

N 70 39828

NASA TECHNICAL
MEMORANDUM

NASA TM X-53991

CASE FILE
COPY

A SOLAR X-RAY ASTRONOMY SUMMARY AND BIBLIOGRAPHY

By Robert M. Wilson
John M. Reynolds
Stanley A. Fields
Space Sciences Laboratory

January 1970

NASA

*George C. Marshall Space Flight Center
Marshall Space Flight Center, Alabama*

TABLE OF CONTENTS

	Page
INTRODUCTION.	1
BIBLIOGRAPHY.	3
AUTHOR INDEX.	83
SUBJECT INDEX	87
APPENDIX	90

LIST OF TABLES

Table	Title	Page
A-1.	Tabulation of Rocket and Balloon Solar X-Ray Flight Experiments.	91
A-2.	Tabulation of Satellite Solar X-Ray Flight Experiments	94
A-3.	Tabulation of Observed Solar Spectral Lines (1- to 100-Å) by Flight Experiment.	96
A-4.	List of Observed Solar Spectral Lines (1- to 100-Å)	114

DEFINITION OF SYMBOLS

Symbol	Definition
Crystals:	
CaF ₂	Calcium fluoride
CaSO ₄ :Mn	Calcium sulfate: manganese
EDDT	Ethylene diamine d-tartrate
KAP	Potassium acid phthallate
LiF	Lithium fluoride
ML	Magnesium lignocerate (multilayer film)
NaI	Sodium iodide
NaI(Tl)	Sodium iodide (thallium)
OHS	Octadecyl hydrogen succinate
Elements:	
Al	Aluminum
Ar	Argon
B	Boron
Be	Beryllium
C	Carbon
Ca	Calcium
Cl	Chlorine
Cr	Chromium

DEFINITION OF SYMBOLS (Continued)

Symbol	Definition
Elements:	
F	Fluorine
Fe	Iron
H	Hydrogen
He	Helium
Li	Lithium
Mg	Magnesium
Mn	Manganese
N	Nitrogen
Na	Sodium
Ne	Neon
Ni	Nickel
O	Oxygen
S	Sulfur
Si	Silicon
Tl	Thallium
Others:	
E	Energy
$h\nu$	Photon energy (Planck's constant \times frequency)

DEFINITION OF SYMBOLS (Concluded)

Symbol	Definition
Others:	
mc^2	Energy (mass \times velocity of light squared)
λ	Wavelength
θ	Incidence angle
f	Focal length
l	Distance
$^{\circ}, ', ''$	Degrees of arc, minutes of arc, seconds of arc
$>$	Greater than
\geq	Greater than or equal to
$<$	Less than
\leq	Less than or equal to
\sim	Approximately
\approx	Approximately equal to
$=$	Equal to
Ca K	Calcium K line (resonance)
H α	Hydrogen line (resonance)
K α	Characteristic X-ray emission
π	Pi (3.1415927)

LIST OF ABBREVIATIONS

Abbreviation

Definition

Groups:

AFCRL	Air Force Cambridge Research Laboratory
ARUCL	Astrophysics Research Unit Culham Laboratory
ASE	American Science and Engineering
CSRL	Convair Scientific Research Laboratory
ESRO	European Space Research Organization
GSFC	Goddard Space Flight Center
HAO	High Altitude Observatory
HCO	Harvard College Observatory
LASL	Los Alamos Scientific Laboratory
MSFC	Marshall Space Flight Center
MSSL	Mullard Space Science Laboratory
NASA	National Aeronautics and Space Administration
NRL	Naval Research Laboratory

Ionosphere:

CR	Cosmic-ray
SCNA	Sudden cosmic noise absorption
SEA	Sudden enhancement of (low frequency) atmospherics
sfe	Solar flare effect

LIST OF ABBREVIATIONS (Continued)

Abbreviation	Definition
--------------	------------

Ionosphere:

SID	Sudden ionospheric disturbance
-----	--------------------------------

SWF	Short-wave fadeout
-----	--------------------

Measurements:

Å	Angstrom
---	----------

ΔÅ	Angstrom band
----	---------------

A. U.	Astronomical Unit
-------	-------------------

mm	Millimeter
----	------------

cm	Centimeter
----	------------

km	Kilometer
----	-----------

in.	Inch
-----	------

eV	Electron volt
----	---------------

keV	Kiloelectron volt
-----	-------------------

MeV	Megaelectron volt
-----	-------------------

MHz	Megahertz
-----	-----------

Mc	Megacycle
----	-----------

Mc/sec	Megacycle per second
--------	----------------------

°K	Degrees Kelvin
----	----------------

°C	Degrees Centigrade
----	--------------------

LIST OF ABBREVIATIONS (Continued)

Abbreviation	Definition
Measurements:	
UT	Universal Time
MST	Mountain Standard Time
min	Minute
sec	Second
lb	Pound
Satellite-Rocket:	
ATM	Apollo Telescope Mount
IMP	Interplanetary Monitoring Probe
IRIS	International Radiation Investigation Satellite
OGO	Orbiting Geophysical Observatory
OSO	Orbiting Solar Observatory
SL	Skylark
SOLRAD, SR	Solar Radiation
UK	United Kingdom (Ariel)
Tabular:	
SC	Solar condition
A	Active
Q	Quiet

LIST OF ABBREVIATIONS (Continued)

Abbreviation	Definition
--------------	------------

Tabular:

R	Rocket
B	Balloon
S	Satellite
CRG	Cosmic-ray group
Obs.	Observatory
Ref	Reference
No.	Number
Uid.	Unidentified
Ly	Lyman
Diff. grating spect.	Diffraction grating spectrograph
spect.	Spectrograph
photo.	Photometer
g. i.	Grazing incidence
g. i. spect.	Grazing incidence spectrograph
g. i. s.	Grazing incidence spectrometer
p. c.	Proportional counter
p. c. s.	Proportional counter spectrometer

LIST OF ABBREVIATIONS (Continued)

Abbreviation	Definition
Tabular:	
p. h. a.	Pulse height analyzer
p. h. c.	Pulse height counter
i. c.	Ionization chamber
s. c.	Scintillation counter
B. c. s.	Bragg crystal spectrometer
G. c.	Geiger counter
Others:	
α	Alpha
β	Beta
γ	Gamma
δ	Delta
cm- λ	Centimeter-wavelength
B, L	Heliographic coordinates
IQSY	International Quiet Sun Year
IGY	International Geophysical Year
IGC	International Geophysical Cooperation
NE	Northeast
NW	Northwest

LIST OF ABBREVIATIONS (Concluded)

Abbreviation	Definition
Others:	
f-f	Free-free
f-b	Free-bound
T	Temperature
T_e	Electron temperature
EUV, XUV	Extreme ultraviolet
UV	Ultraviolet
el	Electrons
Ne	Electron density
V	Volume
Δn	Transition
$N_{\text{Si}}/N_{\text{H}}$	Ratio of silicon atoms to hydrogen atoms

A SOLAR X-RAY ASTRONOMY SUMMARY AND BIBLIOGRAPHY

INTRODUCTION

This review summarizes the results of the solar X-ray astronomy work that has been reported in the literature. Included are tables prepared from the surveyed literature, which are used to summarize certain information concerning the X-ray Sun. Also included is a bibliography, an author index, and a subject index.

The bibliographic section represents the working body of the report. It is arranged in alphabetical order by author, and each abstract is preceded by the abstract number. This number is the key to the abstract-cross-reference system. For example, one wishing to find all articles written by L. W. Acton in this review would turn to the author index, find Acton's name, and list the abstract number or numbers indexed beside the reference. This number refers to the abstract contained in the body of the report. Likewise, one wishing to determine all articles concerning balloon X-ray flight experiments would refer to the subject index under the heading "X-Ray Flight Experiments" and under the subheading "Balloon". These numbers are the abstract numbers.

Four interrelated tables were constructed from the surveyed literature and are included in the appendix. Table A-1, Tabulation of Rocket and Balloon Solar X-Ray Flight Experiments, lists by date and time (UT) the solar X-ray rocket and balloon flight experiments contained within this review. Other information included in the table are solar condition (SC), investigating group (Lab), designation of project, instrumentation, Angstrom band ($\Delta\text{\AA}$), and references (Ref). The numbers in the reference column refer to the abstracts.

Table A-2, Tabulation of Satellite Solar X-Ray Flight Experiments, lists by satellite designation the various satellite solar X-ray experiments. This table is similar to Table A-1 in that the period of observation, the instrumentation, the Angstrom band and the references are included as well. Again, the numbers in the reference column refer to the abstracts.

Table A-3, Tabulation of Observed Solar Spectral Lines (1- to 100- \AA) by Flight Experiment, lists by date of observation the observed solar spectral

lines (λ observed) in the 1- to 100-Å region. Also included are type of flight experiment (R, B, S), predicted wavelength (λ predicted), ion, transition, remarks, and references (references again refer to the abstracts). The number column (No.) enumerates the flights from earliest (1) to most recent (11). This number cross-references Tables A-3 and A-4.

Table A-4, List of Observed Solar Spectral Lines (1- to 100-Å), lists observed solar spectral lines (λ observed) from shortest wavelength (1.91-Å) to longest wavelength (98.24-Å). Included in this table are the ions and predicted wavelengths (λ predicted), which may be identified with the observed spectral lines. The number column (No.) cross-references with Table A-3.

These four tables comprise the appendix section of the review and are definitely interrelated. Table A-3 is connected to tables A-1 and A-2 by the date or period of observation and the R, B, S column, which signifies a rocket, balloon or satellite flight experiment. Table A-4 is related to Table A-3 by the number column (No.) and represents a reordering of the data contained in Table A-3.

To exhibit the interrelationships among the tables an example is given. Suppose one wishes to obtain more information about an observed spectral line listed in Table A-4. From this table he has already secured the ion or ions and their predicted wavelengths that may be associated with the observed line in question. Also, he has a cross-reference to Table A-3, the No. column, which will give him more data. From Table A-3 he learns when the spectral data was obtained and the type of flight experiment it was (R, B, S). The transition of the ion identified with the observed spectral line may be given as well as any useful remarks. From this table he also is referred to the abstract-bibliography by the reference column. Knowing the date of observation and the type of flight experiment, he can go to Tables A-1 and A-2 and determine the solar condition at the time of observation, the investigating group (Table A-1) the instrumentation, and the Angstrom band. He is also referred to the abstracts by the reference column.

The bibliography contains abstracts from 153 papers related to solar X-ray astronomy. It is realized that all articles that may have been published have not been included; however, the articles reviewed provide a comprehensive summary of solar X-ray astronomy.

BIBLIOGRAPHY

1. Acton, L. W.: Contribution of Characteristic X-Rays to the Radiation of Solar Flares. *Nature*, vol. 207, Aug. 1965, pp. 737-738.

The purpose of this communication is to point out that characteristic X-rays emitted as a result of inner-electron transitions may make an important contribution to the X-ray emission of solar flares. The detection of the characteristic radiation of Fe atoms in the X-radiation from flares would indicate that nonthermal processes are important in the production of X-rays in the 1- to 3-Å wavelength range, something which is not yet known with certainty. In order to evaluate the relative contribution of the characteristic radiation excited by nonthermal electrons, the author compares this emission to the bremsstrahlung emitted by the same electrons at the same wavelength. Thus, he calculates the intensity of the bremsstrahlung emission per angstrom and compares this to the estimated value in the characteristic lines of Fe that he derived. From this comparison it is seen that if sizable numbers of energetic electrons are created by a flare, then the characteristic radiation from neutral or weakly ionized Fe may make a substantial contribution to the X-ray emission of the flare in the wavelength interval around 2 Å.

2. Acton, L. W.: X-Ray and Microwave Emission of the Sun with Special Reference to the Events of July, 1961. *Astrophys. J.*, vol. 152, Apr. 1968, pp. 305-318.

X-ray ($\lambda < 14 \text{ Å}$), microwave ($\lambda = 10.7 \text{ cm}$), optical, and ionospheric observations are utilized together with theoretical X-ray spectra to derive physical models of some X-ray emitting volumes on the Sun. The following kinds of emitting regions are studied: (1) a large "permanent" coronal condensation; (2) a flare in its flash phase; and (3) a yellow-line condensation associated with a postflare loop prominence system. Most of the observational data were gathered during the month of July 1961. This period presented the opportunity to study the X-ray emission of the Sun over a wide range of solar activity and at the same time unambiguously to identify the sources of emission. The data were observed from the following two satellite-borne instruments in orbit: (1) the X-ray monitoring satellite Solar Radiation 3 (SR3) of the NRL and (2) the Injun I satellite of the State University of Iowa. Both thermal and nonthermal emission processes seem to be required to account for the X-ray emission from flares. This study indicates that it is not necessary to invoke temperatures higher than $4 \text{ to } 5 \times 10^6 \text{ K}$ to account for the thermal radiation of

flares. The prolonged enhancements of soft X-rays which follow some large flares appear to be thermal emission from the same "sporadic" coronal condensations that emit the yellow line of Ca XV. In the case of the yellow-line condensation studied here, the observations are best fitted if 1 percent of the volume contains 90 percent of the material. Various topics discussed are (1) X-ray and microwave emission from a hot gas, (2) Nonflare X-ray and microwave emission, and (3) X-ray and microwave emission associated with flares.

3. Acton, L. W.; Chubb, T. A.; Kreplin, R. W.; and Meekins, J. F.:
Observations of Solar X-Ray Emission in the 8 to 20 Å Band.
J. Geophys. Res., vol. 68, June 1963, pp. 3335-3344.

This paper reports 101 observations of the solar X-ray flux in the 8- to 20-Å band. The observations were made by NRL solar X-ray monitoring satellite Solar Radiation 3 (SR3) from June 29 to November 26, 1961. Two ionization chambers made up the X-ray detectors for the satellite. A table of observations for the period discussed in the 8- to 20-Å region is presented. The fluxes range from a high value of greater than $0.4 \text{ erg cm}^{-2} \text{ sec}^{-1}$, during a 3^+ limb flare, to below the limit of detectability, $0.002 \text{ erg cm}^{-2} \text{ sec}^{-1}$. The intensity of this radiation is correlated with general solar activity and is greatly enhanced during some flares. Solar X-ray flux in the 8- to 20-Å band versus time is shown graphically. The authors report the results of two solar X-ray flare observations. These flares were on June 29, 1961 and July 20, 1961. Also included is a time history of the July 11, 1961 flare X-ray event. X-ray enhancements may persist for hours after the end of large flares. Comparison of SID and the X-ray enhancements indicates that the spectrum of the X-radiation differs from one flare to the next and with time during a given flare event.

4. American Astronomers Report: Solar Observations in the Extreme Ultraviolet. Sky and Tel., vol. 27, Apr. 1964, pp. 213-214.

A brief discussion concerning solar observations in the XUV by the NRL group (Tousey, Austin, Garrett, Purcell, and Widing) as presented at the 115th meeting of the AAS at Washington, D. C. on December 26 to 28, 1963, is given. The May 10, 1963 and September 20, 1963 rocket flights are compared, and data observed on these flights are presented (the Sun's XUV spectrum between 33 and 188 Å). A 1960 X-ray photograph of the Sun, taken with a rocket-borne pinhole camera, is also included.

5. Anastassiadis, M; and Boviatsos, D. S.: Distribution of X-Ray Emission from the Sun Deduced from Measurements of Ionospheric Absorption. *Nature*, vol. 219, Sept. 1968, pp. 1139-1141.

During the annular solar eclipse of May 20, 1966 solar flux and ionospheric absorption measurements were made from several points along the central line of the path of the eclipse. Solar flux was measured at various frequencies in the cm and mm bands. All the data obtained during the eclipse showed characteristic variations in flux related to local active sources on the solar disk. Three sources giving an increase in flux were identified during this eclipse: one on the west limb, the second in the middle of the disk, and the third on the east limb. These centers of activity were also strong X-ray emission sites, producing absorption in the D-layer, as measured on 1.98 MHz. Direct measurements on X-ray radiation made during the same eclipse by Landini et al., using data from NRL satellite 1965A, show a large change in the 1- to 8-Å band at the covering of the active source in the middle of the solar disk, and also at the uncovering of the active source on the east limb. These results support the authors' observations. Thus, the authors assume that parts of local sources emitting hard X-rays are causing the changes in the D-layer absorption, and that soft X-rays, especially from the solar limb, are associated with absorption in the E-layer.

6. Anderson, K. A.; and Winckler, J. R.: Solar Flare X-Ray Burst on September 28, 1961. *J. Geophys. Res.*, vol. 67, Oct. 1962, pp. 4103-4117.

The bright chromospheric flare of September 28, 1961 emitted a burst of X-rays observed by high-altitude balloon-borne detectors (scintillation counters and three channel pulse analyzers for the 20- to 150-keV energy range) at three locations over North America. The data presented here are mostly that obtained over Flin Flon, Manitoba, Canada by a Berkely Cosmic Ray Group. The other flights were conducted from Minneapolis and International Falls by the University of Minnesota Cosmic Ray Group. The burst had a small precursor, a very rapid rise, and a three-component decay. The main part of the burst is therefore interpreted as being made up of three separate pulses. The X-ray burst shows two remarkable associations with the flare's radio noise emission: (1) microwave bursts at the highest radio frequencies coincide precisely in time with the precursor and the main peak; and (2) groups of type III bursts occur at or near the time of discontinuities in

the decay of the X-ray burst and thus are associated with the leading edges of the three energetic electron pulses whose bremsstrahlung constitutes the observed X-ray flux. The appearance of both type III radiation originating in the corona at about 10^5 km and bremsstrahlung X-rays that cannot reasonably be produced above roughly 5000-km height in the chromosphere gives strong evidence that energetic electrons undergo large-scale motions in the solar atmosphere during chromospheric flares. For this particular flare a filamentary structure appears to be rooted near the sunspot where the flare occurs. Although no direct observations exist on this point, the filament no doubt extends into the lower corona perhaps to heights of 10^5 km. This leads to the possibility that the electrons are contained and guided by this structure. The photon energy spectrum is found to be nearly constant in form, whereas the X-ray intensity varies greatly. This fact makes it extremely unlikely that the bremsstrahlung originates from a thermal distribution of high temperature electrons. A detailed analysis of the spectral variation shows that the solar electrons must spend most of their time above the 15 000-km level. Various charts and tables are included giving pictorial information about the solar X-ray event.

7. Argo, H. V.; Bergey, J. A.; Evans, W. D.; and Singer, S:
16-40 Å Coronal X-Ray Emission during the 12 November
1966 Eclipse. Sol. Phys., vol. 5, 1968, pp. 551-563.

The solar eclipse of November 12, 1966 was used to study the coronal emission near the limbs in selected emission lines [C, N, O] between 16 and 40 Å. Eight fixed-wavelength, curved crystal spectrometers were carried in each of three rocket launches and monitored the flux in each of the eight wavelength intervals of the selected emission lines. The rockets were launched from Rio Grande, R. G. do Sul, Brazil. All three instrumented payloads experienced an anomalously high background counting rate, presumably from the South Atlantic magnetic anomaly. At totality the emissions dropped to background levels of 1 percent or less of the full Sun values, showing that on the solar limbs on that day there was very little emission above 17 000 km in these lines. A schematic chart and table, representing the most prominent emission lines in the 16- to 40-Å wavelength band, are also included.

8. Arnoldy, R. L.; Kane, S. R.; and Winckler, J. R.: A Study of Energetic Solar Flare X-Rays.
Sol. Phys., vol. 2,
1967, pp. 171-178.

A new series of solar flare energetic X-ray events has been detected by an ionization chamber on the OGO-I and OGO-III satellites. These X-rays lie in the 10- to 50-keV range, and a study has been made of their relationship to 3- and 10-cm radio bursts and with the emission of electrons and protons observed in space. The onset times, times of maximum intensity, and total duration are very similar for the radio and X-ray emission. Also, the average decay is similar and usually follows an exponential type behavior. However, this good correlation applies most often to the "flash" phase of flares, whereas subsequent surges of activity from the same eruption may produce microwave emission or further X-ray bursts not closely correlated. The X-ray and microwave emission may have a common energizing process that determines the time profile of both. The recording of electrons greater than 40 keV by the IMP satellite has been found to correlate very well with flares producing X-ray and microwave emission, provided the propagation path to the Sun is favorable. There is evidence that the acceleration of solar protons may not be closely associated with the processes responsible for the production of microwaves, X-rays, and interplanetary electrons. The observations covered the period from September 5, 1964 to June 30, 1966.

9. Arnoldy, R. L.; Kane, S. R.; and Winckler, J. R.: Energetic Solar Flare X-Rays Observed by Satellite and Their Correlation with Solar Radio and Energetic Particle Emission. *Astrophys. J.*, vol. 151, Feb. 1968, pp. 711-736.

The ionization chambers on the OGO-I and OGO-III satellites have detected numerous solar X-ray increases associated with flares and solar radio bursts. Approximately 30 solar flare X-ray bursts have been detected between September 5, 1964 and June 20, 1966. These energetic X-ray bursts have been correlated with 3- and 10-cm solar radio emission and solar-flare electron and proton events measured in space. An analysis of the observations and correlations follows. Tables showing X-ray events observed by OGO satellite corresponding to known radio bursts, X-ray solar radio correlations (September 1964 through June 1966, OGO events), and many others are presented. It is found that the total energy released during a solar flare in the form of X-rays between 10 and 50 keV is approximately proportional to the energy simultaneously released in the form of microwave emission in either the 3- or 10-cm range of frequencies. For a given flare burst the rise time, decay time, and total duration are similar for the 10- to 50-keV X-rays and for the 3- or 10-cm radio emission. The decay is roughly exponential with time constants between 1 and 10 minutes. All 3- or 10-cm radio bursts with peak intensity greater than 80 solar flux units are accompanied by an X-ray

burst greater than 3×10^{-7} erg cm⁻² sec⁻¹ peak intensity in the 10- to 50-keV range. The probability of detecting an X-ray event under the energy and sensitivity limits of this investigation is negligible unless the radio spectrum extends into the centimetric range of wavelengths. The 10- to 50-keV range of X-rays measured shows an excellent correlation with the occurrence of SID events. A very high percentage of large SWF's during OGO observation periods were accompanied by detectable X-rays in the OGO experiments. There exist a number of very large flare events in which one observes all of the energetic processes — solar protons, solar electrons, energetic bremsstrahlung and high-frequency radio emission. In comparing energetic X-rays with solar particle emission, the better correlation seems to exist with the solar electron events observed in space. Many solar proton events occurred without a detectable burst of energetic X-rays.

10. Arnoldy, R. L.; Kane, S. R.; and Winckler, J. R.: The Observation of 10-50 keV Solar Flare X-Rays by the OGO Satellites and Their Correlation with Solar Radio and Energetic Particle Emission. I. A. U. Symp. No. 35, 1968, pp. 490-509.

More than 70 cases have been observed of energetic solar flare X-ray bursts by large ionization chambers on the OGO satellites (I and III) in space. The ionization chambers have an energy range between 10 and 50 keV for X-rays and are also sensitive to solar protons and electrons. A study has been made of the X-ray-microwave relationship, and it is found that the total energy released in the form of X-rays between 10 and 50 keV is approximately proportional to the peak or total energy simultaneously released in the form of microwave emission. For a given burst the rise time, decay time, and total duration are similar for the 10- to 50-keV X-rays and the 3- to 10-cm radio emission. Roughly exponential decay phases are observed for both emissions with time constants between 1 and 10 minutes. All 3- or 10-cm radio bursts with peak intensity greater than 80 solar flux units are accompanied by an X-ray burst greater than 3×10^{-7} erg cm⁻² sec⁻¹ peak intensity. The probability of detecting such X-ray events is low unless the radio spectrum extends into centimetric range of wavelengths. The best correlation between cm-λ and energetic X-rays is observed for the first event in a flare. Subsequent structure and second bursts may not correspond even when the radio emission is rich in the microwave component. The mechanism for the energetic X-rays is shown to be bremsstrahlung probably of fast electrons on a cooler plasma. If the radio emission is assumed to be synchrotron radiation, then a relationship is developed between density and magnetic field which meets the observed quantitative results. A strong correlation between interplanetary solar flare

electrons observed by satellite and X-ray bursts is shown to exist. This correlation is weak for solar proton events. One may infer a strong propagation asymmetry for solar flare electrons along the spiral interplanetary magnetic field.

11. Atkinson, P. A.; and Pounds, K. A.: Laboratory Calibration of Several High-Speed Films with 2-14 Å X-Rays. J. Photographic Sci., vol. 12, 1964, pp. 302-306.

The use of photographic emulsions in rocket-borne instruments for the study of the solar X-ray emission has led to a program of laboratory studies of four high-speed X-ray films. Results are given for the absolute photon sensitivities of commercial Ilford Industrial X-ray film, type G, a single layer unsupercoated Ilford Industrial G, unsupercoated Kodirex, and Kodak-Pathé-SC5, over the 2- to 14.5-Å wavelength range. The precision and repeatability of calibration for a given batch of film are discussed. Measurements of the inherent grain photon equivalence for two emulsions are also given. No significant exposure temperature coefficient is found for the Ilford and centrifuged Kodak emulsions over the 20° to 78° C range. Various plots of density versus exposure, aging, and photon detection efficiency are included. This paper was originally presented at a symposium on "Photographic Aspects of Ionizing Radiation," organized by the Science Committee on April 15 to 17, 1964, in Oxford.

12. Austin, W. E.; Purcell, J. D.; Snider, C. B.; Tousey R.; and Widing, K. G.: Recent Extreme Ultraviolet Solar Spectra and Spectroheliograms. Space Res. VII, 1967, pp. 1252-1261.

Extreme ultraviolet spectroheliograms obtained on October 20, 1965, February 1 and April 28, 1966 show that the chromospheric coarse mottling and network are characteristic of He II (304 Å); high chromospheric lines, such as Mg IX (368 Å) are emitted mostly from the limb and plages; coronal lines like those from Fe XV and XVI come only from plages and the corona above them. Spectra obtained on February 1, 1966 show that Fe XV (284 Å) and Fe XVI (335.361 Å) are of low intensity in the quiet Sun, compared to September 20, 1963 when the Sun was active. The solar X-ray spectra photographed over the 30- to 80-Å range is shown. The long wavelength end of the spectrum from 60 to 100 Å is also shown. In the new spectrum all three lines of Fe XIV $3p^2P^0-3d^2D$ are resolved, but the identification of Fe XIV $3s^2P^0-3p^2P$ remains questionable. The 70- to 105-Å range was photographed using a filter of indium instead of aluminum. Many new lines are present including lines of Fe IX, X, and XI.

13. Austin, W. E.; Purcell, J. D.; Tousey, R.; and Widing, K. G.: Coronal Emission-Line Intensities in the Extreme Ultraviolet. *Astrophys. J.*, vol. 145, Aug. 1966, pp. 373-379.

On May 10, 1963, and again on September 20, 1963, photographic spectra containing many resonance lines from the solar corona extending to wavelengths as short as 33 Å were obtained by rocket. Calibrated fluxes are given for approximately 30 identified resonance lines of coronal ions in the 250- to 370-Å wavelength region obtained from the rocket spectrum of May 10, 1963. Estimated fluxes for 30 coronal lines and multiplets in the 33- to 70-Å wavelength region obtained from the rocket spectrum of September 20, 1963 are also given. Data are presented for the solar active centers of September 20, 1963 from measurements of rocket spectroheliograms in the 300-Å region.

14. Austin, W. E.; Purcell, J. D.; Tousey, R. and Widing, K. G.: Solar Spectrum Photographed to 33 Å. *Astron. J.*, vol. 69, 1964, p. 133.

Spectrographs were flown twice during 1963 in Aerobee rockets. On May 10, 1963 first-order lines were photographed over the 44- to 630-Å range. On September 20, 1963 spectra from 33 to 188 Å were secured with a resolution of 0.1 Å and a wavelength accuracy of 0.03 Å for strong lines. About 50 emission lines were recorded from 33 to 75 Å; some 70 emission lines from 148 to 188 Å; 100 from 188 to 342 Å; and a few strong lines from 342 to 630 Å. New identifications were determined. For the most part, however, the strongest lines were unidentified.

15. Baez, A. V.: A Proposed X-Ray Telescope for the 1- to 100-Å Region. *J. Geophys. Res.*, vol. 65, Sept. 1960, pp. 3019-3020.

The author describes two telescopes for the 1- to 100-Å wavelength region. The first telescope consists of two thin, plane glass mirrors, each approximately 1 inch by 3 inches, disposed like the shades of a venetian blind, followed by an identical array at right angles to the first. This system gives good resolution, and is also capable of producing an image of an extended object. A distant point source would be imaged as a small rectangle, since each crossing of two mirrors at right angles to each other presents effectively a small rectangular "window" for the radiation. The second telescope, a contemplated improvement of the first, is to be made by curving the mirrors

so that each one effectively becomes a section of a right-circular cylinder. Curving the mirrors would greatly improve the resolving power of the system and the intensity of illumination at the image. At grazing incidence, spherical surfaces may be used instead of cylindrical ones with no practical loss in resolution. The advantages of this multiple-crossed-mirror system include simplicity of construction, approximately true point-to-point image-forming characteristics, absence of chromatic aberration, and speed (large flux-gathering capabilities).

16. Blake, R. L.; Chubb, T. A.; Friedman, H.; and Unzicker, A. E.:
Interpretation of X-Ray Photograph of the Sun. *Astrophys. J.*, vol. 137, 1963, pp. 3-15.

The authors report the results of two rocket (Aerobee) flights carrying X-ray pinhole cameras. Both were launched from White Sands, New Mexico, and both obtained X-ray photographs of the Sun. The first flight was launched on April 19, 1960. The best photograph of the four obtained from that flight is reproduced and discussed in their paper. The exposure was made on Ilford Industrial G X-Ray Film. On this date, solar activity was typical of the period near sunspot maximum. Analysis of the X-ray photographs and Ca K pictures has shown that there is a close correlation between X-ray emission regions and plage regions. An analysis of the April 19 photograph in terms of the X-ray contribution of the individual emitting plage regions has been tabulated in the paper. A density contour map of the solar X-ray photograph is also presented. The authors calculated the total solar X-ray emission flux arriving at the earth to be $0.27 \text{ erg cm}^{-2} \text{ sec}^{-1}$ under a 10^6 K Planckian distribution. A probable correlation between plage X-ray brightness and plage activity was noted. The relative brightness of X-ray sources and decimeter radio-emission sources at 9.1 and 21 cm are plotted. These curves show the ratios of integrated X-ray and radio flux from four groups of plages plotted as a function of radius vector. The 21-cm radio emission seems to show less limb darkening relative to the X-ray emission than the 9.1-cm flux and hence may be a good index of solar X-ray emission. A second set of exposures was obtained on June 21, 1961. Three of the resulting photographs are shown with information on angular resolution and filter characteristics for each. The second set of photographs revealed several pieces of new information: the strongly emitting regions are small (comparable in size with camera's resolution 2 minutes); the plage regions were much stronger in emission than the quiet corona, even at wavelengths extending to 90 Å ; correlation of these photographs with drawings from the Sacramento Peak Observatory and Ca K photos from the McMath-Hulbert Observatory indicates that the plage regions

coincide with regions of X-ray emission; and the photographic exposures obtained through the Ni and Ti filters are compatible with expected intensities in these bands based on an assumed 10^6 °K solar emission. In conclusion, the pinhole-camera X-ray photographs of the Sun represent the patterns of solar X-ray source distributions over the broad range of wavelengths from 10 to 100 Å. At least 75 percent of the total X-ray flux comes from active regions smaller in area than underlying Ca plages. It seems likely that increased resolution would reveal finer detail within the presently resolved "X-ray plages" and a dependence of source dimensions on wavelength.

17. Blake, R. L.; Chubb, T. A.; Friedman, H.; and Unzicker, A. E.:
Measurement of Solar X-Ray Spectrum between 13 and 26 Å.
Annales D'Astrophysique, vol. 28, 1965, pp. 583-585.

This present note concerns a study of the solar X-ray spectrum between 13 and 25 Å, carried out with a Bragg crystal X-ray spectrometer on July 25, 1963 from an Aerobee rocket launched from White Sands, New Mexico. The spectrometer was made up of a KAP analyzing crystal and a thin window Geiger counter. A photograph of the spectrometer appears in the article. The spectrum scan of the sun provided three types of information. First, it provided data on the wavelengths and strengths of the X-ray emission lines making up the solar spectrum. Second, it provided evidence on each line as to whether the line originated mainly from the entire solar disk or mainly from the single strong plage region that happened to be present at the time of launch. Third, it established an upper limit to the strength of the solar X-ray continuum. A plot of uncorrected line strengths is shown. Also given is a table showing wavelengths and probable identifications of the observed lines together with the computed energy contained in each line. The wavelengths are believed to be accurate to about ± 0.1 Å. The final column describes the line shape. A spectrum of about 12 lines between 12 and 25 Å was recorded on the flight. The lines were made up mainly of lines from O VII, O VIII, N VII, and Fe XVII. The O VII and N VII lines appeared to come from the entire solar disk, while the Fe XVII lines appeared to originate almost entirely in a single plage region. This communication was originally presented at Symposium No. 23 on Astronomical Observations from Aboard Space Vehicles held at Liège on August 17 through 20, 1964.

18. Blake, R. L.; Chubb, T. A.; Friedman, H.; and Unzicker, A. E.:
Solar Emission Line Spectrum from 1 to 25 Å. Astron. J.,
vol. 69, 1964, pp. 134-135.

A KAP crystal spectrometer was flown on an Aerobee rocket on July 27, 1963 to measure the solar spectrum from 1 to 25 Å. A table of emission lines that were detected and their tentative identifications is presented. No lines shorter than 13.7 Å appeared in the spectrum.

19. Blake, R. L.; Chubb, T. A.; Friedman, H.; and Unzicker, A. E.:
Solar X-Ray Spectrum below 25 Angstroms. *Science*, vol. 146, Nov. 1964, pp. 1037-1038.

A Bragg crystal spectrometer was flown by rocket on July 25, 1963 to measure the solar X-ray emission. The spectral range viewed was 10 to 25 Å. Below 25 Å, the solar spectrum consists primarily of the emission lines of Fe XVII, O VIII, O VII, and N VII. The lines of the more highly ionized atoms, Fe XVII and O VIII, originate in localized active regions. Lines of O VII and N VII emanate from the full disk. The solar X-ray spectrum as recorded by the Bragg spectrometer is shown in tabular form.

20. Blake, R. L.; Chubb, T. A.; Friedman, H.; and Unzicker, A. E.:
Spectral and Photometric Measurements of Solar X-Ray Emission below 60 Å. *Astrophys. J.*, vol. 142, July 1965, pp. 1-12.

NRL launched two Aerobee rockets on April 4, 1963 and on July 25, 1963 to observe the spectrum of solar X-rays (8 to 60 Å) and their brightness distribution over the disk. The experiments carried aloft were Bragg-type X-ray crystal spectrometers, pinhole cameras, and slit scanners. The first flight failed to produce useful spectral data (8 to 15 Å and 44 to 60 Å), but did provide information on the size and distribution of sources on the disk. Sources of 8- to 15-Å X-rays were geometrically smaller than 44- to 60-Å sources. Some 8- to 15-Å sources had dimensions of the order of 1 minute. Essentially all the radiation observed in the 8- to 15-Å band originated in active regions; about half the 44- to 60-Å emission was localized in the same regions, the remainder being distributed over the disk. The second flight (8 to 20 Å and 44 to 60 Å) recorded an X-ray line spectrum in the 13- to 25-Å spectral band. Line emissions from O VII, O VIII, N VII and Fe XVII were recorded in the 13- to 25-Å band. The O VII line emission came mainly from the solar disk as a whole; the Fe XVII emissions came from a localized active region near the center of the Sun. The authors also describe the X-ray spectral measurements, and then discuss developments in X-ray photography and the results of slit-scan observations carried in the two reported flights. The wavelengths

and computed photon fluxes of the lines in the 13- to 25-Å spectral band are tabulated. Also given is a plot of spectrum line counting rates versus wavelength.

21. Blake, R. L.; and House L. L.: K- α X-Ray-Type Transitions in the Solar Atmosphere and Laboratory Plasma. *Astrophys. J.*, vol. 149, July 1967, pp. L33-L35.

A recent observation of the solar X-ray spectrum has led to the suggestion that two lines, one at 1.91 Å and another at 23.28 Å, arise from K- α type X-ray transitions in ionized iron and oxygen, respectively. The purpose of this paper is to confirm the above interpretation by means of preliminary laboratory data and theoretical calculations and, furthermore, to suggest additional identifications of the same type.

22. Bowles, J. A.; Culhane, J. L.; Sanford, P. W.; Shaw, M. L.; Cooke, B. A.; and Pounds, K. A.: A Measurement of the Solar X-Ray Flux in the Wavelength Range below 5 Å. *Planet. Space Sci.*, vol. 15, 1967, pp. 931-935.

Two beryllium windowed proportional counters were used to measure the solar X-ray flux below 5 Å. They were flown on a Centaure sounding rocket launched from a site near Karystos, Greece on May 15, 1966. The counters and their associated electronics are briefly described. The shape of the spectrum is estimated by considering the variation in counting rate as the rocket ascended through the atmosphere. A comparison of the present result with other measurements (2 to 12 Å) suggests that the spectral slope and intensity are extremely variable in this part of the spectrum. A table comparing X-ray and radio intensities is also included.

23. Boyd, R. L. F.: Techniques for the Measurement of Extra-Terrestrial Soft X-Radiation. *Space Sci. Rev.*, vol. 4, 1965, pp. 35-90.

The author reviews the techniques characteristic of the 1- to 100-Å band by following a historical approach discussing the various instruments, the wavelength band, and the groups responsible for the observation. A brief description of Burnight's experiment to detect solar X-radiation by means of

emulsions is presented. The author describes the introduction of photon counters and pulse height analyzers into the study of X-ray emission. A discussion of dispersed spectra and the X-ray spectroheliograph follows. Concluding the historic section is a description of the discovery of galactic X-radiation. The remainder of the report discusses six major topics: (1) photometers; (2) wavelength discrimination; (3) spatially resolved observations; (4) some signal-to-noise ratio problems; (5) calibration and testing; and (6) electronic circuits. The photometer section discusses photographic emulsions, their response curves, a photon-emulsion photometer, emulsions for dispersed spectra, phosphor and semiconductor devices, photoelectric detectors, and photoionization detectors. The wavelength discrimination section discusses the use of filters, filling gases and cathode response, proportional counting, and dispersion systems. The spatially resolved observation section discusses pinhole cameras, Fresnel zone plates, object scanning X-ray spectroheliographs, and reflection of X-rays. The signal-to-noise ratio section discusses noise from celestial sources, cosmic ray noise, and trapped radiation. The calibration and testing section discusses laboratory sources of soft X-rays and the calibration and checking of systems away from the laboratory. The last section discusses electronic circuits, a broad-band counter spectrometer for solar X-rays, an E. H. T. supply for proportional counters, and a pulse height analysis circuit. A lengthy bibliography concludes the report.

24. Broadfoot, A. L.: Coronal Fine Structure in X-Ray Emission. *Astrophys. J.*, vol. 149, Sept. 1967, pp. 675-680.

An X-ray pinhole camera was flown by Aerobee rocket launched from White Sands, New Mexico on June 23, 1965. The pinhole camera was designed to detect limb brightening and the X-ray intensity gradient through the quiet corona during solar minimum. Solar X-rays were detected which were emitted by five regions of coronal condensation. These active regions were also detected in microwave emission at 9.1 cm.; they were closely correlated in position and roughly correlated in intensity. Plage areas were located below each of the active regions. Three of the X-ray sources were within a few degrees of being on the limb of the Sun at the time of flight. This allowed the height of the center of the sources above the photosphere to be estimated at $2.2 \pm 0.3 \times 10^4$ km. A relative intensity profile across the most intense X-ray source was obtained with angular resolution of about 0.5 minute. Coarse spectral resolution showed that X-ray emission, attributed to the 0 VII lines, increased about a factor of 5 in intensity over the threshold of detection. Emission attributed to coronal condensation appeared to be concentrated in a region with an angular dimension of about 1 minute.

25. Chitnis, E. V.; and Kale P.: Study of Solar X-Rays. Space Res. VI, 1966, pp. 1034-1040.

Preliminary results of the observations of X-ray fluxes in the 8- to 14-Å and the 44- to 60-Å bands, as detected by the NRL Solar Radiation Satellite 1964-01-D, are presented. The satellite instrumentation was designed to provide data on the soft component of solar X-ray emission. The 2- to 60-Å wavelength range was covered by five gas-filled ion chamber photometers over the following ranges: 2- to 8-Å, 8- to 14-Å, 8- to 16-Å, 44- to 55-Å, and 44- to 60-Å. The photometers for the 8- to 16-Å band and the 44- to 55-Å band failed about 1 month after the launch. This paper also gives a brief description of the telemetry receiving station and the results of the data monitored. For purposes of comparison, the 10-cm radiation flux observed at NRL, Ottawa, Canada, is plotted along with the observed X-ray flux in the 44- to 60-Å and 8- to 14-Å bands. The real time telemetry signals were monitored with the 136 Mc/sec receiving facility at Ahmedabad, India, during the period February 20 to October 7, 1964. A detailed summary of the results is listed in tabular form.

26. Chubb, T. A.: X-Ray Astronomy. Endeavor, vol. 25, 1966, pp. 136-140.

The author presents a general review of the study of X-ray astronomy. The author traces the growth of solar X-ray astronomy from 1948 to the present, mentioning the early work of Edlen in 1920 on the character of the solar corona. Also discussed is the rapid growth of stellar X-ray astronomy from 1962 to the present. The Crab Nebula, Sco X-1, and the Cygnus X-ray objects are briefly discussed. The author closes with a look at future work in X-ray astronomy.

27. Chubb, T. A.: X-Ray Emissions from Solar Flares and from Celestial Sources. Astron. Soc. of Australia, Proceedings, vol. 1, Jan. 1967, Accession # A68-17983, pp. 4-5.

A discussion of the measurement of high-energy X-ray photons during solar flares and of the spectral character and angular width of the strongest type 1 and type 2 X-ray stars is given. A type 1 X-ray star, as designated by the author, is an X-ray source associated with no peculiar visible or radio object. A type 2 X-ray star, therefore, is a source associated with well-known peculiar visible and radio objects of the supernova remnant type. Most X-ray stars appear to be of type 1. Concerning solar X-rays, the author concludes

that there has as yet been no detection of nonthermal solar X-rays. Traces are plotted which show the response of a large-area collimated X-ray source counter during sky scans across high galactic latitudes. A brief discussion of Sco X-1 is presented with the conclusion that Sco X-1 has the appearance of an intense corona surrounding a collapsed star.

28. Chubb, T. A.; Friedman, H.; and Kreplin, R. W.: Measurements Made of High-Energy X-Rays Accompanying Three Class 2⁺ Solar Flares. *J. Geophys. Res.*, vol. 65, June 1960, pp. 1831-1832.

The authors report the preliminary results of rocket measurements of high-energy X-rays accompanying three class 2⁺ solar flares. The rocket measurements were made on August 24, August 31, and September 1, 1959. Also, four measurements were made during times in which no flare activity occurred on the Sun, but which were typical of sunspot maximum conditions. The most interesting results concern the detection of a considerable flux of solar X-rays of energy greater than 20 keV during each of the three class 2⁺ flares. Each flare was accompanied by a sudden ionospheric disturbance (SID). No X-rays of $E > 20$ keV were observed in the firings conducted for background data in the absence of flares. X-ray flux measurements were also made in the 2- to 8-Å and the 8- to 20-Å regions, both during quiet sun and during flare conditions. A plot of number of X-ray quanta as a function of energy, measured during the medium-intensity class 2⁺ flare of August 31, 1959 is shown. The X-ray distributions were determined from pulses produced in a scintillation spectrometer. The energy distribution shown, however, suggests a somewhat different emission character from that postulated by Peterson and Winckler. The energy distribution shown suggests bremsstrahlung from thermalized electrons, possibly an extension of the normal coronal emission. Also, the presence of quanta with $E > 20$ keV in each of the three class 2⁺ flares measured indicates that this type of X-ray emission is probably a common phenomenon in SID flares. Peterson and Winckler concluded that the flux they measured had relatively few low-energy quanta. It therefore appears that the Peterson-Winckler X-ray flash is a different phenomenon from the X-ray tail observed in the present series of experiments. A table giving launch dates, counts, and flux measurements over the 2- to 8- and 8- to 20-Å bands is also presented.

29. Chubb, T. A.; Friedman, H.; and Kreplin, R. W.: Solar X-Ray Spectra in the 2-20 keV Range. *Astron. J.*, vol. 68, 1963, p. 276.

In 1959 three sounding rockets were launched with proportional counters to measure the spectral energy distribution of solar X-rays from 2 to 20 keV. One rocket was fired when the Sun was quiet; the remaining two when the activity was characterized by subflares. The spectrum of the quiet Sun fell rapidly and monotonically from 2 to 11 keV. A temperature of about 10^7 °K was derived. The other two flights gave similar results, but departed markedly from the quiet spectrum at higher energies. Above 4 keV the flux was found to rise to a maximum near 10 keV on one flight and 12 keV on the other. The presence of the emission peak may be evidence of an intensification of line emission or recombination radiation associated with Fe XXV and XXVI.

30. Chubb, T. A.; Friedman, H.; and Kreplin, R. W.: X-Ray Emission Accompanying Solar Flares and Non-Flare Sunspot Maximum Conditions. *Space Res. I*, 1960, pp. 695-701.

Preliminary results from a series of rockets fired during the summer of 1959 on the X-ray emission accompanying a class 2^+ solar flare are presented. A table summarizing early flight results of NRL rocket firings studying the Sun in the 2- to 8- and 8- to 20-Å regions and also of the two firings in 1959 is presented. A second table showing preliminary results for one of the background firings and the middle intensity flare is shown. The energy values indicated in the table are based on assumed solar emission curves having the shape of a 500 000°K Planck curve for the 20- to 100-Å region and a 2×10^6 °K Planck curve for the 2- to 8-Å band. The energy in the spectral band below 0.6 Å is calculated from the absolute X-ray emission determined directly from a scintillation spectrometer. There is also a measure of the 8- to 20-Å radiation. Data is presented on the solar cycle variation during nonflare Sun conditions. For nonflare conditions, the X-ray emission of the Sun at a sunspot maximum in the 8- to 20-Å region is 40 times the emission of sunspot minimum. An additional increase of at least a factor of five accompanied the class 2^+ flare. In addition during the flare an X-ray emission extending up to quantum energies of 70 keV and penetrating below 43 km was observed. The energy contained in this emission tail for quantum energies $E > 20$ keV was of the order of 2×10^{-5} erg cm⁻² sec⁻¹ and changed noticeably in a time period of 3 minutes. X-ray emissions of $E > 20$ keV were observed in a rocket equipped with identical detectors flown during nonflare solar conditions.

31. Chubb, T. A.; Friedman, H.; Kreplin, R. W.; and Kupperian, J. E., Jr.: Lyman Alpha and X-Ray Emissions during a Small Solar Flare. *J. Geophys. Res.*, vol. 62, Sept. 1957, pp. 389-398.

Balloon-borne Rockoon rockets were fired from sea from the U. S. S. Colonial (LSD-18) approximately 350 miles southwest of San Diego. During the operation, one rocket was successfully fired during a solar flare and two additional rockets gave background data on the level of solar Lyman α emission. Four types of radiation detectors were flown in each of the rockets: (1) an ion chamber was used to measure the incident intensity of solar Lyman α radiation, (2) a Geiger counter was used to measure X-rays of wavelength less than 8 Å, (3) a NaI(Tl) crystal, combined with a photomultiplier, was flown as an X-ray pulse amplitude spectrometer to measure any hard X-ray flash that might be encountered during a flare, (4) and two photocells sensitive to visible light were flown to determine rocket orientation in space. Rocket measurements were made during a small flare in progress on June 20, 1956. The rocket reached peak altitude about 10 minutes after the flare was first seen visually. An unusually high X-ray flux was observed extending to a short wavelength limit of 3 Å. Although the flare was still visible in H α , Lyman α was not appreciably different from normal. A table of solar Lyman α emission as measured by nitric-oxide ion chambers for six rocket firings for the period October 18, 1955 to July 25, 1966 is presented. A table summarizing the solar X-ray emission as measured by beryllium and aluminum Geiger counters for nine rocket flights between September 29, 1949 and July 20, 1956 is shown. Also included is a graph of spectral distribution of incident X-ray quanta as a function of quantum energy. The observed emission spectrum of the coronal X-rays most closely approximates the thermal type with the form to be expected from a collection of solar regions at different states of temperature excitation. The measurements would seem to indicate that the coronal excitation lingers long after the primary flare event has dissipated. They also lend strong support to the theory that a hardening of the coronal X-ray spectrum is the source of the low-level D-layer ionization responsible for SID.

32. Chubb, T. A.; Friedman, H.; Kreplin, R. W.; Nichols, W. A.; Unzicker, A. E.; and Votaw, M. J.: Results from the NRL Solar Radiation Satellite. *Space Res.* II, 1961, pp. 617-623.

The NRL Solar Radiation Measuring Satellite, 1960 Eta 2, was launched as the piggy-back rider of the Transit II-A navigational satellite on June 19, 1960. The instrumentation consisted of an ionization chamber for measuring

solar X-rays in the 2- to 8-Å wavelength band and a pair of ionization chambers operated in parallel as a unit to measure the intensity of solar Lyman α radiation (1216 Å). Its wavelength sensitivity band was 1040 to 1340 Å. The Lyman α payload failed after 3 months, but the X-ray photometer continued to operate for the full 10-month operational period. With the approach toward solar minimum, X-ray emission from the quiet Sun in the 2- to 8-Å region dropped to a level below the detectability limit. This radiation was observed only during periods of solar activity. An attempt to summarize the information derived from data analysis to date then follows.

33. Chubb, T. A.; Kreplin, R. W.; and Friedman, H.: Observations of Hard X-Ray Emission from Solar Flares. *J. Geophys. Res.*, vol. 71, Aug. 1961, pp. 3611-3622.

Spectral measurements of solar X-rays with photon energy greater than 20 keV were carried out in 1959 during portions of three class 2⁺ solar flares. Four rockets were flown with scintillation counter pulse amplitude spectrometers; three rockets were flown with proportional counters. Two tables summarizing the results of these seven flights are presented. Photon flux spectra are presented graphically for all flights. Also, scintillation counter pulse amplitude distributions were obtained at several times during the flares of August 31 and September 1, 1959. A proportional counter study of the Sun's emission in the 2- to 20-keV spectral region during microflare activity is presented. The spectra for this region are suggestive of the existence of a peaking in the solar X-ray spectrum in the 8- to 15-keV region, presumably caused by the Fe line and recombination continuum emissions. Two of the flares observed showed strong fluxes with spectra equivalent to that expected from a thermal plasma with temperature approximately 10^8 °. The emission spectra obtained on September 1, 1959 were indicative of a rapidly cooling plasma with initial temperature of about 285 million degrees. It is argued that a similar plasma could have explained the observations of Peterson and Winckler in 1958 and that there currently exists no definitive observational evidence for nonthermal solar X-ray emission.

34. Cline, T. L.; Holt, S. S.; and Hones, E. W., Jr.: High-Energy X-Rays from the Solar Flare of July 7, 1966. *J. Geophys. Res.*, vol. 73, Jan. 1968, pp. 434-437.

A low-energy positron detector incorporating two X-ray spectrometers was mounted on one of the solar panels of OGO 3, and observed continuous

data (80 keV to 1 MeV) from the Sun over the period of the July 7, 1966 event. The flare was unusually intense in hard X-rays and in microwave emission. It was also the first known event in which a detectable intensity of relativistic solar electrons was observed in interplanetary space. The time history of X-rays of energy > 80 keV was recorded and was found to be well correlated with the microwave bursts. The dynamic spectrum of the solar radio burst is reproduced. The integral X-ray energy spectrum (80- to 500-keV) of solar X-rays of July 7, 1966 is derived. Also, the best power-law fit to the first three integral levels (80, 136, and 203 keV) as a function of time after background has been removed is shown. The spectral shape, time characteristics, and radio correlation for the July 7, 1966 flare strongly suggest a nonthermal bremsstrahlung origin for the hard X-rays. However, the NRL data for the 1959 events have very different spectral and temporal characteristics. Their data have been interpreted in terms of rapidly cooling isothermal plasma bremsstrahlung.

35. Conner, J. P.; Singer, S.; and Stogsdill, E. E.: Solar X-Ray Measurements. Space Res. VI, 1966, p. 893.

Measurements of solar X-rays (0.5 to 15 \AA) have continued from the Vela satellites of 1963 and 1964. The slowly varying component of X-ray flux from the quiet Sun at solar minimum has been measured for wavelengths less than 20 \AA . Variations of the slowly varying component correlate well with solar activity indices, such as 2800-Mc solar radio flux and with sunspot numbers. Many X-ray bursts, which were usually correlated with flares and also ionospheric disturbances were observed. Peak intensities of strong bursts were found to exceed $0.1 \text{ erg cm}^{-2} \text{ sec}^{-1}$ for wavelengths less than 20 \AA .

36. Culhane, J. L.; Sanford, P. W.; Shaw, M. L.; Pounds, K. A.; and Smith, D.: Preliminary Results of Solar X-Ray Studies with a Proportional Counter Spectrometer on OSO-IV. Astron. J., vol. 73, June 1968, pp. S58-S59.

The authors briefly discuss three X-ray events that took place between October 23, 1967 and December 21, 1967 as viewed from OSO-IV. Three wavelength bands were observed: (1) 1 to 9 \AA (1 to 3 and 3 to 9), (2) 8 to 18 \AA , and (3) 44 to 60 \AA . The daily average X-ray flux in the three wavelength bands studied was correlated in general, but not in detail with the 10.7-cm average flux.

37. Culhane, J. L.; Willmore, A. P.; Pounds, K. A.; and Sanford, P. W.:
Variability of the Solar X-Ray Spectrum below 15 Å.
Space Res. IV, 1964, pp. 741-758.

Over 150 low resolution X-ray spectra obtained during the first 3-week period of satellite Ariel have now been reduced. These measurements, together with those of a series of rocket flights in the period 1959-63, illustrate the variations of the short wavelength "tail" of the solar X-ray spectrum in both intensity and spectral slope, under nonflare and flare-active conditions. Typical nonflare and flare-enhanced spectra are given in the paper. It is shown that the difficulty in describing the measured intensity of nonflare X-rays in this short wavelength band, by the emission from a thermalized coronal plasma, may be removed by consideration of both line and continuum radiations from one or more discrete hot regions in the corona. The X-ray enhancement associated with many chromospheric flares may also be interpreted as the thermal emission of a localized hot region, though the variability in the X-ray emission from one flare to another is quite marked. Three flares are described in detail in the paper, and of these, two appear to be of the "simple" thermal type. In the third flare an unusually rapid enhancement or X-ray "burst" occurs about 20 minutes after the flare commencement. The spectral and time development of this burst are described and the excellent correlation with an impulsive microwave burst and with the onset of the ionospheric effects are noted. The possibility of both microwave and X-ray bursts having a non-thermal origin is discussed.

38. Dicke, R. H.: Scatter-Hole Cameras for X-Rays and Gamma Rays.
Astrophys. J., vol. 153, Aug. 1968, pp. L101-L106.

A random, scatter-hole, pinhole camera is described in the text and is shown to be a very effective way of forming images of a complex system of X-ray sources. A simple statistical trick is used to reduce the multitudinous overlapping images to a single image. Less than 40 detected photons are needed to form an image of a single star.

39. Dolan, J. F.; and Fazio, G. G.: Gamma-Ray Spectrum of the Sun.
Astron. J., vol. 69, 1964, p. 137.

Mechanisms for the production of gamma radiation ($h\nu > 10$ keV) by the Sun are investigated and fluxes at the earth are predicted. The gamma

radiation emitted by the quiet Sun is negligible compared to emission during a solar flare. The most important emission mechanism in the 10-keV to 1-MeV energy region is bremsstrahlung by flare accelerated electrons.

40. Donnelly, R. F.: The X-Ray and Extreme Ultraviolet Radiation of the August 28, 1966 Proton Flare as Deduced from Sudden Ionospheric Disturbance Data. *Sol. Phys.*, vol. 5, 1968, pp. 123-126.

Sudden ionospheric disturbances (SID) associated with the proton solar flare of August 28, 1966 have been analyzed to deduce the flare enhancements of soft X-ray (1 to 100 Å) and extreme ultraviolet (100 to 1030 Å) radiation. The time dependence of this burst agrees closely with the 8800- and 10 700-MHz solar radio bursts, but does not agree with radio bursts at frequencies less than 2800 MHz. The soft X-ray enhancement deduced from ionospheric data peaked about 4 minutes after the extreme ultraviolet (EUV) burst.

41. Dvoryashin, A. S.; Levitskii, L. S.; and Pankratov, A. K.: X-Ray Emission from Flares. *Soviet Astron.-AJ*, vol. 6, Nov.-Dec. 1962, pp. 340-348.

World data on the ionosphere (f_{\min}), radio outbursts on cm wavelengths, and chromospheric flares are used in this paper. The study of the connection between the time characteristics (time of commencement, maximum, and termination) of X-ray and radio emission from flares and characteristics obtained from observations in the optical region of the spectrum show that the time variations of X-rays and radio emission are practically the same. The radiation of the flare in $H\alpha$, however, commences before the other phenomena are observed. From a comparison of the minimum reflection frequencies f_{\min} , registered during ordinary and proton flares, it is found that proton flares produce a considerable increase in X-ray intensity. A strong hardening of the X-ray spectrum of the intense proton flares of March 23, 1958 and July 14, 1959 was detected. On the assumption that additional ionization in ionosphere originates at heights of 60 km, it is concluded that protons with energies up to approximately 1 MeV are generated during the development of intense proton flares.

42. Ellison, M. A.: Solar Flares and Associated Phenomena. Planet. Space Sci., vol. 11, 1963, pp. 597-619.

A review is made of some of the more important papers on solar flares and their associated effects that have been contributed since the beginning of the IGY. Important flares emit X-rays, UV, emission lines in the visible region, radio waves, and a variety of particles. During the 18 months of the IGY, the Sun was kept under observation for about 95 percent of the possible observing hours. Various instruments and techniques were used to acquire the observations. A review of the solar flare X-ray and SID association is presented. The authors state that the particle acceleration in the flare generates the X-ray burst as well as the microwave continuum of type IV. Also discussed are the particle emissions from flares and flare radio emissions. The author briefly describes energy release in proton flares and concludes with a section on flare theories. An extensive bibliography accompanies the paper.

43. Elwert, G: Comparison of Tousey's X-Ray Spectrum of the Sun with Theory. Space Res. VII, 1967, pp. 1287-1295.

Tousey et al. succeeded in taking a high resolution photograph of the solar X-ray spectrum. This spectrum shows a group of lines between 30 and 60 Å, a gap extending to 150 Å, and then dense lines, predominantly originating in the transition layer of the corona. This spectrum is presented and compared with earlier calculations. If one uses the abundance of the elements of Pottasch instead of the abundance distribution used earlier, then at a temperature of 10^6 K one obtains a spectrum with the observed strong lines between 34 Å and 55 Å and the observed absence of strong lines between 55 Å and the line of oxygen at 150 Å. If dielectronic recombination is included in the calculation of the ionization rate, then at 1.6×10^6 K the qualitative intensities of the strong lines are also in agreement with the observations. This new computation of the solar X-ray spectrum is depicted. In conclusion it appears noteworthy that both the spectrum of Tousey et al. and that of Friedman et al. can to a large extent be explained by using the relative abundances of the elements, computed for the upper layers of the Sun's atmosphere, and a temperature of the corona deduced from equal intensity of the red and green lines, corresponding to average conditions in the corona.

44. Elwert, G.: Röntgenstrahlung Koronaler Kondensationen (X-Radiation of Coronal Condensations). Zeitschrift für Astrophysik (J. for Astrophys.), vol. 41, 1956, pp. 67-83 (Translation).

The X-ray emission of coronal condensations is investigated. The model of Waldmeier and Müller is used for the electron density. Temperatures of 6×10^6 K and 3×10^6 K are considered. Below about 30 Å there appears an appreciable increase of the intensity of radiation and a short-wave limit of the spectrum appears at 6 to 7 Å. These results are in good agreement with the observations gained from rocket flights. The ionospheric effects of this radiation are investigated. A mechanism for the production of a radiation between 1 and 2 Å by eruptions is pointed out. X-rays in this range of wavelengths have been postulated by Siedentopf and Friedman as the cause for the ionization of the D-layer in the Mögel-Dellinger effect. A tabular compilation of early rocket flights, dates, and wavelength bands of interest is presented.

45. Elwert, G.: Theory of X-Ray Emission of the Sun. *J. Geophys. Res.*, vol. 66, Feb. 1961, pp. 391-401.

The radiation of the Sun at X-ray wavelengths is a consequence of the high temperature of the emitting layers, namely the corona and the region of transition to the chromosphere. Since the flux is dependent on the electron density, the relative abundance of the elements, and the temperature, the physical state of the radiating gas must first be considered. Physical conditions of the solar corona are reviewed. The cross sections for electronic collisions computed by Schwartz and Zirin for s waves yield an upper limit of $T = 1.3-1.4 \times 10^6$ K. X-ray emission of the corona by f-f and f-b as well as by line emission is discussed. The theoretical results are compared with the observations. An X-ray spectrum of the Sun for August 31, 1959 is presented. The effect of the radiation in the atmosphere of the earth and the intensity distribution across the solar disk is summed up. The emission of the transient region to the chromosphere and of hot spots is considered. Finally the X-ray radiation during a flare is investigated. Some conclusions are drawn from the observations on the physical state of the emitting gas. This paper was originally presented at the Symposium on Solar Emissions and the Interplanetary Medium, which was held in Washington, D. C. on April 27 and 28, 1960.

46. Evans, K.; and Pounds, K. A.: The X-Ray Emission Spectrum of Solar Active Region. *Astrophys. J.*, vol. 152, Apr. 1968, pp. 319-336.

Two slitless Bragg spectrometers were successfully flown on a Skylark rocket (SL 304) from Woomera, South Australia on May 5, 1966 to

measure the solar X-ray emission between 11 and 25 Å. Absolute intensities are presented for 28 identified and 4 unidentified solar X-ray emission lines between 11 and 22 Å in tabular form from the Skylark experiment. It is found that the total line emission exceeds the X-ray continuum by at least a factor of 5, and this is shown to be consistent with an emission model derived from the observed line spectra. Excellent agreement is found between the total flux and a simultaneous observation obtained with a broadband (8- to 20-Å) ion chamber of the NRL SOLRAD satellite series. Of the measured emission lines, those of O VII are distinct, both in their observed profiles and in consideration of the coronal temperatures at which they are efficiently produced. These lines are interpreted as arising principally from the general coronal disk at a temperature between 10^6 and 1.5×10^6 K. In contrast, all the other observed lines show a strong component clearly associated with a coronal active region, and the absolute line intensities are used to derive a model of this region. Good agreement of the calculated and observed spectra of O VIII, Ne, Fe, and Ni is obtained with the bulk of the active region plasma at a temperature of 3×10^6 K. The corresponding value of $N_e^2 V = 1.7 \times 10^{48} \text{ cm}^{-3}$ is consistent both with the nonobservation of a solar continuum below 14 Å and with the separate values of N_e^2 and V obtained for similar active regions from recent broadband X-ray photographs. Element abundances for Ne, Fe, and Ni are determined relative to O and are found to be in good general agreement with values obtained from analyses of solar ultraviolet spectra.

47. Evans, K; Pounds, K. A.; and Culhane, J. L.: X-Ray Emission Line Spectrum of a Coronal Active Region. *Nature*, vol. 214, Apr. 1967, pp. 41-42.

Two slitless Bragg spectrometers were successfully used on a Skylark rocket flight (SL 304) on May 5, 1966 to measure the solar X-ray emission in the 11- to 25-Å band. The crystals were of potassium acid phthalate (KAP), with a lattice constant of 13.3 Å, and photons were detected with thin plastic window proportional counters. The experiment was carried out during a period of relatively quiet solar activity. Wavelengths were determined for the stronger emission lines with an overall precision corresponding to a Bragg angle error not exceeding 5 minutes. The observed "active region" emission lines are listed in tabular form. A comparison with the only previous solar X-ray line spectrum shows all the lines reported there below 20 Å together with additional lines of Fe XVII and new line series of Ne IX and X, Fe XVIII and Ni XIX. The proposed identifications of weak lines in the spectrum have been checked by a consideration of the expected intensity

ratio compared with the well determined strong lines. Ten statistically significant features were not identified.

48. Friedman, H.: Recent Experiments from Rockets and Satellites. *Astron. J.*, vol. 65, June 1960, pp. 264-271.

The author summarizes the results of three active groups studying the solar UV spectrum. These groups are NRL, University of Colorado, and the U.S. Air Force Cambridge Research Center. He also discusses the UV radiation from celestial sources. Rocket experiments succeeded in advancing several areas of UV and X-ray astronomy in 1959. The solar disk was photographed in Lyman α with a resolution of better than 1 minute of arc. Spectrograms were obtained down to wavelengths below the He I and He II resonance lines. Solar X-ray emission coincident with visible flares was mapped from 60 down to 0.2 Å. For the first time a small optical telescope was used for the study of UV emissions in the night sky. It demonstrated the feasibility of UV color mapping of the stars and has given some new clues into the nature of the UV nebulosities surrounding the early stars.

49. Friedman, H.: Rocket Astronomy. *Sci. Am.*, vol. 200, June 1959, pp. 52-59.

The author briefly reviews rocket astronomy as applied to solar X-ray and XUV radiation observations (as of June 1959). The Sun's UV spectrum between 500 and 1800 Å is presented. A brief discussion concerning the absorption of X-ray and UV radiation is given. A UV image of the Sun is shown, as well as some results of UV experiments to determine UV areas on the celestial sphere. Rocket X-ray measurements indicate high temperatures correlated with solar activity.

50. Friedman, H.: Solar Observations Obtained from Vertical Sounding. *Institute of Physics and the Phys. Soc. of London*, vol. 25, 1962, pp. 164-217.

Rocket spectroscopy has mapped the solar spectrum from the ground level cut-off near 3000 Å down to the short wavelength limit of the X-ray region. The spectrum has been photographed to 84 Å and scanned photo-electrically to somewhat shorter wavelengths. Throughout most of the UV the spectrum is known with a resolution of about 0.5 Å. The profile of Lyman α

has been measured with a resolution of 0.03 \AA . In the X-ray region, the spectrum is known only in broad outline from measurements made with narrow-band photometers. Fraunhofer lines disappear near 1500 \AA , beyond which chromospheric and coronal emission lines dominate the spectrum. The strongest lines observed are H Lyman α (1216 \AA) and He II Lyman α (304 \AA). In the X-ray region the total flux (1 to 100 \AA) varied by a factor of 7 over the past solar cycle under quiet conditions and exhibited a progressive hardening with increasing solar activity. From sunspot minimum to maximum the flux in a 2 - to $8\text{-}\text{\AA}$ bandwidth increased several hundred times. At 8 to 18 \AA the increase was a factor of 40 to 60. Solar flares were accompanied by large overall increases, especially enhancements of the shorter wavelengths. Solar disk photographs in H Lyman α and X-rays show that short wavelength emissions are intensified over active regions. In the UV, the intensity from plage areas averages four times the background brightness. In the X-ray spectrum, active regions may be 80 times as bright as the quiet background. A strong correlation exists between X-ray sources and centimeter wave sources. A tabular listing of preliminary X-ray measurements from SR-I and an extensive bibliography conclude the review.

51. Friedman, H.: The Solar XUV Spectrum. *Astron. J.*, vol. 73, June 1968, p. S61.

The author briefly summarizes what has been learned from the satellite and rocket observations of solar X-ray and ultraviolet astronomy. Valuable information has been collected from the series of NRL SOLRAD satellites, the British Ariel satellite, NASA's OGO-1, -2, and -4, the Air Force's OV-1, the USSR Electron 2 and 4, and many rocket flights. From these observations a broad picture of the maximum to minimum variations of the quiet Sun spectrum, the nature of transient variations under quiet conditions, the time-dependent growth and decay of flare spectra, and evidence of the degree of departure from thermal equilibrium under various conditions of solar activity can be developed.

52. Friedman, H.: Ultraviolet and X-Rays from the Sun. *Ann. Rev. Astron. Astrophys.*, vol. 1, 1963, pp. 59-96.

The author presents a general review of solar X-ray and XUV astronomy as observed by rockets and satellites through November 1962. The solar spectrum over various wavelength ranges is shown. Various methods and techniques of solar X-ray astronomy are discussed. Tables presented

summarize the present state of knowledge regarding the existence of all ions of atomic numbers 1 to 16 and of Fe in the solar chromosphere and corona. Also to summarize the best available flux data on solar UV emission lines from about 1900 Å down to 100 Å is summarized. A discussion of the coronal X-ray spectrum, solar flares and X-ray emission is made. Pinhole camera photographs of the Sun are also presented. An extensive bibliography concludes the review.

53. Friedman, H.; Lichtman, S. W.; and Byram, E. T.: Photon Counter Measurements of Solar X-Rays and Extreme Ultraviolet Light. *Phys. Rev.*, vol. 83, Sept. 1951, pp. 1025-1030.

Data telemetered continuously from photon counters aboard a rocket (V-2, No. 49), which rose to 150 km on September 29, 1949, showed solar 8-Å X-rays above 87 km, and UV light around 1200 and 1500 Å above 70 and 95 km, respectively. The rocket was fired from White Sands, New Mexico during a period of no unusual solar activity. The payload consisted of six photon counter tubes contained in two pressurized boxes, comprising in effect photon counter spectroscopes. In addition to the counter tubes, each box also contained one control tube, sensitive only to cosmic rays, and one photocell for determining the roll orientation of the rocket with respect to the Sun. Each tube responded to a relatively narrow portion of the spectrum in one of four bands covering 0 to 10, 1100 to 1350, 1425 to 1650, and 1725 to 2100 Å. The results indicated that solar soft X-rays are important in E-layer ionization (advanced earlier by Hulburt, and later by Bates and Hoyle), that Lyman α radiation of hydrogen penetrates well below E-layer, and that molecular oxygen is rapidly changed to atomic oxygen above 100 km.

54. Fritz, G.; Kreplin, R. W.; Meekins, J. F.; Unzicker, A. E. and Friedman, H.: Solar X-Ray Spectrum from 1.9 to 25 Å. *Astrophys. J.*, vol. 148, June 1967, pp. L133-L140.

An Aerobee rocket was launched by the NRL from White Sands, New Mexico on October 4, 1966 to observe the solar X-ray spectrum. The rocket carried Bragg crystal spectrometers and an array of pinhole cameras. This is a preliminary report of the main features of the X-ray spectrum and tentative identifications of the emission lines recorded by two crystal spectrometers, using EDDT and KAP crystals to cover the wavelength ranges 1.7 to 8.3 and 5 to 25 Å, respectively. Intensities were measured by Geiger counters. An X-ray photograph taken with one of the pinhole cameras is shown.

There were two main sources on the solar disk — one near each limb almost diametrically opposed. The Sun was at a low level of activity; no solar flares or enhanced microwave radio emission were reported during the flight. No collimators were used to restrict the field of view so that the spectrometers acted as "objective grating" instruments. Each discrete source on the Sun produced its own spectrum. Rapid relative variations in the emission spectra of the individual active regions were revealed. No strong emission was produced by the central plages on the ascent scan, but emission lines did flash sporadically from the central plages on the descent scan. The wavelengths of the peaks measured by the spectrometers, together with identifications, are listed in tables. All the ions found by Blake et al. (1965) and also by Evans et al. (1967) were found in this spectrum. The presence of Fe XVII and XVIII, Ne IX and X, O VIII, N VII, and Al XII indicates ionization temperatures ranging from 2×10^6 K to 4×10^6 K. The presence of Si XIII signifies temperatures greater than 7×10^6 K, according to Tucker and Gould (1966).

55. Giacconi, R.; Reidy, W. P.; Zehnpfennig, T.; Lindsay, J. C.; and Muney, W. S.: Solar X-Ray Images Obtained Using Grazing Incidence Optics. *Astrophys. J.*, vol. 142, 1965, pp. 1274-1278.

Three X-ray grazing-incidence telescopes with cameras were flown by Aerobee rocket from White Sands, New Mexico on March 17, 1965. The resolution of the telescopes had been measured in visible light to be better than 20 seconds of arc and with 8-Å radiation to better than 1 minute of arc. Useful solar photographs were obtained in the spectral region 8 to 12 Å. A plage-associated X-ray region with a spectral distribution significantly harder than that associated with the coronal X-ray emission and a significant latitude dependence in the coronal X-ray emission were observed. Also, the photographs showed large regions of low X-ray intensity distributed across the solar disk. The solar X-ray photographs are shown.

56. Giacconi, R.; and Rossi, B.: A 'Telescope' for Soft X-Ray Astronomy. *J. Geophys. Res.*, vol. 65, Feb. 1960, pp. 773-775.

The authors describe the design of an X-ray 'telescope' and analyze some of its characteristics. The instrument consists of one or several parabolic mirrors on which the X-rays impinging at nearly grazing angles undergo total reflection. In the actual design of the instrument it is necessary to consider two limitations: (1) for each wavelength, and for each material, the angle of the incident rays with the reflecting surface must be smaller than

a certain value, θ , so that the reflection coefficient will be of order of unity; (2) in general, the design of the satellite will impose an upper limit to the distance, ℓ , between the detector and the outer edge of the mirror. The problem is to obtain the maximum area of collection consistent with these limitations. The prime advantages of the instrument are the large area of collection, the high resolution, and the large signal-to-noise ratio. Among the obvious applications are a detailed analysis of the distribution of X-ray sources on the solar disk and the solar corona, and a search for weak X-ray sources.

57. Goldberg, L.: Solar Experiments. *Astron. J.*, vol. 65, 1960, pp. 274-277.

Owing to the well-known negative temperature gradient in the solar atmosphere, the solar chromosphere and corona emit strongly in the far UV and X-ray regions of the spectrum, as has already been revealed by observations from rockets. The highly energetic events connected with solar flares also result in strong emissions at very short wavelengths. Hence, solar experiments from satellites will have high priority in the astronomy space program. Design work has been begun on the development of solar instrumentation to be flown in a series of vehicles with progressively larger payloads. The first experiment is being designed for a vehicle that can carry instruments weighing up to about 100 lb and that will be stabilized with a pointing accuracy of a few arc minutes. Two scanning spectrometers will be employed, one covering the spectral region from 1600 to 500 Å and the other from 600 to 75 Å. The resolving power would be about 1 Å, and the spectrometers would have a combined weight of about 45 lb. It is also hoped that some type of X-ray imaging device will be flown in the first vehicle. Plans are being developed for the installation of a small solar observatory with a variety of instruments totaling about 600 or 700 lb, exclusive of stabilization gear, power supply and storage, etc. The instruments would include a high-dispersion spectrometer operating in the region from 3000 to 75 Å, one or more spectroheliometers to register images of the Sun and Lyman α and other monochromatic radiations, an X-ray telescope and spectrometer, and equipment for the observation of low-frequency radio emission from the Sun. Finally, it is pointed out that a number of important problems in solar physics can be solved better by observations from balloons rather than from satellites. These include studies of the hydrodynamic and magnetic properties of the solar photosphere, and observation of the infrared solar spectrum.

58. Goldberg, L.: Ultraviolet and X-Rays from the Sun. *Ann. Rev. Astron. Astrophys.*, vol. 5, 1967, pp. 279-324.

The author presents a general review of solar X-ray and XUV astronomy. The latest observational results (as of January 1967) and a discussion of the current status of certain of the more interesting problems of interpretation of X-ray and XUV spectra are presented. A table summarizes the principal observations of the solar XUV spectrum performed by rockets and the OSO-1 spacecraft since 1962. The discussion is broken into three major areas: (1) solar XUV spectrum, (2) solar imaging, and (3) solar monitoring. The solar spectrum over various wavelength ranges is shown. Interpretation of spectra and abundance determination is discussed as well as the various techniques used in solar X-ray astronomy. Solar images at various wavelengths is presented. A discussion of X-ray flares, nonflare X-ray emission, and production mechanisms of X-rays is made. An extensive bibliography is also included.

59. Gregory, B. N.; and Kreplin, R. W.: Observations of Solar X-Ray Activity below 20 Angstroms. *J. Geophys. Res.*, vol. 72, Oct. 1967, pp. 4815-4820.

Observations of solar X-ray emission in the wavelength region of 1 to 8 and 8 to 16 Å have been made by Explorer 30 (NRL SOLRAD 8) (1965-93A), a small, spin-stabilized satellite. The satellite is equipped with ion-chambers to monitor solar radiation in the following wavelength regions: 1 to 8 Å, 1 to 20 Å, 8 to 16 Å, 44 to 60 Å, 1080 to 1350 Å, and 1225 to 1350 Å. In addition, it carries 0.5- to 3-Å and 1- to 8-Å Geiger counter photometers. The dynamic ranges of the X-ray experiments aboard Explorer 30 as well as the ranges of experiments flown on earlier satellites and several levels measured during rocket flights are shown. The efficiency curves of the X-ray detectors are reproduced. The 8- to 20-Å photometer also has a window from 1 to 7 Å, and the 44- to 60-Å photometer has a window from 0 to 20 Å. The analog real-time records from this satellite show slowly varying changes of up to 40 percent in the 1- to 8-Å region with a time scale of 1 or 2 minutes and of 20 percent in the 8- to 16-Å region with a somewhat longer time scale. No fluctuations of more than 5 to 10 percent are observed within a time scale of 1 second, the highest time resolution of the satellite X-ray photometers. Data from OSO-2 and the SOLRAD satellites 1964-O1D and 1965-16D have shown that X-ray flares below 20 Å are often accompanied by no change or an actual decrease in the flux in the 44- to 60-Å region. It now appears that such behavior is characteristic of small flares occurring when the X-ray emission below 20 Å is confined to a fairly small portion of the solar disk; that is, when only one or two small plages are visible on the Sun. Data from SOLRAD 8 taken during periods of generally increased activity show that X-ray flares below 20 Å may be accompanied by significant increases in 44- to 60-Å

emission. The decrease in 44- to 60-Å emission observed during several small flares by earlier satellites was interpreted to be the result of flare heating confined to an X-ray plage that is already at a temperature of about 2.8×10^6 K. Also, the volume of the flares was believed to be a significant portion of the total volume of the X-ray plage, a condition to be expected only during periods of low activity. The present data, however, indicate that flare heating is not always confined to such localized areas, and that during some flares, large, previously cooler regions of the chromosphere or corona are heated to the point that they contribute significantly to the background plage emission in the 44- to 60-Å wavelength region.

60. Gursky, H.; and Zehnpfennig, T.: An Image-Forming Slitless Spectrometer for Soft X-Ray Astronomy. *Appl. Opt.*, vol. 5, May 1966, pp. 875-876.

The authors describe the design of a slitless spectrometer that can produce high resolution spectral data, simultaneously yielding high-resolution spatial data. The instrument consists of the combination of a soft X-ray transmission grating and an image forming soft X-ray telescope, the grating being positioned in front of the entrance aperture of the telescope in order to disperse a portion of the incident radiation before it is collected by the telescope. The advantages of this instrument are a large collecting area, a favorable ratio of collecting area to detector area, and the capability of examining a source at high angular resolution, and simultaneously, at all wavelengths in a given range. It can be used in a spectral region where application of Bragg crystal spectrometers is difficult because of the size of available crystal lattice constants. Also, it does not share with the Bragg spectrometer the difficulty of measuring continuous spectra.

61. Hall, L. A.; Schweizer, W.; Heroux, L.; and Hinteregger, H. E.: Solar XUV Spectrum of March, 1964. *Astrophys. J.*, vol. 142, 1965, pp. 13-15.

The authors describe the results from a rocket experiment on March 30, 1964 from White Sands, New Mexico. The Aerobee rocket carried monochromators with photoelectric detection of the radiation dispersed by gratings in grazing incidence. The grating was ruled on a gold-coated surface, and the detector cathode was coated with LiF. The solar spectrum covered was from 312 to 55 Å. The instrumentation was similar to earlier launches of AFCRL. The main features of the observations of May 2, 1963, reported previously, were confirmed except for an apparently real decrease of the Fe XV (284 Å) line intensity.

62. Harries, J. R.: Impulsive X-Ray Emission by the Sun. Astron. Soc. of Australia, Proceedings, vol. 1, Nov. 1967, Accession #A68-18308, pp. 51-52.

Measurements of solar X-ray bursts have been observed by a xenon-methane filled proportional counter on the satellite IMP-F. The X-ray threshold is in the vicinity of 4 keV; for electrons it is about 80 keV, and for protons it is 2.1 MeV. The charged particle and X-ray background is found to be isotropic most of the time. The solar X-ray flux is observed to consist of impulsive bursts of X-rays with a time scale of about 1 hour superimposed on a slowly varying X-ray flux with a time scale of about 3 days. Figures are shown comparing X-ray bursts and radio emission. The background shows no variation, and the radio burst shows a close agreement with X-ray burst. During very active periods, many X-ray bursts occur together. Although the X-ray bursts, the radio bursts, and the optical flares are obviously related, the correspondence is not perfect.

63. Hindley, K.: The Unsettled Sun. New Scientist, vol. 39, Aug. 1968, pp. 228-231.

The author reviews the flare of July 9, 1968 and briefly discusses some of the terrestrial effects. He reviews the discovery of sunspots and how the 11-year solar cycle was determined. The yearly average Wolf Sunspot Numbers from 1750 to the present is shown. The solar flare is described schematically.

64. Hinteregger, H. E.; Hall, L. A.; and Schweizer, W.: Solar XUV-Spectrum from 310 Å to 55 Å. Astrophys. J., vol. 140, 1964, pp. 319-327.

A grazing incidence grating monochromator (AFCRL) with photoelectric detection carried by an Aerobee rocket to an altitude of 234 km on May 2, 1963 recorded the solar XUV-spectrum from 310 to 55 Å. For wavelengths from 310 to 250 Å, the new data agree rather well with earlier values from 1960-62 experiments covering the 1300- to 250-Å region; for wavelengths from 250 to 55 Å the new data represent a substantial improvement in both spectral resolution and background suppression beyond the experimental state of photoelectric XUV spectrophotometry reflected in earlier space experiments. The spectra of the flight is reproduced.

65. Holt, S. S.; and Cline, T. L.: On the Generation of Synchrotron and X-Ray Emission from Electrons with Energy below mc^2 in Solar Flares. *Astrophys. J.*, vol. 154, Dec. 1968, pp. 1027-1038.

An attempt is made to reconcile a single source of electrons with both the hard X-ray and microwave radio emission observed at the peak of the solar flare of July 7, 1966. The spectral and temporal characteristics of the X-ray emission are used to determine the total number of electrons involved in the emission, as well as the shape of the generating electron spectrum. This is the first instance in which a generating electron spectrum has been directly inferred from experimental data. The differential X-ray spectrum at flare maximum for July 7, 1966 is shown. The bulk of the microwave emission originates from electrons with energies below mc^2 . Both the observed X-radiation and synchrotron radiation can be explained in terms of the same electron source if the source region is high in the chromosphere, where the maximum field may be as high as 1000 gauss.

66. House, L. L.: Theoretical Wavelengths for X-ray $K\alpha$ -Type Lines in the Spectra of Ionized Atoms (Carbon to Copper). *Astrophys. J.*, vol. 154, Dec. 1968, pp. 1172-1173.

Recent solar rocket observations by NRL have led to the suggestion that certain lines in the X-ray spectrum originate as characteristic $K\alpha$ -type X-ray transitions in atoms in which some of the outer shielding electrons have been removed. Theoretical calculations that should aid in the identification problem are presented.

67. Hudson, H. S.; Schwartz, D. A.; and Peterson, L. E.: Hard Solar X-Ray Bursts Observed by OSO-III. *Astron. J.*, vol. 73, June 1968, p. S64.

A description of some of the results observed by OSO-III of the solar X-ray spectrum above 7.7 keV since March 9, 1967 is presented. The occurrence of solar X-ray bursts is well correlated with the occurrence of 2800-MHz solar radio bursts. Although solar X-ray bursts are very frequent, they are only partially correlated with flares and radio-wave emission. Sixty-five percent of the solar X-ray bursts were found to coincide with flares; on the other hand, about 85 percent of all important flares produced detectable X-ray emission. Most solar X-ray bursts were found to exhibit a simple fast-rise (nonthermal), slow-decay time structure (thermal). Rise and fall times were highly variable, as were the peak energy flux ranges of the bursts.

68. Jones, B. B.; Freeman, F. F.; and Wilson R.: XUV and Soft X-Ray Spectra of the Sun. *Nature*, vol. 219, July 1968, pp. 252-254.

X-ray and XUV spectra of the Sun were observed by a Skylark rocket launched from Woomera, South Australia on March 20, 1968. Included in the rocket experimental payload were two grazing incidence spectrographs. The wavelength ranges covered by the spectrographs were (1) approximately 12- to 70 Å and (2) approximately 140- to 500-Å. Both instruments carried thin Al filters over the entrance slits to exclude the intense longer UV and visible wavelength radiation. X-ray and XUV pinhole camera photographs were obtained and showed a belt of active regions extending across the north and south equatorial zones of the Sun. The soft X-ray spectrum and XUV spectrum of the total Sun is presented as recorded by the film. For the X-ray spectrum, an exposure time of 240 seconds on Kodak Pathé S.C-7 film at an altitude of 140 to 217 km was made. For the XUV spectrum, the same film was used, but an exposure time of approximately 200 seconds was required. The altitude was between 170 and 217 km. Numerous emission lines were found, and the spectrum is in good agreement with the findings of previous investigators. The spectral accuracy is ± 0.04 Å for most of the spectrum. Photometric reduction is under way and will be published in the future. The intensity of some of the more prominent lines has been calculated, and a coronal temperature of $2.1 \pm 0.5 \times 10^6$ K has been observed. This temperature is also in agreement with previous measurements. The presence of very highly ionized species in the soft X-ray spectrum indicates that higher temperatures can occur in the active region.

69. Kawabata, K.: The Relationship between Post-Burst Increases of Solar Microwave Radiation and Sudden Ionospheric Disturbances. *Rep. Ionos. Space Res. Japan*, vol. 14, 1960, pp. 405-426.

The purpose of the present paper is to find the astronomical evidence to support the idea that very hot condensations exist within the solar corona. In the first part of the paper, the author makes a statistical study of the relationship between SID and post-burst increases. In the second part of the paper, the author investigates the spectra of some post-burst increases so that the temperature and density of the very hot condensation will be obtained. From these investigations it follows that the post-burst increases as well as the X-rays responsible for SID are emitted within the same very hot condensation. The physical connection between the solar flare and very hot condensation is also briefly discussed. Various graphical representations of flare events and various spectra are shown. In conclusion, the statistical investigation

concerning the relation between SID and post-burst increases suggests that SID are more likely to be associated with a post-burst increase rather than with a microwave outburst. It seems that only those microwave outbursts which give rise to the post-burst increases are also able to cause SID. Investigation of the excess flux of post-burst increase shows that a part of the coronal condensation is heated to a temperature of 10^7 to 10^8 ° K. Such a very hot condensation may emit the X-rays that may be responsible for the SID. The calculated intensity of the X-rays is in good agreement with the rocket observation by Friedman et al. during the solar flare. The present investigations support the X-ray theory of SID. The degrees of magnitude of the total energy released and stored in a solar flare and in a very hot condensation are roughly checked. It is suggested that the primary energy release of a flare-associated phenomena takes place in the solar corona and that the solar flare may be generated by heat conducted from a very hot condensation in the solar corona.

70. Korchak, A. A.: Possible Mechanisms for Generating Hard X-Rays in Solar Flares. *Soviet Astron.-AJ*, vol, 11, Sept. - Oct., 1967, pp. 258-263.

To explain the nonthermal X-rays that have been detected in solar flares, three possible radiation mechanisms have been discussed in the literature: bremsstrahlung, synchrotron, and inverse-Compton. A comparison is made between the spectral radiant power of bremsstrahlung and synchrotron and inverse-Compton radiation in this article. The region of the X-ray spectrum in which each mechanism will predominate is determined, depending on the physical conditions in the radiating region and the behavior of the accelerated-electron energy spectrum. If the electrons have a power spectrum extending with constant slope into the region $E_k \leq 10^6$ eV, bremsstrahlung will predominate throughout the X-ray region $E_\gamma \geq 1$ keV. In solar flares, inverse-Compton radiation can be dominant only if certain restrictive conditions are satisfied; thus inverse-Compton radiation can hardly be a universal mechanism for all flares. A brief discussion concerning polarization observations concludes the paper.

71. Kreplin, R. W.: Solar X-Rays. *Annales De Géophysique*, vol. 17, Apr. - June 1961, pp. 151-161.

Over the past 11 years and especially during the IGY and IGC the NRL conducted rocket-borne experiments in which solar X-ray radiation was measured both during quiet periods and periods of intense solar activity. These measurements were made using ion chamber, photon counter, and

scintillation counter techniques and covered the following wavelength ranges: 2- to 8-Å, 8- to 20-Å, 44- to 60-Å, 2- to 20-keV, and 20- to 200-keV. The results of these measurements have revealed increases of X-ray radiation from sunspot minimum to sunspot maximum which correlate with the increase of E-region critical frequencies and with coronal green line intensities over the same period. Measurements made during solar flares have shown large increases in X-ray flux as well as a "hardening" of the X-ray spectrum at these times. The solar eclipse experiment of October 12, 1958 helped to isolate the sources of X-rays on the solar disk and also indicated that the residual coronal emission could account for the presence of E-region ionization during totality. An X-ray picture of the Sun made with a pinhole camera in 1960 showed a close correlation with the Ca K line plage pictures made on the same day. These two experiments revealed that most of the solar X-ray radiation came from active regions rather than from a uniform corona. A table presenting a comparison of the observed X-ray intensities over a portion of the recent solar cycle is given. A progressive increase in X-ray intensity from the period of minimum solar activity in 1953 to the maximum measured in 1959 is noted. A similar increase is observed in the 8- to 20-Å intensity measurements and at shorter wavelengths. From these data one can conclude that the spectral distribution of X-ray emission from the Sun becomes harder with increasing solar activity. A table showing the characteristics of the X-ray detectors used in the IGC solar flare experiment is presented. A map giving the appearance of the solar disk on October 12, 1958 is shown. The method used for calculating X-ray flux from the detector response is outlined. This communication was originally presented at the Colloquium of Aeronomy (Copenhagen, July 1960) held under the auspices of the Committee on High Atmosphere of the International Association of Geomagnetism and Aeronomy.

72. Kreplin, R. W.; Chubb, T. A.; and Friedman, H.: X-Ray and Lyman-Alpha Emission from the Sun as Measured from the NRL SR-1 Satellite. *J. Geophys. Res.*, vol. 67, June 1962, pp. 2231-2253.

This paper describes the principal scientific results over the period June 22 through November 1, 1960 of the SR-1 satellite, which was instrumented for solar X-ray and UV emission. The monitoring system consisted of a UV photometer (1050 to 1350 Å), an X-ray photometer (2 to 8 Å), and a visible light aspect system using a vacuum photocell. A table listing the main design parameters of the two photocells and their spectral response characteristics are shown. A photograph of the SR-1 satellite showing the location of the instrumentation is given. The method used for calculating the solar X-ray flux is discussed. The X-ray events seen by the SR-1 satellite are listed in a table. This table includes the times of all the records on which X-ray signals

were seen. Another table summarizes the major events seen by SR-1. Various graphs and charts showing the intensities of the X-ray flux, Lyman α flux and the noise are included. Measurements made from SR-1 confirm the hypothesis that solar X-rays are the cause of flare SID events, and that variations in solar Lyman α are not geophysically significant. Results also indicate that active prominence regions, bright surges on the limb, and certain limb flares have the same X-ray characteristics as major disk flares. SID phenomena occur when the solar X-ray flux below 8 Å exceeds 2×10^{-3} erg cm⁻² sec⁻¹ as measured above the earth's atmosphere. Solar X-ray flares can change significantly in a time scale of the order of 1 minute. Long-duration X-ray events of moderate intensity can accompany rising limb prominences.

73. Kreplin, R. W.; and Gregory, B. N.: Solar X-Ray Monitoring during the IQSY. Space Res. VI, 1966, pp. 1011-1021.

Results from NRL satellite 1964-O1D for the period January 1964 to March 1965 are presented. The satellite carried X-ray band sensitive photometers to measure radiation in the 1- to 8-, 8- to 12-, and 44- to 60-Å regions. An aspect sensor was also included to allow the photometer signals to be corrected for the time varying angle between the Sun and the X-ray photometers' normal direction. This correction was required in developing the time history of solar X-ray emission over the experiment lifetime. The spectral response of the 44- to 60-Å photometer is shown. Real time data was transmitted continuously and recordings of the transmissions were made whenever the satellite was in range of a telemetry station. The plot of daily flux averages appears in graphical form. The daily averages show a broad minimum in 44- to 60-Å radiation in the months of May, June, and July 1964. In this same period there were no observations of 8- to 12-Å flux greater than the threshold for detection. After July the X-ray emission from the Sun began increasing and by October, 8- to 12-Å signals were observed whenever the photometer viewed the Sun. The X-ray flux shows a small peak in July, about the 18th. It decreases on the 19th, 20th, and 21st, reaching about 0.015 erg cm⁻² sec⁻¹ on the 22nd. No observations could be made from the 23rd to the 27th of July because the precession of the satellite produced an aspect angle greater than 35 degrees. On the 28th the flux had risen to 0.02 erg cm⁻² sec⁻¹ and it continued to rise during the next week. From the X-ray measurements the authors conclude that solar minimum occurred during the months of May, June, and July 1964 with the lowest flux values probably occurring between July 23 and 27. These observations of solar minimum are in agreement with measurements of 2800-Mc solar radio emission and with the measurement of plage areas and brightness made by the McMath-Hulbert Observatory. Ca plage photographs are reproduced for this same period at 2-day intervals. Also

monitoring the solar X-ray emission was OSO-II. It provided continuous monitoring from February 3, 1965 through the first week of March 1965. The experiment used three Geiger counter photometers to monitor X-ray radiation in the 1- to 8-, 8- to 20-, and 44- to 60-Å bands, plus a fourth counter to measure background caused by charged particles. Another in the series of NRL solar X-ray monitoring satellites (1965-16D) was launched in early March 1965. The instrumentation was almost identical to the 1964-01D satellite except that: (1) a photometer was added to monitor X-ray emission in the 0.5- to 3-Å band, and (2) the sensitivity of the amplifier employed in the 8- to 12- and 8- to 14-Å experiments was increased to provide on-scale readings of the 8- to 12- and 8- to 20-Å flux. All indications are that solar minimum did occur in mid-1964. The paper concludes with a discussion of the two X-ray flares of April 15 and February 8, 1965. Various graphs showing the X-ray flux in the different bands versus time are presented.

74. Kundu, M. R.: Bursts of Centimeter-Wave Emission and the Region of Origin of X-Rays from Solar Flares. *J. Geophys. Res.*, vol. 66, Dec. 1961, pp. 4308-4312.

The author briefly reviews some of the work by different investigators concerning X-ray bursts and associated phenomena and also mechanisms for production of X-rays. The author has examined the solar radio bursts observed in different meter- and centimeter-wave frequency ranges simultaneously with the X-rays directly measured by balloons and rockets. The details of the observed X-rays and the associated radio bursts are listed in a table. A discussion then follows from the table concerning the various correlations of X-ray bursts with other phenomena. It appears from this table that during all seven cases of flare X-rays observed by balloons and rockets, there were simultaneous centimeter bursts, whereas during only three cases were there meter-wave bursts. Of these three cases, in only one was there a strong group of type III bursts simultaneous with X-rays. In three of the four cases where X-ray maxima were observed, the time of maxima agreed precisely with the peaks of centimeter-wave emission. In the fourth case, the maximum occurred during the 6-minute duration of the centimeter-wavelength burst. Also in one case the X-ray event agrees even in fine structure detail with the centimeter-wave burst, with the ratio of X-ray and centimeter-wavelength intensities nearly constant. The author concludes that solar flare X-ray bursts are intimately associated with centimeter-wave bursts from the Sun, while the relation with type III bursts is much looser. This result provides strong evidence that flare X-rays of energy greater than 20 keV are generated not in the higher levels of the corona, but rather in the region of origin of emission of centimeter-wave bursts; i. e., within about 10 000 to 20 000 km above the photosphere as determined by interferometric and eclipse observations.

75. Kundu, M. R.: Centimeter-Wave Radio and X-Ray Emission from the Sun. Space Sci. Rev., vol. 2, 1963, pp. 438-469.

The generation of solar radio waves on centimeter wavelengths appears to be closely associated with the production of X-rays during both quiet and disturbed periods of the Sun. The theory of solar X-rays shows that the temperature of the corona as deduced, among other methods, from radio observations can adequately account for the quiet X-radiation from the Sun. The dense hot regions (sources of slowly varying component on centimeter and decimeter waves) can be identified with the localized regions of X-radiation of increased intensity and of higher quantum energy and are consequently the sources of slowly varying X-radiation. Both the quiet and the slowly varying radio and X-ray emissions can be explained by thermal bremsstrahlung mechanism. During solar flares bursts of centimeter-wave radio emission and X-rays of high and low energy X-ray bursts are due to nonthermal bremsstrahlung, while the associated centimeter-wavelength radio bursts can be due to synchrotron radiation of the high-energy electrons. In this review, the author discusses the various relationships existing between solar radio emission and X-radiation. Various spectra diagrams and solar X-ray photographs are shown. A table of X-ray events and associated solar radio bursts is also given.

76. Landini, M.: Determination of the Solar X-Ray Spectrum by Using the Atmospheric Extinction. Sol. Phys., vol. 2, 1967, pp. 106-111.

The author investigates the spectral distribution of the solar radiation in the region from 2 to 20 Å, and its variation with solar activity, using the atmospheric extinction. The measurements were obtained from NRL satellites SOLRAD 7 and 8. Telemetry data were received at Arcetri when the satellites passed into or out of the earth's shadow. The satellites were instrumented with ion chambers for monitoring the solar radiation in the 1- to 8-, 8- to 16-, and 44- to 60-Å bands. Absorption curves for these bands were computed according to the theoretical spectra given by Madelstam for $T_e = 1, 2 \text{ and } 3 \times 10^6 \text{ K}$. The measurements were performed for 4 days: July 5, 6, and 8, 1965 (1965-16-d satellite) and July 23, 1966 (1965-93-a satellite). July 5 and 8 had a low solar activity; July 6 and 23 showed higher activity. The spectral distributions obtained from atmospheric extinction for the above 4 days is given, and a comparison is made between active and quiet days.

77. Landini, M.; Russo, D.; and Tagliaferri, G. L.: Solar X-Ray Emission by the Satellite 1965-16D during the Period from 8 April to 31 July 1965. Space Res. VII, 1967, pp. 1281-1286.

Solar X-ray data obtained by telemetering the NRL 1965-16D satellite from April 8, to July 31, 1965 are presented. NRL satellite 1965-16D, the seventh satellite of the SOLRAD series, was launched from Wallops Island on January 11, 1965 and was equipped with ionization chambers and GM counters sensitive to the soft X-ray radiation. Six chambers were aboard and provided measurements of solar flux in the following bands: 0.5 to 3, 1 to 8, 8 to 12, 8 to 20, 44 to 55, and 44 to 60 Å. The threshold limit at normal incidence was 2×10^{-5} erg cm⁻² sec⁻¹ for the 0.5- to 3-Å chamber and 1×10^{-4} erg cm⁻² sec⁻¹ for the 1- to 8-Å chamber, assuming the spectral shape of a black body with $T = 2 \times 10^6$ K. The threshold limits for the other chambers were: 1×10^{-4} erg cm⁻² sec⁻¹ for the 8- to 12- and 8- to 20-Å chambers and 1×10^{-2} erg cm⁻² sec⁻¹ for the 44- to 60-Å chamber. Daily data of solar flux in the 44- to 60- and 8- to 20-Å bands for the period April 8 to July 31, 1965 are given together with the solar aspect angle. The 44- to 60-Å flux shows a gradual rise from April to July. The 8- to 20-Å flux indicates a much greater variability and sensitivity to the presence of localized activity centers on the Sun. The strong relationship of the 8- to 20-Å flux with the decimeter radioflux is well established. The 2800-Mc/sec radioflux (Ottawa) and the 8- to 20-Å solar emission are plotted against time. For this comparison only data with no flare activity in coincidence were taken into account. For the 8- to 12-Å band a comparison was made between the experimental values and the theoretical ones computed by means of the Stanford spectroheliograms and the theoretical X-ray spectrum proposed by Mandelstam. The theoretical computation procedure is briefly described and the results of this computation for July 1965 are shown. The agreement between the computed and the observed values is rather good except for July 12-16. The solar emission below 8 Å was detectable only during outstanding events, all in coincidence with optical flare activity. A table of outstanding events in the 1- to 8-Å band is included.

78. Landini, M.; Russo, D.; and Tagliaferri, G. L.: Solar X-Ray Flux Measured by the 1964-01 D Solar Radiation Satellite during the I. Q. S. Y. Planet. Space Sci., vol. 15, 1967, pp. 231-237.

This paper discusses the results of telemetered data from NRL Solar Radiation satellite 1964-01 D as recorded at Arcetri Observatory from March 1, 1964 to February 28, 1965. The instrumentation aboard the satellite consisted of three photometers working in the 44- to 60-, 8- to 12-, and 0- to 8-Å bands and a detector to measure the aspect angle. Real-time

telemetry was recorded daily. The report discusses the above wavelength bands in the same order, and concludes with a section concerning optical flare correlations. Solar X-rays (44 to 60 Å) and decimetric radio emission (10.7 cm and 20 cm) are compared and the minimum of solar X-ray activity is determined. This comparison reveals a slowly varying component in the X-ray fluxes, evidently caused by localized activity centers. The observed fluxes in the 8- to 12-Å band are compared with the theoretical values (by the method of Mandelshtam) and the brightness distribution on the disk is discussed. X-ray measurements taken at the same time as optical flares are also examined. Detailed investigations reveal the following results: (a) all associated flares were very small (class 1⁻); (b) the flux in the 8- to 12-Å band seems to be approximately proportional to the corrected area of the optical flare, but the optical information on these areas was not always available, and so the small number of events did not allow the authors to make a significant correlation; (c) no outstanding events were observed in the radio waves and only in a few cases were type III outbursts present; and (d) no sudden ionospheric effect was observed.

79. Landini, M.; Russo, D.; and Tagliaferri, G. L.: Three Solar X-Ray Events Observed during the Quiet-Sun Year 1964. Space Res. VI, 1966, pp. 1041-1047.

In this paper are presented some special events in the X-ray band recorded at Arcetri while telemetering the NRL 1964-1-D satellite during 1964. Satellite 1964-1-D was launched on January 11, 1964 and is instrumented with three ion chambers working in the following spectral bands: 2 to 8 , 8 to 12 , and 44 to 60 Å. A detector sensitive to the red and infrared radiation provides the aspect angle. Real-time telemetry data were monitored daily by the Arcetri station. Many high-value fluxes were recorded, three of which were considered outstanding events. There was one long-lived event, which occurred October 7-10, and two short-lived events, which occurred on June 15 and December 21, respectively. Their relationships with the H α flares and centimetric radio flux are investigated. No geophysical effect was recorded during the events. For the event June 15, 1964 an attempt was made to approximate the spectrum of the X-ray burst in the 5- to 25-Å band. The computed spectrum is in good agreement with a bremsstrahlung emission in a region with $T = 2-3 \times 10^6$ K and electron density $N_e \sim 10^9$ el cm⁻³.

80. Lin, R. P.: Correlations of Solar-Flare Electron Events with Radio and X-Ray Emission from the Sun. Can. J. Phys., vol. 46, 1968, pp. S757-S760.

The > 40 -keV solar-flare electrons observed by IMP-III and Mariner IV satellites are shown to be closely correlated with solar radio and X-ray burst emission. In particular, intense type III radio bursts are observed to accompany solar-electron flares. The energies of the electrons, the total number of electrons, and the size of the electron source at the Sun can be inferred from radio observations. The characteristics of the electrons observed in interplanetary space are consistent with these radio observations. Therefore, these electrons are identified as the exciting agents of the type III emission. Impulsive centimeter-wavelength bursts are believed to be generated by non-thermal bremsstrahlung or synchrotron radiation of energetic electrons released onto the chromosphere. X-ray bursts may also be generated by nonthermal bremsstrahlung of energetic electrons that are ejected into the dense chromosphere. X-ray bursts, as evidenced by the sudden ionospheric effects observed at the earth, also appear to be correlated with electron events. Many optical flares exhibit a flash phase — a sudden intensification and expansion during their development. It has been noted that the radio and X-ray bursts are part of this flash phase of flares. The observations indicate that a striking feature of the flash phase is the production of electrons of 10- to 100-keV energies. A table depicting the correlation of solar phenomena with electron events is included as a summary. This paper was originally presented at the Tenth International Conference on Cosmic Rays, held in Calgary, Canada, June 19-30, 1967, MOD-4.

81. Lindsay, J. C.: Comments on X-Rays Emitted by the Sun. *Annales D'Astrophysique*, vol. 28, 1965, pp. 586-588.

Observations from the first Orbiting Solar Observatory have set an upper limit of 3.40 ± 0.95 photons $\text{cm}^{-2} \text{sec}^{-1}$ for the 20- to 100-keV X-ray flux from the "quiet" Sun. Frost utilized a scintillation counter consisting of a cylindrical NaI(Tl) crystal 0.3 cm high and 2.24 cm in diameter coupled to an RCA C-7151 multiplier-phototube to study 20- to 100-keV solar rays and to determine the upper limit estimate. Eight impulsive and short-lived 20- to 100-keV X-ray bursts were observed that were associated with optical flares and cm radio bursts. The 2- to 8-Å X-ray flux from the quiet Sun was observed to be associated with plage groups on the Sun. The intensity for this 2- to 8-Å X-radiation was found to be quite variable, changes of 5 percent being observed almost hourly. White, utilizing a beryllium window ionization chamber filled with xenon gas, determined this result. The slowly varying component of solar X-ray flux is plotted for the period March 1 through May 15, 1962. White made an effort to correlate the slowly varying component of the solar X-ray flux with the Ca plage data and with 2800-Mc flux and found that plage activity is the major source of nonflare 2- to 8-Å solar X-rays. A microdensitometer trace of the photograph obtained for wavelengths between 8 and 20 Å on

October 15, 1963 is shown in comparison with the solar 9.1-cm radio emission. There is obvious similarity. This communication was originally presented at Symposium No. 23 on Astronomical Observations from Aboard Space Vehicles held at Liège on August 17-20, 1964.

82. Lindsay, J. C.: The Solar Extreme Ultraviolet Radiation (1-400 Å).
Planet. Space Sci., vol. 12, 1964, pp. 379-391.

This article reviews the results learned from previous experiments in the solar EUV. The report is divided into two sections: (1) Solar X-Rays (1 to 10 Å) and (2) Solar Radiation (50 to 400 Å). In the first section, three satellite studies are reviewed. They are Solar Radiation 1 (SR-1) launched June 22, 1960 followed by the first Orbiting Solar Observatory (OSO-1), launched March 7, 1962 and Ariel, launched April 26, 1962. OSO-1 measurements are discussed in more detail than the other two studies. A comparison is made of the slowly varying component of the 10-Å X-ray flux with 2800-Mc radiation and plage activity. Typical transient X-ray events and the 1- to 10-Å X-ray flux observed by OSO-1 for March 7-14, 1962 are shown. SR-1 results have led to the conclusion that if the X-ray flux $\lambda < 8 \text{ Å}$ exceeded $2 \times 10^{-3} \text{ erg cm}^{-2} \text{ sec}^{-1}$, radio fadeout and other SID phenomena occurred simultaneously. In the second section, many graphical comparisons are shown; for example, a typical solar spectrum (170 to 400 Å) from OSO-1, a comparison of two spectra representing "quiet" and "active" Sun, a comparison of the He II Lyman α with ground-based measurements of solar activity, and a comparison of Fe XIV and Fe XVI lines with ground-based measurements of solar activity. The author concludes with a summary of the principal observations discussed. They are as follows: (1) A slowly varying component has been observed in the solar X-ray flux that correlates with the slowly varying component of the 2800-Mc solar radiation and with the plage activity. It is evident that plages are the major source of solar X-rays for relatively quiet Sun conditions. (2) The lowest X-ray flux that has been measured from satellites was for $\lambda < 8 \text{ Å}$, $3.6 \times 10^{-5} \text{ erg cm}^{-2} \text{ sec}^{-1}$; for $\lambda < 11 \text{ Å}$, $1.8 \times 10^{-4} \text{ erg cm}^{-2} \text{ sec}^{-1}$. This may be considered as an upper bound from a "quiet" Sun. (3) When the Sun emits an X-ray flux of $\lambda < 8 \text{ Å}$ in excess of $0.6 \times 10^{-3} \text{ erg cm}^{-2} \text{ sec}^{-1}$ some optical indication of activity is usually observed. If the flux is in excess of $2 \times 10^{-3} \text{ erg cm}^{-2} \text{ sec}^{-1}$, radio fadeout and other SID phenomena occur. (4) Variations of a factor of two in X-ray emission have been observed to occur in the order of 1 second. (5) Active prominences and bright limb sources have been observed to produce X-ray events. (6) The X-ray flux from the Sun is quite variable. Out of several hundred hours of observation only 6 hours were found in which the X-ray flux did not vary by more than 5 percent. (7) The flare associated X-ray spectrum was observed to harden as compared with preflare spectrum. (8) No definite statement can be made

at this time concerning correlation of X-ray events with H α flares since X-ray events have been observed when no H α event was reported although observations were presumably being made. (9) The He II (304 Å) emission is enhanced by a factor of about 33 percent during a period when the Zurich Provisional Relative Sunspot Number increased from zero to a maximum of 94 and the 2800-Mc flux varied from approximately 76 to $125 \times 10^{-22} \text{ Wm}^{-2}/\text{Hz}$. (10) The Fe XV (284 Å) and Fe XVI (335 Å) coronal lines were enhanced during the same period by a factor of approximately four. (11) The enhancements of He II (304 Å) and Fe XV (284 Å) and Fe XVI (335 Å) caused by plage activity were much larger than enhancements caused by flares that occurred during the 3-month interval of the observations. (12) The variations in intensity of the He II (304 Å) and Fe XVI (335 Å) lines represent the extremes observed. If one averages 60 of the reliably observed lines between 171 and 342 Å, the enhancement is between 50 and 80 percent for the time interval March 9-23. (13) Although there appears to be a gross correlation between solar activity indexes (such as 2800-Mc flux) and the He II, Fe XV, and Fe XVI fluxes, there are indications that the relative prominence of the spectral lines may depend upon the age of the center of activity.

83. Lundbak, A.: Solar X-Rays and Related Phenomena. Annales De Géophysique, vol. 24, 1968, pp. 799-805.

An extraordinary high level of solar X-ray activity with several peaks in the 0- to 3- and 0- to 8-Å intervals is characteristic of the period from March 14 to April 13, 1966. It was preceded by a rather quiet period (March 3-12) and was evidently connected with two active regions on the Sun. The magnetic properties of these regions are classified as gamma type (Mt. Wilson System) during some central days for X-ray activity. Further, both of these regions were active sunspot regions during the preceding revolution. For comparison, a period of corresponding high X-ray activity took place in the beginning of July 1966, and again an active sunspot region with gamma type magnetism occurred. Reference is also made to the active period at the end of May 1967. The March X-ray activity followed just after high geomagnetic activity early on March 14 with no sudden commencement, whereas similar geomagnetic activity preceded by sudden commencement occurred on March 23, 1 1/2 to 2 days after the central meridian passage of an active region. More moderate geomagnetic activity took place on April 1 and 2 and also on July 8 and 9. These days were preceded by sudden commencement. The X-ray results in question are due to real-time receipt from the NRL Satellite Explorer 30, mainly at Rude Skov near Copenhagen, and it is estimated that 5 to 10 percent of the X-ray peaks that occurred in the above periods are actually recorded here. It is noteworthy in any case, that the highest peak recorded was contemporary with a very great increase in cosmic

noise absorption (called SCNA), which had its maximum just before 10.00 UT on March 20, 1966. Important SCNA's for three periods with sfc's, flares, and X-ray records are reproduced in tabular form. In conclusion, well established correlation exists between great X-ray bursts from the Sun and some ionospheric effects. Further, great geomagnetic disturbances and displacements of the outer radiation belt are well correlated. Also, the solar X-radiation and geomagnetic disturbance correlation appears to be weak. This paper was originally presented at the IAGA Symposium on Special Events, Saint-Gall Switzerland, October 2, 1967.

84. Machlum, B.; Frank, L. A.; and Van Allen, J. A.: Solar X-Ray Observations by Injun I. State University of Iowa, SUI-64-27, Accession #AD 603 427, July 1964, pp. 1-30.

Injun I satellite, which was launched on July 29, 1961, was to measure solar X-rays ($\lambda < 14 \text{ \AA}$). Calculations are carried out to determine the photon efficiency of the 213 Geiger tube for soft X-rays. The relationship between X-ray energy flux and counting rate of the 213 GM tube is determined. A discussion of the flight results of Injun I follows. A table of observed counting rates for the period June 29 through August 22, 1961 is presented. A comparison of the data to the SR-3 experimental data is given. Several conclusions are determined based on the 36 random observations of the Sun during the period July-August 1961. (a) The "quiet day" solar X-ray flux at 1 A. U. in the wavelength range $\lambda < 14 \text{ \AA}$ is about $1 \times 10^{-2} \text{ erg cm}^{-2} \text{ sec}^{-1}$, a value approximately independent of the assumed black body temperature of the emitting areas of the Sun over the temperature range $0.8 \times 10^6 \text{ K}$. (b) There is clear enhancement of such X-ray flux during visual solar flares by a factor of about 4 during 1 or 1^+ flares and by a factor of about 40 during a 3^+ flare. The highest flux in the region $\lambda < 14 \text{ \AA}$ is $0.04 \text{ erg cm}^{-2} \text{ sec}^{-1}$ during a 3^+ flare on July 20, 1961. The corresponding total flux for an assumed black body temperature of $2 \times 10^6 \text{ K}$ is $0.2 \text{ erg cm}^{-2} \text{ sec}^{-1}$. (c) The time required for the solar X-ray emission to return to quiescent values after a flare of importance 1 is 1 to 2 hours. For more important flares the time is greater.

85. Malitson, H. H.: The Solar Energy Spectrum. Sky and Tel., vol. 29, Mar. 1965, pp. 162-165.

The author reviews the construction of the solar energy spectrum and discusses briefly the various topics — black-body curves, spectral windows, optical windows, millimeter range, radio windows, and the X-ray-UV region. A visual presentation of the solar energy spectrum is presented.

86. Mandel'shtam, S. L.: On X-Ray Radiation of the Quiet Sun. *Annales D'Astrophysique*, vol. 28, 1965, pp. 614-622.

The conditions for production of the solar X-rays are briefly discussed. The comparison of the results of recent calculations and experimental measurements supports the assumption of a thermal origin of the X-ray radiation. In the tail of the solar spectrum below 15 Å, the main contribution comes from the free-bound radiation of electrons and ions of carbon, oxygen, and other elements. The solar X-ray radiation consist of a quasi-stable component produced in undisturbed coronal regions and a slowly varying component generated in the active regions of the corona. A table showing the spectral energy distribution in the 2- to 20-Å region is given. Calculated and experimental values of the solar X-ray fluxes are compared. The energy of bremsstrahlung, recombination and line emission in the 2- to 20-Å region of the solar spectrum is reproduced with the various line identifications. A radiospectro-heliogram of the Sun at 9.1 cm is also shown. This communication was originally presented at Symposium No. 23 on the Astronomical Observations from Aboard Space Vehicles, held at Liège on August 17-20, 1964.

87. Mandel'shtam, S. L.; and Efremov, A. I.: *Issledovaniya Korotkovolnovogo Ul'trafiol'tovogo Izlucheniya Solntsa* (Investigations of Short-Wave Ultraviolet Solar Radiation). *Uspekhi Fizicheskikh Nauk* (Advances in Physical Sciences), vol. LXIII, 1957, pp. 163-180 (pp. 218-242) (Translation).

The authors review the experimental and theoretical work on investigations of the short-wave radiations of the Sun. Their discussion covers four main topics: (1) the radiation of the photosphere, (2) chromosphere radiation, (3) corona radiation, and (4) variations and experiments with the aid of artificial earth satellites. In the first section the authors give the basic results of the Clearman (1953) experiment concerning the identification of lines in the 2285- to 3000-Å region. A comparison between the theoretical and experimental results produced from the work of De Jager (1955) in the region of 2000- to 3000-Å is given. In the second section the authors review the experiments carried out to determine chromospheric radiation in the 1000- to 5000-Å range. Discussion of Lyman α radiation is the main subtopic of this section. In the third section the authors discuss two flights of NRL rockets in 1953. They give the results of measurements obtained during six rocket flights in tabular form. A correlation is observed between the radiation intensity in the 0- to 20-Å region and the intensity of the lines Fe XIV and Ni XV. The author also discusses the results of calculations made by Elwert (1954). Elwert defined the ionization state of the atoms of elements which can exist in the conditions of the corona. Further, Elwert calculated

approximate values of the wavelengths of their resonance lines. These data were compared with the experimental wavelength values available for some ions, and the values were corrected. All these data appear in tabular form. Later, Elwert calculated the intensities of these lines. The results of these calculations are given. Examination of these data show that the line spectrum radiation plays a basic role in the radiation of the corona. The last section closes out the report and mentions several experiments that may be fruitful for the understanding of the chromosphere and corona.

88. Mandel'stam, S. L.: Studies of Shortward Solar Radiation in the U. S. S. R., Appl. Opts., vol. 6, Nov. 1967, pp. 1834-1844.

A history is presented of measurements of solar vacuum UV and soft X-ray radiation made by rocket and satellite-borne instruments in the U. S. S. R.. The origin and mechanism of the production of solar X-rays are discussed. The author separates his discussion into two sections: (1) studies of shortward ultraviolet solar radiation (100 to 3000 Å) and (2) studies of X-ray solar radiation (< 100 Å). The spectrograms confirm that the chief agent in the earth's atmosphere that absorbs UV solar radiation below 3000 Å is ozone. The results obtained in the U. S. S. R., U. S. A., and Great Britain are in good mutual agreement. Comparison of these data indicate the following conclusions: (a) The flux of X-radiation remains practically constant during a period on the order of 1 day under quiet Sun conditions. (b) During a longer period, the intensity of radiation in the region $\lambda < 10 \text{ Å}$, also in the absence of flares, may change by several orders of magnitude, in the region of 10 to 20 Å by a factor of 10 and in the region of 40 to 100 Å by a factor of between 2 and 3. (c) During a still longer period of time (several years), the variation of X-radiation flux may be still more considerable, and during the 11-year solar cycle the radiation flux in the absence of flares may vary in order of magnitude within the following limits: $\lambda \leq 10 \text{ Å} \sim 1 \times 10^{-5} \text{ erg cm}^{-2} \text{ sec}^{-1}$ to $\sim 2-3 \times 10^{-3} \text{ erg cm}^{-2} \text{ sec}^{-1}$, $\lambda \sim 10-20 \text{ Å} \sim 1 \times 10^{-4} \text{ erg cm}^{-2} \text{ sec}^{-1}$ to $\sim 1-2 \times 10^{-2} \text{ erg cm}^{-2} \text{ sec}^{-1}$, $\lambda \sim 40-60 \text{ Å} \sim 1 \times 10^{-2} \text{ erg cm}^{-2} \text{ sec}^{-1}$ to $\sim 5 \times 10^{-2} \text{ erg cm}^{-2} \text{ sec}^{-1}$. (d) There is a close correlation between the intensity of X-ray solar radiation and other manifestations of solar activity, such as the radio-frequency solar radiation in the range from a few centimeters to 10-20 cm, the Wolf numbers, etc. X-ray and Ca K photographs of the Sun are compared. Spectral lines observed in the X-ray (9.5 to 33.75 Å) region of the solar spectrum are shown. A schematic spectrum of the Sun in the 2- to 25-Å range is presented. It follows from the calculations and experiments that the X-ray solar radiation has a varying-constant component corresponding to the undisturbed corona, on which is superimposed hotter radiation from the active regions of the corona. The author concludes that studies of the X-ray solar radiation has led him to experiments involving observation of the

X-radiation of the moon. A brief discussion of these lunar fluorescence X-rays completes the report. A lengthy bibliography is attached to the report.

89. Mandel'stam, S. L.: X-Ray Emission of the Sun. Space Sci. Rev., vol. 4, 1965, pp. 587-665.

The author presents a general, comprehensive review of solar X-radiation from a quiet Sun as well as an active Sun. In this review the author does not discuss the physics of the solar corona and of the ionosphere nor the experimental measuring techniques. The author includes rocket data and satellite data. A table summarizes the measurements of X-ray flux in the 2- to 10-, 8- to 20-, and 44- to 100-Å regions and launch data and indicates a correlation between the X-ray flux and the 11-year cycle of solar activity. The method of calculation for converting the recorded signal to the energy in the spectral regions given above is described. The author uses the data gathered from the second and third Soviet Spaceship-Satellites, Electron-2, Electron-4, SR-1, SR-3, SR-4, OSO-1, and Ariel-1. Brief discussions of the above satellites are given. Various X-ray photographs of the Sun are presented. A discussion of regions of preferential generation of X-rays in the solar corona resulted in the conclusion that some regions of enhanced X-ray emission have angular dimensions of the order of 1 minute or less. The dimensions of these regions are smaller in the 8- to 15-Å interval by a factor of 2 than in the 44- to 60-Å range. A table of lines in the coronal spectrum between 13 and 25 Å is presented. Tables of solar X-rays during flares are given. The X-ray flux measurements of SR-1 (2 to 8 Å) and Electron-2 (2 to 10 Å and 8 to 18 Å) during flares are included. The data shows that during flares there is a shift towards shorter wavelengths of the X-radiation. There is also an increase in the flux for $\lambda \leq 3$ to 5 Å. The author presents a section comparing theory and experimental data. Degrees of ionization and absolute ion concentrations are shown; the energy distribution between 2 and 20 Å is given; a table of principal lines and their flux for $\lambda < 25$ Å is presented; the relative contribution of the various processes to the X-ray intensity is included; and the calculated and experimental values of the X-ray lines of the Sun are compared. Also shown is a table giving the spectral energy distribution between 20 and 100 Å. The author concludes with a resume and conclusion section. For $\lambda \leq 15$ -26 Å, the spectrum is mainly continuous and is due to recombination emission by the ions of carbon, nitrogen, oxygen, and other elements in the corona. Between 20 and 100 Å the main contribution is due to the line spectrum of these ions and to the continuous bremsstrahlung and recombination emission resulting from the interaction of coronal electrons with hydrogen and helium ions. The X-ray emission appears to be divided into a quasi-stable component emitted by undisturbed coronal regions and a slowly varying component emitted by active (hotter and denser) coronal regions.

According to X-ray measurements, the temperature of active regions may reach 2 to 2.5×10^6 K while the temperature of the undisturbed regions amounts to 1 to 1.3×10^6 K. The electron density in active regions may exceed the electron density in undisturbed regions by factors of 5 to 10 . Regions of preferred generation of X-rays coincide with regions of enhanced radio emission in centimeter and decimeter ranges, and lie above strong calcium plages in the chromosphere. These regions of increased heating appear to penetrate the entire atmosphere above the photosphere, up to the corona, and may persist for a considerable time. An extensive bibliography completes the report.

90. Mandel'stam, S. L. ; Vasilyev, B. ; Voron'ko, J. ; Tindo, I. ; and Shurygin, A. : Measurements of Solar X-Ray Radiation. Space Res. III, 1963, pp. 822-835.

A summary is given of the results of the measurements of solar X-ray radiation in the region of the spectrum below 10 \AA performed at the Levedev Physical Institute of the U. S. S. R. Academy of Sciences. The flux of solar X-ray radiation below 10 \AA was measured on July 21, 1959 by vertical flights of two geophysical rockets, on August 19, 20, 1960 during the flight of the spaceship Sputnik II; on December 1, 2, 1960 during the flight of the spaceship Sputnik III; and on February 15, 1961 by vertical flight of geophysical rocket during the total phase of the solar eclipse. The results of the measurements are listed in tabular form. A good correlation between the radiation flux and the green coronal line intensity is observed, which was also observed by H. Friedman. It is therefore believed that solar short-wave radiation comes from all the corona regions in which the $5303\text{-}\text{\AA}$ line is excited. Preliminary results of calculations show that in the 2- to $10\text{-}\text{\AA}$ spectrum region the principal contributions to the coronal radiation are made by f-b transitions of electrons in the fields of "heavy" ions present in the corona. It seems that the contributions of lines of these ions and f-f transitions and also f-f and f-b transitions in the fields of protons and helium ions are relatively weak. Measurements have shown that in the region of interplanetary space in the vicinity of the Earth, at altitudes of 200 to 300 km in the latitude range approximately 35 degrees N and 35 degrees S the X-ray radiation of the solar origin is the main "hard" radiation. In the region of higher latitudes radiation caused by the radiation belt particles is imposed on it.

91. Mangus, J. D. ; and Underwood, J. H. : Optical Design of a Glancing Incidence X-Ray Telescope. Appl. Opts., vol. 8, Jan. 1969, pp. 95-102.

The optical design of a Wolter type 1 glancing incidence X-ray telescope for the wavelength 6- to 100-Å region is described. Basic design criteria are reviewed. The theoretical performance of the instrument is evaluated by ray tracing. The results of laboratory and rocket tests on a prototype instrument are briefly described. A schematic diagram of the Wolter type 1 X-ray telescope, as well as actual X-ray photographs taken with the system, is included. This paper describes the larger solar X-ray telescope version that is being built for the ATM.

92. Manson, J. E.: The Spectrum of the Quiet Sun Between 30 and 128 Å for November, 1965. *Astrophys. J.*, vol, 147, 1967, pp. 703-710.

The AFCRL grazing-incidence grating monochromator was modified for use with a thin-window Geiger detector and a 2400-line/mm gold replica grating. This combination allowed coverage of the wavelength region from 30 to 128 Å with a resolution of 0.2 Å in an experiment launched by Aerobee rocket on November 3, 1965 from White Sands, New Mexico. Preliminary analysis of the data indicates the presence of over 100 lines, each less than $0.003 \text{ erg cm}^{-2} \text{ sec}^{-1}$ in intensity. The total intensity for the entire 30- to 128-Å interval was between 0.1 and 0.2 $\text{erg cm}^{-2} \text{ sec}^{-1}$ at Earth distance. A table of major line intensities is presented as well as tables concerning unresolved and marginal lines and continuum regions and summed flux and intensity values per 10-Å interval.

93. Maxwell, A.: X-Ray, Radio, and Particle Emissions from the Solar Atmosphere. *Astron. J.*, vol. 67, 1962, pp. 276-277.

At the time of larger solar flares, electrons and protons are accelerated to quasi-relativistic energies, possibly by the Fermi mechanism. A brief description of these particles and their effects is presented. It appears that jets of electrons are projected downward into regions of higher density in the lower chromosphere where they give rise to X-ray emission by the bremsstrahlung process. The energy range of the X-radiation is generally consistent with electron energies of about 10^5 - 10^6 eV.

94. Meekins, J. F.; Chubb, T. A.; Kreplin, R. W.; and Friedman, H.: 1-8 Å X-Ray Spectra of the Active Sun from OSO-IV. *Astron. J.*, vol. 73, June 1968, p. S106.

The authors report the results of a satellite flight experiment on board OSO-IV. Two Bragg crystal spectrometers covering the 0.5- to 8.4-Å range

(0.5- to 3.9-Å and 1.4- to 8.4-Å) were used to view X-ray emissions during active periods on the Sun. Continuum emission dominated the line emission by about one order of magnitude during class 2 and 3 flares.

95. Meisel, D. D.: Identification of a Solar X-Ray Source Using D Layer Ionization Behavior during an Eclipse. *Sol. Phys.*, vol. 5, 1968, pp. 575-587.

Semiquantitative reports of short-wave radio reception during the November 12, 1966 total solar eclipse have been used to determine the characteristics of a major source of D layer ionization. An effective electron depletion coefficient was found empirically and used to reduce the data. Analysis of the radio absorption shows that the source was located near heliographic coordinates, $B = +7$ degrees, $L = 340$ degrees and was probably less than 0.5 minutes of arc in diameter. At the time of the eclipse, the source accounted for 40 percent of the radio absorption on a single, vertical pass through the D layer. Preoccultation behavior of the signal strength is interpreted by assuming a portion of the source X-ray flux was reflected at grazing incidence from the limb of the moon. A crude source spectrum in the 3- to 140-Å range is derived from the data. X-ray absorption edges of various elements arising from the terrestrial atmosphere have been identified. A source temperature approximately twice that of the corona is indicated. A summary of radio frequency monitoring efforts is included.

96. Muney, W. S.; and Underwood, J. H.: Soft X-Ray Photographs of the Sun Obtained on 3 October 1967. *Astron. J.*, vol. 73, June 1968, pp. S72-S73.

The authors report of solar X-ray photographs taken from an Aerobee rocket on October 3, 1967 obtained with a glancing incidence X-ray telescope. Four band pass regions were used: 6 to 11, 8 to 20, 27 to 40, and 44 to 60 Å. The photographs show the familiar aspects of the Sun's X-ray emission, bright X-ray regions in the corona above plages, and a general disk emission at longer wavelengths showing limb brightening. Other features of the X-ray emission also viewed were: (a) X-ray emission from the region of a disappearance brusque about 1 hour after the disappearance of the filament. (b) X-ray emission from active prominences at the limb. (c) Complex structures, such as jets and arches, extending high above the limb. (d) There is no longer a gap in the limb brightening at either pole as there was earlier in the solar cycle.

97. Negus, C. R.; and Glencross, W. M.: Spatial Variability of the Solar X-Ray Spectrum below 20 Å. *Nature*, vol. 220, Oct. 1968, pp. 48-50.

An instrument consisting of a gas-filled proportional counter with a six-channel, pulse-height discriminator utilizing grazing incidence optics has been flown on Skylark rockets and has obtained X-ray images of the Sun below 20 Å. Two sets of pictures in the 8- to 20-Å wavelength region were obtained. The first flight took place on May 5, 1966, nearly 2 years after the solar minimum (1964). The general features of the X-ray emission below 20 Å were clearly shown. There were no flares during the flight, nor did any occur near the time of launch. Strong emission came from regions of the corona that lay above the plage areas seen in Ca II K radiation. The more intense X-ray emission was associated with the larger plage areas. There was weak X-ray emission from the plage-free disk and this came predominantly from the northern hemisphere where the initial development of solar activity occurred during this present solar cycle. A second flight took place on August 8, 1967. No reported flares occurred during or near the time of flight. This rocket flight looked at the 8- to 20-Å band and the H Lyman α (1216 Å) line. All contour maps showed that an increase in solar activity had occurred since the earlier flight. The 15- to 20-Å map shows the general features of X-ray emission. The Lyman α contour map is also shown. By the second flight strong X-ray emission below 20 Å came from the nonplage area in the southern and northern hemispheres. The intensity of this emission had increased. There was also an increase in the number of X-ray active regions. The regions of enhanced X-ray emission were associated with known centers of activity. Thus, the increase in the intensity of the slowly varying component of X-ray emission, which is known to occur as the solar maximum is approached, is caused by an intensification of the emission from the quiet corona and a rise in the number of active regions. The X-ray emission is seen to come from a wide range of heights in the corona. By assuming that the X-ray flux can be expressed as a polynomial in wavelength, smooth spectra that gave the observed count-rate histograms were constructed. Smooth spectra for two active regions and that of the undisturbed Sun on August 8 have been constructed, using a fourth order polynomial, and are shown. All the observed spectra were similar in shape to the spectrum calculated by Mandel'stam for the emission from a plasma at 2×10^6 K. An uncollimated spectrometer flown on the first vehicle measured a line spectrum in the 12- to 22-Å region. The line profile indicated that the lines came predominantly from the two active regions present at that time. The only detected emission lines from the undisturbed corona lay in the 17- to 22-Å region and were identified as resonance transitions in the ion of O VII. The spectrum of the nonactive corona clearly indicates X-ray emission down to 9 Å. The X-ray spectroheliograph reported here had insufficient angular resolution to discriminate between the cores of high-density, high-

temperature, and the bulk of the active region. The overall size of active regions was found to be typically 5 arc minutes in diameter. Assuming that the main difference between the active and the undisturbed corona is due to a change in density, then density variations of approximately 3 would be required. X-ray emission from the undisturbed corona was observed to have increased in intensity by a factor of 2 in the 15 months between the flights. Assuming again that the increase in X-ray emission is due solely to an increase in density, then the increase would be consistent with a 40-percent rise in the electron density. Observations of the scattered photospheric light by electrons in the corona indicate a difference in density of a factor of 2 between solar minimum and solar maximum.

98. Neupert, W. M.: Emission of Extreme Ultraviolet Line Radiation from Solar Centers of Activity. *Astron. J.*, vol. 68, 1963, p. 288.

A scanning monochromator, mounted as a pointed experiment on OSO-1, has been used for observation of the solar EUV emission line spectrum in the spectral range from 50 to 400 Å. It is found that increases in UV fluxes over those observed from the quiet Sun can be localized to plage areas existing on the solar disk. The development of these regions of enhanced emission (coronal centers of activity) can be traced through observations covering nearly three solar rotations. The intensity ratio of Fe XVI to Fe XV is found to remain nearly constant in time. An electron temperature of 1.8×10^6 K has been derived from the ratio of Fe XVI to Fe XV for a quiet Sun.

99. Neupert, W. M.; Behring, W. E.; and Lindsay, J. C.: The Solar Spectrum from 50 Å to 400 Å. *Space Res. IV*, 1964, pp. 719-729.

A grazing incidence spectrometer has been flown on OSO-1 to monitor the EUV spectrum of the Sun from 50 to 400 Å. Over 6000 spectra were obtained at the rate of about 100 per day over a period of time from March through May 1962, corresponding to nearly three solar revolutions. This paper presents, in a condensed form, the variations observed in three of the more reliably identified lines of the spectrum: 284-Å (Fe XV), 304-Å (He II) and 335-Å (Fe XVI). The period of observation was sufficient to observe a slowly varying component having a period of approximately 27 days and correlating with solar activity. The enhancement of radiation during periods of activity was observed to vary from line to line in the spectrum, depending upon the origin of the line in the solar atmosphere. Data showed an

increase in the He II Lyman α flux, integrated over the solar disk, of 33 percent, during a period when the Zurich Provisional Relative Sunspot Number increased from zero (March 11, 1962) to a maximum of 94 (March 22, 1962). Enhancements of approximately a factor of four were observed for the 284-Å (Fe XV) and the 335-Å (Fe XVI) lines. Although there appears to be a gross correlation between solar activity indices (such as 2800-Mc flux) and the He II, Fe XV, and Fe XVI fluxes, there are indications that the relative prominence of the spectral lines may depend upon the age of the center of activity.

100. Neupert, W. M.; Gates, W.; Swartz, M.; and Young, R. M.:
Observation of the Solar Flare X-Ray Emission Line
Spectrum of Iron from 1.3 to 20 Å. *Astrophys. J.*, vol.
149, Aug. 1967, pp. L79-L83.

Solar X-ray spectra have been obtained during solar flares with two uncollimated, single-crystal Bragg spectrometers, each having a crystal-detector combination optimized for a specific range. In one, a LiF analyzing crystal is coupled with a conventional photomultiplier using a 5-mil Be filter and a NaI conversion phosphor. The spectral resolution of the system is 0.01 Å in the 1.3- to 3.1-Å spectral range. A similar instrument with KAP crystal, together with a Bendix magnetic electron multiplier using a 2- μ thick filter of polypropylene overcoated with 2×10^3 Å of Al, scans the 6.3- to 25-Å region with a resolution of 0.05 Å at 10 Å. The X-ray spectrometers were part of the OSO-III payload, which was launched on March 7, 1967. To date more than 1600 hours of observation have been accumulated. Two spectra, obtained with the LiF spectrometer during the build-up of X-ray emission associated with a flare of importance 2b on March 22, 1967, are shown. Spectra for the 6.3- to 20.0-Å region are also given. The data presented here are the first observations of the spectrum during a solar flare. In addition to increases in intensity of all lines observed in the preflare spectrum, the authors observed a new group of lines between 9.0 and 14.0 Å, which appear not to have been present prior to the flare. The new emission lines observed in the 1.3- to 20-Å range are tentatively identified by the authors as transitions in Fe XXVI through Fe XX.

101. Neupert, W. M.; Swartz, M.; and White, W. A.: Observations of the
Solar X-Ray and Extreme Ultraviolet Spectrum for OSO-III.
Astron. J., vol. 73, June 1968, p. S73.

The authors briefly describe some of the results observed by OSO-III. Solar X-ray and XUV emission spectra between 1 and 400 Å were obtained by

two single crystal spectrometers (1- to 3- and 6- to 25-Å) and a grating spectrometer (20- to 400-Å). The spectrum was scanned with a resolution of 0.01 Å at 2 Å, 0.05 Å at 10 Å, and 0.6 Å at 300 Å. Fe emission lines as well as continuum emission were observed during flares. Also, peak emission at 304 Å (He II) usually occurred before maximum intensity in the 1- to 8-Å region of the spectrum.

102. News Notes: X-Ray Solar Photograph. Sky and Tel., vol. 20, Sept. 1960, pp. 143-144.

Using an Aerobee-Hi rocket carrying a pinhole camera sensitive to 20- to 60-Å radiation, the NRL group has succeeded in taking the first X-ray photograph of the Sun. This was reported by H. Friedman of NRL at a symposium of the National Academy of Sciences and the American Geophysical Union. The Sun appears as a bright, spotty coronal ring in the photograph.

103. Paolini, F. R.; Giacconi, R.; Manley, O.; Reidy, W. P.; Vaiana, G. S.; and Zehnpfennig, T.: Preliminary Results from the AS ± E X-Ray Spectroheliograph on OSO-IV. Astron. J., vol. 73, June 1968, pp. S73-S74.

Various observations of solar X-ray flares were conducted on OSO-IV with the ASE X-ray spectroheliograph. The instrument utilizes image-forming grazing optics and has an angular resolution of 1 minute of arc. The results of observations over the period from October to December 1967 are: that X-rays are produced about 4×10^4 km above the photosphere; that sizes in X-radiation tend to correlate with sizes in H α ; that X-ray spectra tend to soften as the flares decay; that flares are observable in X-rays after they are no longer so in H α ; that X-ray plages are of the order of minutes of arc in diameter; and that X-ray brightness of plages tend to correlate with 9.1-cm radiation brightness temperatures.

104. Pecker, C.; and Rohrllich, F.: Some Attempts at Identification of Spectral Lines in the Solar Rocket Ultraviolet Spectrum. Astrophys. J., vol. 138, 1963, pp. 1322-1323.

Rocket and satellite data of the XUV spectrum of the Sun have been accumulating over the past 10 years. Four groups have been especially active in this work: AFCRL, NRL, GSFC, and the University of Colorado. This paper represents an attempt to identify many of the numerous solar emission

lines that occur between 84 and 1216 Å. Comparison of laboratory and computed wavelengths are made with rocket measurements made available mostly by the first and last of the above mentioned groups. The lines are listed according to the laboratory and computed wavelengths for each of the elements considered, along with the observed rocket wavelengths. This table however, does not appear in this supplementary article. Many lines corresponding to an ionization potential of less than 70 eV were found. For ionization potentials between 80 and 120 eV the most abundant ions have observed lines that are sometimes very faint. This result indicates that the temperature gradient in the corresponding region of the solar atmosphere must be very large.

105. Peterson, L. E.; Hudson, H. S.; and Schwartz, D. A.: Preliminary Results of the University of California X-Ray Experiment on the OSO-III. NASA-CR-96950, Accession #N68-35493, Nov. 1967, pp. 1-28.

The authors describe the University of California X-ray experiment on OSO-III, indicate its present operational status, and present a preliminary discussion of the results obtained thus far. The satellite was designed to search for X-rays over the 7.7- to 210-keV region. Results are presented covering the period March 8, 1967 through October 1, 1967. Both cosmic X-rays and solar X-rays were detected. The diffuse cosmic flux as detected by OSO-III is given. Preliminary data analysis has generally confirmed the previous knowledge of solar X-ray emission. The outstanding characteristic of the Sun in the hard X-ray region is its variability. The hard X-ray continuum of the normally quiet Sun obtained by various rocket observations and on the OSO-III during this solar cycle is shown. A typical medium size X-ray burst is presented. This burst was observed on March 16, 1967 and shows the correlation of microwave radio flux and the visible flare. A plot of the ratio of channel 3 (12.5 to 22 keV) to channel 2 (7.7 to 12.5 keV) is given and indicates that the larger the X-ray event, the harder the spectrum. The large event of March 22, 1967 is presented. The lower channels were completely saturated for many hours. Even at energies of 100 keV, a detectable intensity was emitted for nearly an hour. This shows clearly the softening of the spectrum with time.

106. Pounds, K. A.: Recent Solar X-Ray Studies in the United Kingdom. *Annales D'Astrophysique*, vol. 28, 1965, pp. 132-145.

Solar X-ray data obtained over the past year by scientists in the United Kingdom are reviewed. These include several new X-ray events reduced from the Ariel satellite results, soft X-ray flux measurements from NRL satellite

1963-21 C and notes on recent rocket studies in this field. In section 1 results are presented of several X-ray events measured by the proportional counter spectrometer on satellite Ariel I, and the present position of this work is reviewed. Section 2 summarizes the X-ray data recorded and analyzed at the Radio Research Station, Slough England, from the ion chambers on board the NRL satellite 1963-21 C. Some notes on the present low level of nonflare solar X-rays are given in section 3, followed by a brief report on the recent successful firing of a stabilized Skylark rocket X-ray payload. In the final section is a short discussion on the nature of solar flare X-rays and their measurement. The results of the Ariel I satellite cover the period April 26, 1962 through May 6, 1962, and they cover the 5- to 13-Å spectral region. Data of the X-ray enhancements associated with a number of flares are given. Also shown are the burst profiles of microwave solar radio noise associated with each flare. Brief notes are given on each event. In general the time resolution of the spectrometer was 51 seconds. Despite the lack of time resolution, interesting changes in the spectral distribution of the short wavelength solar emission during a fairly representative selection of flares have been obtained. Examples are given. A summary of the 44- to 60-Å measurements over the period January through August 1964 from the NRL satellite 1964-01-D is given. Combination of Skylark rocket measurements with those of the NRL satellite data given in section 2 provide the following figures for near-minimum X-ray fluxes:

$$\begin{array}{ll}
 < 8 \text{ Å} = 5 \times 10^{-5} \text{ erg cm}^{-2} \text{ sec}^{-1} & \text{for a 2800-MHz} \\
 8-12 \text{ Å} = 2 \times 10^{-4} \text{ erg cm}^{-2} \text{ sec}^{-1} & \text{daily index} \\
 & \text{of 74.0} \\
 44-60 \text{ Å} = 1.3 \times 10^{-2} \text{ erg cm}^{-2} \text{ sec}^{-1} &
 \end{array}$$

Also reported is a Skylark rocket flight launched on August 11 from Woomera, Australia to study the solar image in several wavelength bands with an array of pinhole cameras and to obtain high resolution spectra by means of a photographic bent crystal spectrometer. X-ray images of the Sun in the 10- to 60-Å wavelength region were obtained. This communication was originally presented at Symposium No. 23 on Astronomical Observations from aboard Space Vehicles held at Liège on August 17-20, 1964.

107. Pounds, K. A.: The Use of Photographic Emulsions in Rocket Studies of the Solar X-Radiation. *J. Photographic Sci.*, vol. 13, 1965, pp. 20-24.

The unique properties of a photographic emulsion have been used to advantage in a number of rocket-borne instruments recently designed for studies of the solar X-ray emission. It is found that with suitable laboratory calibration absolute X-ray intensities can be measured with satisfactory precision. Brief details are given of four instruments, three of which have been in production for some time, and the particular advantages of the emulsion as radiation detector are noted in each instance. The four instruments are: the ionosphere X-ray monitor, the spectroheliograph, the crystal spectrograph, and the Fresnel zone plate. This paper was originally presented at a symposium on Photographic Aspects of Ionizing Radiation, organized by the Science Committee on April 15-17, 1964, in Oxford.

108. Pounds, K. A.; and Russell, P. C.: Some X-Ray Photographs of the Sun. *Space Res.* VI, 1966, pp. 38-52.

A number of pinhole photographs of the Sun in various wavelength bands below 50 Å obtained during a rocket flight of December 17, 1964 are presented. Skylark 302 was launched from Woomera, Australia on December 17, 1964 and carried a pinhole camera with a special Ilford-G emulsion without a gelatin supercoat. Details of the camera and transmission curves for the different filters used in the camera are given. Six X-ray images could be seen on the negative. A number of bright emitting regions on the disk are found to correlate well with Ca plages and sources of the slowly varying component of 9.1-cm radio emission. The bright X-ray emission centers require a coronal densification similar to the "condensation" proposed by Waldmeier. Emission from the disk between the active regions is also visible and in fact provides the major part of the total solar flux above 25 Å. The greater relative X-ray brightness of the active regions below 25 Å indicates that generally the coronal condensations are somewhat hotter than the adjacent corona. Examination of the true extent of the individual X-ray "bright spots" indicates that more than half the emission arises from a central core less than 1-arc minute diameter. Similar study of a region whose base lies beyond the solar limb shows that the emission region extends up to at least 6.7×10^4 km. A list of the active regions on the visible solar hemisphere for December 16-18 is presented. A table of excess emission of active regions and one giving mean film densities on various parts of the solar image are given. Several conclusions are drawn from the initial analysis and are summarized: (1) All nine main plages on the Sun are associated with a region of enhanced X-radiation. These plages cover an age group up to fourth rotation. (2) The active region X-rays form some 20 percent of the total emission at wavelengths near 30 to 50 Å, rising to 50 percent below 25 Å and 85 percent below 15 Å. (3) At least half of the emission from one region appears to arise from a vertical densification extending from about 0.3 to 1.0×10^5 km above the photosphere. (4) The

coronal active regions on the disk have the appearance of a very bright central core, less than 1 arc minute in diameter, surrounded by a weaker halo to some 2 or 3 arc minutes in diameter. When allowance is made for the real sizes of the active emitting regions, the peak-to-disk ratios of emission increase to near 100 for three of the images and even higher for the shorter wavelength images.

109. Pounds, K. A.; and Willmore, A. P.: Instrumentation of Satellite UK1 for Obtaining Low Resolution Solar X-Ray Spectra. Space Res. III, 1963, pp. 1195-1206.

A satellite instrumentation is described which employs the energy (or wavelength) resolution of a proportional gas counter to study the spectral shape of the Sun's X-ray emission near its short wavelength limit, and the variation of this spectral "tail" with solar activity. It is noted that the experimental limitations of this type of spectrometer are in principle determined by the properties of the gas counter itself and these are examined in some detail in order that the expected precision of spectral measurement may be described. Some additional limitations imposed by the space vehicle itself are noted. A brief discussion of the standard Skylark spectrometer is presented. Some preliminary results from UK1 (Ariel) from its first week of operation are presented. Counting rates covering the 4.7- to 13.8-Å wavelength band and the solar energy fluxes for intervals of this band are given.

110. Reidy, W. P.; and Vaiana, G. S.: An Analysis of Solar X-Ray Photographs Obtained with Grazing Incidence Optics. Space Res. VII, 1967, pp. 1247-1249.

An analysis is presented (in the *Astrophys. J.*) of six X-ray photographs of the Sun obtained using grazing incidence optics during low solar activity (March 17, 1965). Transmission filters of Al, Be, and Mylar were used to obtain broadband spectral information. The harder X-radiation was localized to a plage associated region. A general coronal emission characterized by limb brightening and the presence of several extended weakly emitting regions which have no obvious correspondence to visible or radio observations was seen. The emission at the limb is enhanced in regions where enhanced coronal green line emission is observed. Spectral differences between various solar features were determined. The spectral character of the X-radiation was expressed in terms of an effective electron temperature calculated on the basis of an assumed exponential spectrum. The effective temperature for the plage associated radiation is 1.8×10^6 K in the 8- to 20-Å wavelength region. The plage associated emission in the 44- to 60-Å region is relatively more intense than the

simple exponential model would predict. The relative intensity of the emission in the 8- to 20-Å and 44- to 60-Å regions is consistent with an effective exponential temperature of 1.45×10^6 K. The effective temperature of the observed limb emission is significantly smaller than the plage associated emission, with an upper limit of 1.1×10^6 K. The total plage associated flux at the top of the atmosphere is calculated to be 6.7×10^{-4} erg cm⁻² sec⁻¹ in the 8- to 20-Å region and 1.2×10^{-2} erg cm⁻² sec⁻¹ in the 44- to 60-Å band. The total solar radiation in the 44- to 60-Å region is estimated at 4.5×10^{-2} erg cm⁻² sec⁻¹. The plage associated X-ray source is less than 1 minute of arc while the H α plage is 3 minutes of arc across its longest dimension. It is of particular interest that the H α plage consists of two similar regions while the X-ray emission appears to be localized to a single region. There is some indication that the peak position is not circularly symmetric with respect to the solar disk and that the position of peak intensity in the northeast quadrant is at somewhat greater altitude than for the other sectors. This would appear to be related to the large prominences observed in that region.

111. Reidy, W. P.; Vaiana, G. S.; Zehnpfennig, T.; and Giacconi, R.:
 Study of X-Ray Images of the Sun at Solar Minimum.
 Astrophys. J., vol. 151, Jan. 1968, pp. 333-350.

Three X-ray telescopes were flown by rocket from White Sands, New Mexico on March 17, 1965 to obtain X-ray photographs of the Sun. Two types of film were used for the X-ray pictures, Ilford Commercial G and Ilford Special G (unsilvered). The set of solar X-ray photographs obtained using grazing-incidence optics at solar minimum is analyzed. The spatial distribution of the X-ray radiation above 20 Å is shown to be consistent with models of the general coronal emission by Elwert. A model for the X-ray emission from a plage is constructed by use of the experimental data on temperature, volume, and density of the emitting regions. The results obtained in X-rays are compared to the 9.1-cm spectroheliogram, the H α spectroheliogram, and the magnetogram of the Sun obtained simultaneously by ground observation. It is shown that the ionized plasma that produces the observed X-ray emission also accounts for the observed radio emission at 9.1 cm. Thus, the correlation between enhanced radio emission and X-rays from this plage region is due to a common physical process that is responsible for both. The lifetime and mode of confinement of such as ionized plasma are discussed. It is shown that energy injection must occur during the life of the plage to account for the observed persistence. It is also shown that the observed magnetic field would be capable of containing the plasma if it extends to the coronal heights in which the plasma is maintained. A table summarizing the solar conditions for March 17, 1965 is given. This was a joint experiment by ASE and GSFC.

112. Rense, W. A.: Solar Ultraviolet Spectroscopy and Applications to Problems of the Upper Atmosphere and the Solar Corona. Space Res. I, 1960, pp. 608-614.

This paper was originally presented at the 1st International Space Science Symposium at Nice in January 1960. Results obtained from rocket spectrographs equipped with photographic-type detectors are reviewed. These include: (1) extension of the solar Fraunhofer spectrum to about 1500 Å and their identification of over 1000 absorption lines, (2) the detection of hydrogen Lyman α and the measurement of its absolute intensity, (3) the determination of the half-width and profile of the hydrogen Lyman α line, (4) the detection of several members of the Lyman series and the continuum, (5) the detection of the ionized He resonance line at 303.8 Å and the establishment of its relatively high intensity, (6) the wavelength measurements and identification of several hundred emission lines extending from about 1900 to 80 Å, (7) the measurement of the approximate absolute intensities of several less-intense emission lines, and (8) successful photography of the Sun's disk in H Lyman α radiation. Examples of application to solution of problems of the upper arc and solar corona are presented.

113. Rugge, H. R.; and Walker, A. B. C., Jr.: Solar X-Ray Spectrum below 25 Å. Air Force Report #SAMSO-TR-67-128, Aerospace Report #TR-0158 (9260-02)-1, Accession #AD663415, Laboratory Operations Aerospace Corporation, Oct. 1967, pp. 1-16.

A pulsed-height analyzed proportional counter and a Bragg crystal spectrometer, both mounted on a compact solar pointer, were flown on the polar, earth-oriented satellite 1966-111B and obtained solar X-ray spectra below 25 Å. The pulsed-height analyzed proportional counter obtained low-resolution spectra below 13 Å with a time resolution of 1 second and the scanning Bragg X-ray crystal (KAP) spectrometer yielded one highly resolved spectrum from 7 to 25 Å every 250 seconds. This paper presents some of the spectra from the crystal spectrometer experiment. The satellite was in operation from launch (mid-December 1966) to early March 1967, and then resumed operation in mid-April 1967 and effectively ceased operating in mid-June 1967. Over the observed range, much of the X-ray energy is in line radiation. The predominant lines are those of the ions N VII, O VII, O VIII, Fe XVII, Ne IX, Ne X, and Mg XI. At least 50 emission lines were observed, a number of them for the first time. Spectra taken with the crystal spectrometer under various conditions of solar activity showed that large enhancements in flux are confined to the shorter wavelength lines. The proportional counter also showed a distinct hardening of the spectrum, as well as an increase in

flux with solar activity. A tabular chart of solar X-ray lines from 8- to 25-Å is given.

114. Rugge, H. R.; and Walker, A. B. C., Jr.: Solar X-Ray Spectrum below 25 Å. *Space Res.* VIII, 1968, pp. 439-449.

The solar X-ray spectrum below 25 Å has been studied with two X-ray experiments mounted on a compact solar pointer on the polar earth-oriented satellite OV1-10 (1966-111B). The experiments consisted of a pulsed-height analyzed proportional counter that obtained low-resolution spectra below 13 Å with a time resolution of 1 second and a scanning Bragg crystal (KAP) spectrometer which yielded one highly resolved spectrum from 7 to 25 Å every 250 seconds. This paper presents some of the spectra from the crystal spectrometer experiment. The satellite operated from launch in mid-December 1966, to early March 1967, and then resumed operation in mid-April 1967 and operated effectively until mid-June 1967. Over its observed range, much of the X-ray energy is in line radiation. The predominant lines are those of the ions N VII, O VII, O VIII, Fe XVII, Ne IX, Ne X, and Mg XI. At least 50 emission lines have been observed, a number of them for the first time. Spectra taken with the crystal spectrometer under various conditions of solar activity indicates that large enhancements of flux are confined to the shorter wavelength lines. The proportional counter also shows a distinct hardening of the spectrum as well as an increase in flux with solar activity. Tables giving identified solar X-ray lines (8 to 25 Å) and solar X-ray flux ratios for selected lines are presented.

115. Russell, P. C.: Further Soft X-Ray Images of the Sun. *Nature*, vol. 206, Apr. 1965, pp. 281-282.

A Skylark rocket was launched on December 17, 1964 from Woomera, Australia and carried an X-ray pinhole camera to produce a soft X-ray image of the Sun. Part of the negative obtained from the flight is reproduced. A table giving details of the filters and the pinholes used to obtain these images is presented. An enlargement of one of the X-ray emitting regions is reproduced. This may be compared with the Fraunhofer Institute Solar map for the same day. The correlation between the bright patches on the X-ray photograph and the continuous plage areas shown on the Fraunhofer Institut solar map is very clear. The presence of limb brightening is clearly evident. It is particularly interesting to note that the area of the NE limb on the pinhole photograph does not coincide with any plage area observed on the Fraunhofer Institut solar map for December 17, 1964. However, examination of the Fraunhofer Institut solar map for December 18, 1964 shows that a plage area appears at

this position. The X-ray emitting region at a greater altitude is visible before the plage area. Moreover, examination of the Fraunhofer map for December 16 shows that the small area at the NW limb on the map of December 17 is a larger plage region, which has partially disappeared around the limb, but on the X-ray photograph is still showing the greater activity of the larger area.

116. Russell, P. C.: Soft X-Ray Image of the Sun. *Nature*, vol. 205, Feb. 1965, pp. 684-685.

A Skylark rocket launched from Woomera, Australia on August 11, 1964 carried a pinhole camera device consisting of nine pinholes, covering five wavelength ranges. A soft X-ray photograph of the Sun was obtained from this launch. The photograph reproduced was obtained from a camera of $f = 7.5$ in. with a 0.005 in. pinhole. The filter used over the pinhole was 1.5μ plastic foil with a 1000-Å coating of Al. This filter passes soft X-rays in the region up to about 25 Å and also in the 44- to 70-Å region. Comparison of this photograph with the Ca K plage photographs of Tokyo Observatory and the Fraunhofer Institut solar map shows a good correlation between the plage areas and the patches on the X-ray photograph. The X-ray emission defining the external edge of the disk of the photograph does not correlate with the plage areas and is thought to be due to coronal emission of soft X-rays and the limb brightening that would be expected due to the optically thin nature of the corona at these wavelengths. Comparison with the 9.1-cm spectroheliograph obtained by the Radio Astronomy Institute, Stanford, on August 10, 1964, 8 hours before the X-ray photograph, shows generally good correlation of the bright patches and the limb areas. The photograph was taken at a period of quiet Sun and does not show the activity visible of the previous X-ray photographs; it thus has the advantage of limited X-ray activity and limited Ca K plage activity for comparison.

117. Sakurai, K.: Energetic Electrons Associated with Solar Flares. *Pub. Astron. Soc. Jap.*, vol. 19, 1967, pp. 316-322.

Energetic electrons in the 10- to 100-keV range associated with solar flares have been detected by means of the deep-space probe, Mariner IV, and the satellites, IMP-1 to -3. The results indicate that the electrons generated in solar flares are ejected from the flare region into interplanetary space. The positions of those electron-generating flares are mainly restricted with the western hemisphere of the Sun, and, furthermore, the transit time of the electrons from the Sun to the earth tends to become shorter as the associated sunspot goes westward on the Sun. Those electron flares are almost always associated with the emission of microwave impulsive bursts and X-ray bursts,

although the importance of most of these flares is small. Generation and propagation mechanisms of these electrons are considered. A table summarizing data concerning solar electron flares and associated phenomena is presented.

118. Shklovskii, I. S.: Nature of Solar X-Ray Emission. Soviet Astron. -AJ, vol. 8, Jan.-Feb. 1965, pp. 538-544.

It is shown, on the basis of an analysis of simultaneous observations of X-ray emission, the coronal lines Fe XV and Fe XVI, and radio emission at 10.7 cm, that a coronal temperature of $\sim 1.5 \times 10^6$ is sufficient to account for the X-ray emission of the quiescent Sun. The X-ray emission of flares is accounted for by the inverse-Compton effect on relativistic electrons of $\sim 10^7$ - 10^8 eV energy moving in the solar radiation field. The total energy associated with these electrons must be $\sim 10^{30}$ erg or less in the region of a flare (if the emission density of Lyman α quanta trapped in the flare region is sufficient high).

119. Shklovsky, J.: The Inverse Compton Effect as a Possible Cause of the X-Ray Radiation of Solar Flares. Nature, vol. 202, Apr. 1964, pp. 275-276.

The author reviews the major difficulties of the thermal origin theory of X-radiation of flares, and briefly investigates a nonthermal origin of X-radiation by the inverse-Compton effect. The author further states that the inverse-Compton effect may be a very efficient mechanism for the hard photon emission of some types of stars.

120. Smith, T. S.: Two-Photon Processes in the Solar X-Ray Spectrum. Astron. J., vol. 73, June 1968, p. S78.

Two-photon decay of the metastable 2s levels of hydrogen has been shown to be important in providing continuous emission from planetary nebulae. The author attempts to show briefly that this process is active in the formation of continuous emission X-ray spectra.

121. Snijders, R.: Theory of Deka-keV Solar X-Ray Bursts. Sol. Phys., vol. 4, 1968, pp. 432-445.

Beginning with the hypothesis that X-rays and radio waves are generated in the same coronal region and emitted by the same electrons, (thus phenomena

caused by one coronal disturbance) the author attempts to investigate theoretically the time-profile of deka-keV X-ray bursts. The energy distribution of fast electrons that emit the hard X-ray burst has been computed as a function of time. On the basis of these expressions the time-profile has been calculated. Two initial electron distributions were chosen: (1) a monoenergetic distribution and (2) a maxwellian distribution of electron energies. It has been proven that the process of an electron is completely governed by losses caused by magnetic bremsstrahlung emission. This implies that the decay shape of a burst is determined by the value of the magnetic-field strength existing in the plasma. A typical decay time of about 3 minutes can be expected theoretically from a thermal plasma of $T = 10^9$ K confined by a magnetic field of about 750 gauss. The theory developed indicates that the soft X-ray burst accompanying the deka-keV burst lasts much longer than the deka-keV burst itself.

122. Stein, W. A.; and Ney E. P.: Continuum Electromagnetic Radiation from Solar Flares. J. Geophys. Res., vol. 68, Jan. 1963, pp. 65-81.

Continuum electromagnetic radiation from solar flares is discussed in terms of the energy loss processes of electrons in the solar atmosphere. The discussion covers radio emission, visible light and X-ray and γ -ray radiation. The various possibilities for the description of continuum emission at visible wavelengths are discussed. The intensity of electromagnetic radiation from flares as a function of frequency is depicted. A discussion concerning synchrotron radiation as the source of white light from flares is presented. It is shown that it is possible to attribute the continuum radiation both at radio frequencies and at visible frequencies to synchrotron radiation by exponential rigidity distributions of electrons. The magnetic field necessary to produce white light is of the order of 500 gauss, and the number of electrons necessary is of the order of the number of protons accelerated in a large flare. Nonwhite light flares would be expected to be flares in which the maximum in the synchrotron spectrum occurs at a frequency less than the frequency of visible light. These flares would be expected to have accelerated particles with steep spectrums, small magnetic fields and/or small numbers of accelerated electrons. Bremsstrahlung as observed at X-ray frequencies would be expected from the relatively low-energy electrons that are probably accelerated even in those flares of less importance. The observed flux of X-rays is too large to be accounted for by synchrotron radiation even in large flares that are observed in white light. It is possible however that some of the very largest flares could produce bursts of synchrotron X-rays or γ -rays. Several astronomical experiments on solar flares are suggested by this discussion. A number of tables and graphs are included in the discussion of synchrotron radiation.

123. Stuhlinger, E.; and Clark, T. A.: The Apollo Telescope Mount. *Astron. J.*, vol. 73, June 1968, p. S119.

The authors present a brief statement on the ATM manned orbital astronomical observatory being developed by MSFC in conjunction with the five sponsors representing the five solar experiments. They are NRL and HCO (UV spectrographs and spectroheliographs); ASE and GSFC (X-ray investigations); and HAO (White Light Coronagraph).

124. Takao, K: X-Ray Events at the End of August, 1966. *Rep. Ionos. Space Res. Japan*, vol. 21, 1967, pp. 125-131.

The author has been receiving signals from the SR-8 (Explorer 30) satellite at Uji Radio Observatory of Kyoto University since its launching in 1965. In this paper the X-ray events observed during the period of August 28-31, 1966 are discussed. Solar activity was very high in this period. Showing a similar variation is the 3750-MHz solar radio emission observed at ToyoKawa, Nagoya University. For comparison, solar-terrestrial events were examined in the CRPL Solar-Geophysical Data. The 0- to 3-Å emission is below the threshold level most of the time. The 0- to 20-Å sensor suffers an unfavorable effect of 0 to 8 Å when the latter is too strong. The channel for 44 to 60 Å is sometimes switched to another 0- to 8-Å sensor when the normal 0- to 8-Å sensor is saturated. Data on the UV band were omitted because there was no significant time variation even at a flare time. The author concludes with the following suggestions: (1) At the solar flare time there arises a hardening in the X-ray spectrum. (2) As a consequence, the time variation is more sensitive for a shorter wavelength. (3) There is a close correlation between solar X-ray and solar radio emission in the microwave band. (4) H Lyman α does not show any great variation even at flare time. (5) As to the SID's, one example was discovered that did not result from a solar X-ray burst. (6) From the observation of SID's it is concluded that the time constant of recovery of the ionosphere is sometimes shorter than the decay time of the solar X-ray burst. (7) The decay time of 0- to 8-Å emission is calculated to be about 10 minutes.

125. Teske, R. G.: Description of OSO-III Soft X-Ray Experiment. *Astron. J.*, vol. 73, June 1968, p. S80.

A brief description of some of the results of the Michigan experiment on board OSO-III is presented. Data obtained have confirmed the variability of the Sun in the soft X-ray region. Also, soft X-ray emission seems to be

associated with other indices of solar activity. The X-rays appear to be primarily of thermal origin.

126. Thomas, L: Observations of Solar X-Ray Emission in the Band 44-60 Å from U. S. Naval Research Laboratory Satellite 1963-21-C. *Nature*, vol. 203, Aug. 1964, pp. 962-963.

This paper presents some results for X-rays in the 44- to 60-Å band derived from telemetry recorded from satellite 1963-21-C at the D. S. I. R. Radio Research Minitrack Station at Winkfield during June and July 1963. The X-ray fluxes measured at 1/2-minute intervals during a satellite pass on July 23, 1963 are shown. These fluxes have been derived assuming a spectrum corresponding to a source temperature of 0.5×10^6 K. The accuracy of these measurements is estimated to be better than 5 percent. Measurements near sunrise and sunset have shown marked changes in flux during a single pass. The measurements made at 1/2-minute intervals during a pass on June 25, 1963 are shown. It seems reasonable to conclude that the variations of flux observed during passes near sunrise and sunset are almost entirely caused by atmospheric absorption. In conclusion, the observations indicate that the flux of solar X-rays in the 44- to 60-Å band during the period of low solar activity of June and July 1963 was near 8×10^{-2} erg cm⁻² sec⁻¹. In general, measurements made near 190 km show little evidence of atmospheric absorption except near sunrise and sunset.

127. Thomas, L.; Venables, F. H.; and Williams, K. M.: Measurements of Solar X-Ray Fluxes by the U. S. Naval Research Laboratory Satellite 1964-01-D. *Planet. Space Sci.*, vol. 13, 1965, pp. 807-822.

The NRL Solar Radiation satellite 1964-01-D was launched January 11, 1964 and was intended to monitor solar X-rays in the following bands: 2- to 8-, 8- to 14-, 8- to 16-, 44- to 55-, and 44- to 60-Å. Also, it was to have monitored solar UV radiation in the 1225- to 1350-Å band. Measurements of X-ray fluxes in the 2- to 8-, 8- to 14-, and 44- to 60-Å bands have been provided over a period of several months, but the 8- to 16-Å and 44- to 55-Å photometers failed during early February. The flux in the 1225- to 1350-Å band was generally below the threshold of the photometer. The detectors were ionization chambers mounted in the equatorial plane of the satellite. Satellite spin modulated the X-ray inputs. This paper describes the results derived from telemetry recorded at Winkfield during the period January-August 1964. The daily measurements of X-ray fluxes are described, including those following a small flare. A comparison is made between the day-to-day changes in the

44- to 60-Å flux and measurements of the E-layer critical frequency in order to investigate the importance of these X-rays in the production of the E-layer. Comparison of fluxes in the 44- to 60-Å band and measurements of the E-layer critical frequency indicate that these X-rays play little part in the production of the E-layer during this period. Measurements of the 44- to 60-Å flux have shown marked variations during passes near sunrise and sunset and these changes have been attributed to atmospheric absorption. Studies of these changes have provided information on the atmospheric model in the 120- to 200-km height range. Measurements of X-ray fluxes made on the photometers and of the 10.7-cm radio noise flux recorded at Ottawa are shown. The fluxes in the 0- to 8- and 8- to 20-Å bands were about 0.3×10^{-3} and 2×10^{-3} erg cm⁻² sec⁻¹, respectively; that for the 44- to 60-Å band, based on a source temperature of 0.5×10^6 K, was about 3×10^{-2} erg cm⁻² sec⁻¹. Attention is drawn to the rather poor correlation between 44- to 60-Å X-ray flux and the 10.7-cm radio noise flux. Also presented are the measurements of X-ray fluxes in the 44- to 60-Å and 8- to 16-Å bands at about 1/2-minute intervals during this satellite pass and the median values measured during passes on January 19 and 20. It is noticeable that the measurements made on January 20 show no evidence of decays in the enhanced fluxes during the satellite pass. It appears, therefore, that the emission in both 8- to 20-Å and 44- to 60-Å bands can remain at enhanced levels for several minutes after the termination of an optical flare of minor importance.

128. Tousey, R.: Highlights of Twenty Years of Optical Space Research. Appl. Opt., vol. 6, Dec. 1967, pp. 2044-2070.

The most important first discoveries in optical space research are reviewed for the 20 years since the beginning in 1946. Only research conducted from space vehicles is included: rockets, earth orbiting vehicles, both manned and unmanned, space probes, and lunar landings. The optical fields involved are: measurements of EUV and X-rays from the Sun, including spectra, spectroheliograms, and monitoring; white light solar corona; X-rays and EUV from stars and nebulae; airglow; photography of the moon, Mars, and the earth; and technical breakthroughs that made the work possible. An extensive bibliography is included. Various schematic spectrograph designs are shown. Also, many spectra representative of the EUV and X-ray regions of the Sun are reproduced. High resolution H Lyman α , H α , Ca K, and white light photographs of the Sun are compared. Also, X-ray images of the Sun are depicted. This communication was originally an invited paper presented at the 50th anniversary meeting of the Optical Society of America, Washington, D.C., March 15, 1966.

129. Tousey, R. : Some Results of Twenty Years of Extreme Ultraviolet Solar Research. *Astrophys. J.*, vol. 149, Aug. 1967, pp. 239-252.

This article is a general review of the experiments in the 30- to 2869-Å range over the period 1946-1966. Some of the results of these experiments are presented. The author discusses the EUV region in more detail than the X-ray region. The author includes the solar X-ray spectrum of July 25, 1963 as recorded by NRL using a Bragg crystal spectrometer. The graph covers the 12- to 26-Å spectral band. The author briefly discusses the < 80-Å range. Here, the intensity depends strongly on solar activity. Identifications in this range are fairly secure. From a study of the relative intensities among the Si lines, using ionization theory and dielectronic recombination coefficients of Burgess (1965), Widing and Porter (1965) have calculated the temperature for the region where Si VIII, IX, X, XI, and XII originate. The value comes out to be $1.6-1.8 \times 10^6$ K. The remainder of the report is concerned with the extreme UV. This paper was originally presented at the Henry Russell Lecture at the 122nd meeting of the AAS, Cornell University, Ithaca, New York, July 26, 1966.

130. Tousey, R. : The Spectrum of the Sun in the Extreme Ultraviolet. *Quart. J. Roy. Astron. Soc.*, vol. 5, 1964, pp. 123-144.

The author reviews the early experiments of UV and X-ray astronomy. He briefly discusses emission from the photosphere and the transition region. Following this is a brief discussion of the solar emission line spectrum between 170 and 2000 Å. A summary of the ions identified by their EUV and soft X-ray lines is presented. It is surprising that certain ions have not as yet been detected. For example, no lines of neon less ionized than Ne VII have been observed. Also Mg III-VI, with 15- to 141-eV production ionization potentials are missing, as are Si V and VI, with 45 and 167 eV. The author briefly discusses some of the measuring techniques and closes with a discussion containing many examples of spectroheliograms and line profiles. The author concludes that EUV and X-ray spectroscopy of the Sun are still in the observational stage. A number of spectra have been obtained, but many lines remain unidentified. Intensities of the emission lines and their profiles are needed. More spatial resolution is required, and other lines must be studied. A lengthy bibliography is presented. This paper was originally presented at the George Darwin Lecture, delivered at Burlington House October 11, 1963.

131. Tousey, R.; Watanabe, K.; and Purcell, J. D.: Measurements of Solar Extreme Ultraviolet and X-Rays from Rockets by Means of a $\text{CaSO}_4\text{:Mn}$ Phosphor. *Phys. Rev.*, Vol. 83, Aug. 1951, pp. 792-797.

The presence of solar EUV and X-rays at high altitude in the atmosphere was detected by means of a thermoluminescent phosphor, $\text{CaSO}_4\text{:Mn}$, which was not sensitive to wavelengths above 1340 Å. Samples of the phosphor were flown in V-2 rockets and exposed to sunlight. By means of filters of Be, LiF, and CaF_2 , response was measured in the 0- to 8-, 1050- to 1340-, and 1230- to 1340-Å wavelength bands. X-rays were observed on one flight which reached 128 km, during which an SID occurred. Wavelengths between 1050 and 1340 Å were observed on all four flights and reached as low as 80 to 90 km. A tentative value of 0.04 microwatt/cm² was calculated for the total intensity in the solar spectrum in the range 1050 to 1240 Å, which includes the H Lyman α line, at an altitude level somewhere between 82 and 127 km. A similar value for the range 1230 to 1340 Å was 0.02 microwatt/cm². A comparison of the responses of the phosphor strips flown without filters and those with filters indicated that radiation between 795 and 1050 Å reaches the region 82 to 127 km with an intensity well above that produced by a 6000° K blackbody Sun. Two tables summarizing the four flight experiments (1949-50) discussed are presented.

132. Tousey, R.; and Widing, K. G.: Ionic Species in the Sun as Identified from XUV and X-Ray Lines. *Astron. J.*, vol. 73, June 1968, pp. S80-S81.

The authors report on the ionic species detected in the Sun by identification of lines in the XUV (extreme ultraviolet) and X-ray spectrum. No lines of Li, Be, and B, as well as of F or Cl, have been found. All stages of C, N, and O are recorded. Most of the Si and Na ions are absent. Fe lines have been observed during flares. The wealth of Fe ions and the strength of their emission lines are taken as further evidence in support of the enhanced abundance of Fe in the corona.

133. Underwood, J. H.; and Muney, W. S.: A Glancing Incidence Solar Telescope for the Soft X-Ray Region. *Sol. Phys.*, vol. 1, 1967, pp. 129-144.

This paper describes the instrumentation of an Aerobee rocket (NASA 4.95 GS), which was launched from White Sands, New Mexico on May 20, 1966 to observe the Sun in the soft X-ray region. The experiment package, which was pointed at the Sun by a control system stabilized about all

three axes, carried two Wolter type I glancing incidence telescopes to photograph the Sun in wavelength regions (determined by bandpass filters) between 3 and 75 Å, and the proportional counters to obtain flux data and rough spectral shapes in the 2- to 11-, and 8- to 20-Å regions. The spatial resolution obtained was about 20 arc seconds. Limb brightening and polar darkening are very pronounced at the longer wavelengths. A tuft of emission was observed at the North Pole in addition to an arch-like structure on the NW limb. Several of the photographs are presented, and some preliminary results are discussed. Sixteen pictures of the Sun were obtained through five different filters which defined different wavelength regions. The relevant data on each exposure is summarized in tabular form, and the transmittance of the five filters are shown plotted as a function of wavelength.

134. Van Allen, J. A.: Solar X-Ray Flares on May 23, 1967. *Astrophys. J.*, vol. 152, May 1968, pp. L85-L86.

The soft X-ray flux from a sequence of three solar flares on May 23, 1967 was observed on satellite Explorer 33. The absolute flux of soft X-rays (2- to 12-Å) from the sequence of three solar flares observed on May 23, 1967 is given as a function of time with a resolution of 163.6 seconds. Maximum flux was measured to be $0.65 \text{ erg cm}^{-2} \text{ sec}^{-1}$, and it occurred at 1846 UT. This is believed to be the most intense X-ray flux that has been observed. On the grounds of time coincidence with terrestrial optical observations, the three X-ray flares of May 23, 1967 are attributed to McMath plage region 8818 at N27 E25 on the solar disk.

135. Van Allen, J. A.: The Solar X-Ray Flare of July 7, 1966. *J. Geophys. Res.*, vol. 72, Dec. 1967, pp. 5903-5911.

By means of a mica window Geiger-Mueller (EON 6213) tube on earth satellite Explorer 33, a major solar X-ray flare was observed with a 81.8-second time resolution on July 7, 1966. The flare had a total duration of about 200 minutes. The maximum energy flux was $3 \times 10^{-2} \text{ erg cm}^{-2} \text{ sec}^{-1}$, and the time integrated flux was 97 erg cm^{-2} over the 2- to 12-Å wavelength range. Assuming equal intensity over 2π steradians at the Sun, the total emission in this wavelength band was about 1.4×10^{29} ergs, and the maximum surface luminosity of the Sun was $2.9 \times 10^6 \text{ ergs cm}^{-2} \text{ sec}^{-1}$ or 4.5×10^{-5} of the whole radiant luminosity of the average solar surface. Charged particles began to arrive at the satellite 35 minutes after the first detection of the X-ray enhancement and remained in the interplanetary system for at least 10 days thereafter. The intensity-time curve of the soft X-rays is compared with those

of 2700-MHz solar radio noise flux and of ionospheric absorption at 22 MHz as observed at Penticton.

136. Van Allen, J. A.; Drake, J. F.; and Gibson, Sr. J.: Solar X-Ray Observations with Explorer 33, Explorer 35, and Mariner V. *Astron. J.*, vol. 73, June 1968, p. S81.

The authors report that nearly continuous observation of the soft X-ray emission of the whole Sun was achieved for the period July 1, 1966 through January 30, 1968 by satellites Explorer 33, Explorer 35, and Mariner V. The Explorer satellites were sensitive to the 2- to 12-Å wavelength range, while the Mariner satellite was sensitive to the 2- to 8-Å wavelength range. The high sensitivity, large dynamic range, and continuous nature of these observations have proved to be of considerable value in coordinated studies of a variety of solar-geophysical phenomena.

137. Vette, J. I.; and Casal, F. G.: High-Energy X-Rays during Solar Flares. *Phys. Rev. Letters*, vol. 6, Apr. 1961, pp. 334-336.

The authors conducted a balloon flight on October 12, 1960 and detected two X-ray bursts with energies exceeding 80 keV during a class 2 and a class 1 flare. Spectrum measurements and complete time histories of these events were obtained. The data for the two events are shown. A NaI scintillation counter was used to obtain the measurements. The background counts are caused mainly by X-rays from cosmic-ray induced showers in the atmosphere. The interesting solar and terrestrial events that occurred during this flight were: (a) a class 2 flare, (b) a class 1 flare, (c) a sudden enhancement of atmospherics (SEA), (d) a sudden cosmic noise absorption (SCNA), and (e) various noise storms. A table containing the solar radio data for October 12, 1960 (1700 to 1800 UT) is given. A balloon flight was also made on August 17, 1960 carrying the same instrumentation during a class 1 flare. However, no increase in counting rate was observed. Also there were no terrestrial effects or radio noise storms observed during this flare.

138. Violet, T.; and Rense, W. A.: Solar Emission Lines in the Extreme Ultraviolet. *Astrophys. J.*, vol. 130, 1959, pp. 954-960.

Solar UV rocket spectrograms were obtained from Aerobee-Hi flights on June 4, 1958 and on March 30, 1959 at Holloman Air Force Base, New Mexico. In both cases a modified grazing-incidence concave-grating spectrograph was employed. Intense plage areas were present on the first flight, but

no flare occurred. Solar activity was again high for the second flight, but again no outstanding single event occurred. Measurements from these two flights have yielded wavelengths of about 150 solar UV emission lines in the range between 1216 (H Lyman α) and 83.9 Å. Estimates of the intensity of the He II 303.8-Å line were made. Measured wavelengths corrected for systematic errors and, in some cases, identifications of the lines are given. Eastman Kodak SWR film was used for the flights.

139. Vladimirkii, B. M.; and Pankratov, A. K.: X-Radiation from Solar Flares and Cosmic Rays. Acad. of Sciences U.S.S.R., Bulletin, Physical Series, vol. 28, 1964, pp. 1911-1914.

The authors briefly discuss the results of Wilson and Nehra (1962) that may have considerable significance for understanding the physical processes that occur during periods of development of solar flares; specifically, they found that cosmic-ray (CR) effects are produced only by flares that are accompanied by absorption of short radio waves in the D-layer of the ionosphere at low latitudes (short-wave fadeout — SWF). At present it has been reliably established that SWF are due to bursts of X-radiation with $\lambda < 8$ Å. The results obtained by Wilson and Nehra have been substantiated by the authors on the basis of the data of the IGY and IGC for flares of different importance. The authors show plots of the CR intensity for the effects of flares of importance 2. It proved feasible to investigate roughly the quantitative relation between the strength of the ionospheric effects of the solar flares and the amplitude of the increase in CR. This relation between the absorption in the D-layer on the ionosphere (SCNA) and the amplitude of the increase of the nucleon component is shown. It is important to note that for six flares with absorption ≥ 80 percent, no significant increase in the CR intensity was detected. This shows that not all flares accompanied by significant ionospheric absorption exhibit increase of the CR intensity. There has been established close correlation between the intensities of 10-cm radiowave bursts and bursts of X-radiation. The authors took advantage of this fact for independent verification of the regularity under discussion. Examination of the corresponding data confirmed the conclusion that on the average there is observed a relation between the SCNA strength and the corresponding CR effect at sea level. Apparently, the presence of a flux of X-radiation with $\lambda \leq 8$ Å is a necessary, but not sufficient condition for the appearance of a flare effect in CR at sea level. The existence of a relation between the X-radiation of solar flares ($\lambda \leq 8$ Å) and the relativistic part of the energy spectrum of solar CR ($E > 1$ BeV) can be understood in principle if you assume: (1) that the X-radiation responsible for the SCNA is mainly of bremsstrahlung origin from fast electrons (possibly, synchrotron radiation) and (2) that the electrons responsible for the X-radiation are accelerated during the period of the flare to the same velocities as nuclei or are secondary with

respect to the last. From this point of view the existence of bursts of X-radiation is indicative of the existence of an electron component in solar cosmic-rays.

140. Walker, A. B. C., Jr.; and Rugge, H. R.: Absolute Intensity of the Solar X-Ray Line Spectrum below 25 Å. *Astron. J.*, vol. 73, June 1968, pp. S81-S82.

The authors present flux intensities for several of the strongest lines of O, Fe, Ne, N, and Mg for times of typical and enhanced activity of the Sun. The observations were made by satellite 1966 111B (December 1966) and utilized a scanning Bragg crystal spectrometer sensitive to the 8- to 25-Å wavelength range. The spectrometer had a spectral resolution of 0.15 Å, and a spatial resolution of 15 minutes of arc for discrete sources on the disk of the Sun.

141. Walker, A. B. C., Jr.; and Rugge, H. R.: Variation in the Solar X-Ray Line Spectrum below 25 Å. *Astron. J.*, vol. 72, 1967, p. 835.

A solar-pointed scanning Bragg-type crystal spectrometer flown aboard the satellite 1966-111B made high-resolution measurements of the solar spectrum between 9 and 25 Å from mid-December 1966 to early March 1967. The instrument included a KAP crystal, a photoelectric detector and a scaler. The major lines observed at all times were due to the ions N VII, O VII, O VIII, Fe XVII, Ne IX, Ne X, and Mg XI. The lines with lower ionization potentials appear to come from the whole disk while some of the lines with higher ionization potentials appear to come from several discrete sources. Considerable hardening of the spectrum as well as larger intensity changes in the lines with higher ionization potential have also been observed shortly after the start of a large flare.

142. Watts, R. N., Jr.: Explorer 37 Studies Sun. *Sky and Tel.*, vol. 35, May 1968, pp. 298-299.

The author briefly reviews the NRL Solar Radiation satellite series and some of the results. SR-1 (June 22 through November 1, 1960) was the first successful solar X-ray measuring satellite. SR-1 observations showed that X-rays provide a very sensitive measure of solar activity, sometimes changing significantly within 1 minute. SR-4 found that 44- to 60-Å radiation is especially sensitive to small solar disturbances, and is correlated with solar

plages. Data from Explorer 30 provided evidence that an increase in X-ray background precedes flare activity that can disrupt radio communications on earth. Explorer 37 launched on March 5, 1968 from Wallops Island, Virginia is making observations of solar UV radiation (1080- to 1350-Å), as well as monitoring six bands in the X-ray region between 0.1 and 60 Å.

143. Watts, R. N., Jr.: International Satellite IRIS. Sky and Tel., vol. 35, June 1968, pp. 236.

The author briefly discusses the seven experiments being conducted on board IRIS (ESRO II-B). To monitor the flux of energetic particles in the Van Allen radiation belts, two Geiger-Müller counters are being used. The flux of protons in the energy range of 1 to 100 MeV is being measured. Measurements of the flux and energy of cosmic-ray electrons in combination with radio noise observations are being made. Hard X-rays (1- to 20-Å) from the Sun are being measured. Soft solar X-rays (44- to 70-Å) are also being investigated. The flux and energy spectrum of solar and galactic cosmic ray particles are being studied.

144. White, W. A.: Solar X-Rays: Slow Variations and Transient Events. Space Res. IV, 1964, pp. 771-779.

Solar X-ray flux integrated over the 0.1- to 10-Å interval was measured from the OSO-1 satellite in early 1962 (March-May 1962) using a xenon-filled ion chamber with a thin beryllium window. A slowly varying component of X-ray flux that correlates well with the slowly varying component of 2800-Mc solar radiation was observed. The X-ray flux can be accounted for by localized sources that have the same horizontal extent as Ca plages with thicknesses proportional to their diameter, that have an electron temperature of about 2.8×10^6 K, and that have an electron density of about 5×10^9 electrons per cm^3 . A further conclusion is that for these conditions the ratio of line emission to continuum emission is at least 10:1 and more probably 30:1. In addition to a slowly varying component, transient events (X-ray flares) lasting from 10 minutes to a few hours were frequently observed. Correlations with H α flares, with SID's, and with 2800-Mc transients have been investigated; the results show that as an indicator of local solar activity, the OSO-1 X-ray experiment was more sensitive by a large factor than indicators based on ionospheric wavelengths. X-ray flares were frequently observed to be associated in groups possessing a characteristic pattern; the implications are discussed.

145. Widing, K. G.: Interpretation of the Soft X-Ray Spectrum of the Sun.
Astrophys. J., vol. 143, 1966, pp. 606-609.

A spectrum of the Sun with lines in the soft X-ray region (33- to 72-Å) was obtained from an instrumented rocket by Austin et al. on September 20, 1963. On this spectrum coronal resonance lines from five stage of Si (Si VIII-XII) are seen in the relatively narrow wavelength range of 40- to 61-Å. On a spectrum secured in a rocket flight on May 10, 1963, resonance lines from Si VIII-XI are seen in the 300-Å region. In a preliminary discussion of these Si data it was noted that Si IX and X appear to be the most abundant stages of ionization, corresponding to a temperature of the quiet corona in the range of 1.6 to 1.8×10^6 K. These temperatures result when theoretical ionization equilibria of Si are computed, with recombination rates by the dielectronic process estimated from formulae given by Burgess (1964, 1965). The purpose of this paper is to show that with an isothermal model of the quiet corona at 1.8×10^6 K one may represent other features of the observed soft X-ray spectrum as well as, in particular, the line intensities of the C and Mg ions. Some of the more important lines observed with estimated fluxes are given in graphical form. The total line energy for the 33- to 72-Å band is computed to be about $0.10 \text{ erg cm}^{-2} \text{ sec}^{-1}$. A theoretical plage spectrum is also given. Preliminary computations with temperatures covering the range 1.4×10^6 K showed that the relative intensities of the Si lines in the 40- to 61-Å spectral range were a rapidly changing function of the temperature. The line intensities of C VI, Ne VIII, and Mg X, on the other hand, showed little change. The continuous radiation in the 10- to 100-Å region for the same value of the mass parameter, but a lower temperature of 1.5×10^6 K was also estimated. The results show a continuous energy shortward of the O VII recombination limit at 17 Å exceeding the line energy. The same result is found when the ionic concentrations are computed with only the radiative recombination rates. The predicted continuous flux in the spectral range of the 8- to 12-Å ion chamber is the range 3×10^{-5} erg to 2×10^{-4} erg, depending on the value of $N_{\text{Si}}/N_{\text{H}}$, whereas the observed flux from the quiet Sun is $< 1 \times 10^{-4}$ erg.

146. Widing, K. G.: Interpretation of the Soft X-Ray Spectrum of the Sun.
Astrophys. J., vol. 145, 1966, pp. 380-399.

Coronal resonance-line intensities are discussed in terms of isothermal models of the quiet corona. The ionization theory includes recombination by the dielectronic process. Coronal ions of silicon in the 250- to 370-Å region are best fitted with $T = 1.6 \times 10^6$ K and

$$\frac{N_{\text{Si}}}{N_{\text{H}}} \int N_e^2 dh = 2 \times 10^{22}$$

while the lines in the 33- to 70-Å region are best filled with $T = 1.8 \times 10^6$ K. The relative intensities of the resonance lines of Si indicate a depopulation of the upper level of the ground term which is consistent with an electron density in the quiet corona of 6×10^8 . The intensities of Fe XV and Fe XVI in the active center of September 20, 1963 suggest a temperature in the range 3-5 x 10^6 K and values of $\int N_e^2 dh$ 50 to 80 times the corresponding values in the quiet corona. Line and continuous spectra predicted for the wavelength range below 25 Å are compared with NRL spectrometer measurements and ion-chamber observations in the 8- to 12-Å band. Tables showing relative emission intensities, relative abundances and ionic concentrations, radio-brightness temperatures, theoretical fluxes, comparison of observation and theory below 25 Å, and theoretical continuous and line energy are included.

147. Widing, K. G.; and Sandlin, G. D.: Analysis of the Solar Spectrum in the Spectral Range 33-110 Å. *Astron. J.*, vol. 73, June 1968, pp. S83-S84.

Using the results of Manson (AFCRL) and Austin et al. (NRL), the authors review the soft X-ray region of the solar spectrum. The spectra should be representative of the quiet corona following solar minimum. Approximately 24 ions were identified in the 33- to 110-Å spectral region.

148. Widing, K. G.; and Sandlin, G. D.: Analysis of the Solar Spectrum in the Spectral Range 33-110 Å. *Astrophys. J.*, vol. 152, May 1968, pp. 545-556.

Austin, Purcell, and Tousey had previously photographed the 33- to 72-Å spectral region at 0.1-Å resolution. On February 1, 1966 during a period of minimal solar activity, a second spectrum was obtained at a resolution of 0.2 to 0.3 Å by the same group. The wavelength region was 60 to 110 Å. A reflight of the same instrument on July 27, 1966 when the Sun was active produced a new spectrum with sharper lines. Just before the new NRL spectra were obtained, Manson recorded the solar spectrum in the 33- to 128-Å range, under quiet Sun conditions. There is an excellent correlation of the photographic and telemetered spectra of the quiet Sun. A summary of observational data and results of analysis showing line identifications and intensities with

supplementary notes, references and explanations are given in tabular form in the paper. Approximately 24 ions are identified in the soft X-ray spectrum of the Sun. Further identifications are suggested. Fe and Ni identifications (70-110 Å) are the principal additions to the observational data. Identified as well as unidentified spectral features that enhance with solar activity are pointed out. The lines of lithium-like ions excited by monopole and quadrupole collisions are very strong. Other examples of multipole excitation are pointed out in the spectra of Mg IX, Si XI, and Fe XVI. Element abundances relative to Si are derived by the method of Pottasch. The Fe and Si emission maximizes the stage Fe XI and Si X, respectively, indicating a general coronal temperature of 1.7×10^6 K. Quantitative agreement with the previous analyses of the $\Delta n = 0$ transitions (150 to 300 Å) of the Fe and Si ions by Jordan and Pottasch is found.

149. Winckler, J. R.; May, T. C.; and Masley, A. J.: Observation of a Solar Bremsstrahlung Burst of 1926 UT, August 11, 1960. J. Geophys. Res., vol. 66, Jan. 1961, pp. 316-320.

An observation has been made with balloon detectors of a radiation increase that can be identified with certainty as a burst of bremsstrahlung originating on the Sun during a class 2^+ flare. The observation was made simultaneously with identical detectors on a balloon at Minneapolis, Minnesota at 45 degrees geographic latitude, at Fort Churchill, Manitoba, Canada at 58.5 degrees geographic latitude, at the same longitude of 95 degrees W. The instruments consisted of an aluminum-walled ionization chamber filled with argon gas operating on the pulsing electrometer system, an aluminum Geiger counter, and a copper Geiger counter. The readings of these instruments are shown for both geographic locations. The equality of response at both geographic locations suggests that the X-rays originate outside the earth and are not bremsstrahlung from the precipitation of electrons trapped in the geomagnetic field. The event is very closely correlated with optical and radio emissions from the flare. A plot of the ionization record in comparison to optical ($H\alpha$) and radio emissions over the same time scan depicts the above correlation. The X-ray burst seems definitely correlated with the type III radio emission and not the type II. A table, listing the characteristics of the optical flare, is provided. A comparison with an earlier flight (March 1958) of the average energy observed is made. For this flight this value was about 30 keV. For the previous flight (also observing a class 2^+ flare) the value was about 500 keV. The total energy content of the two events is very similar. The authors close with a discussion of De Jager's (1960) theory on the generation of solar flare X-rays. The arguments for the production of both X-ray bursts and type III emission by electron jets accelerated

in the flare are briefly outlined. The authors conclude that the correlation determined in this experiment (August 11, 1960) is a verification of De Jager's suggestion.

150. Yefremov, A. I.; Podmoshensky, A. L.; Yefimov, O. N.; and Lebedev, A. A.: Investigations of Solar X-Rays and Lyman Alpha Radiation on August 19-20, 1960. Space Res. III, 1963, pp. 843-854.

A radiation detector consisting of an open type secondary emission multiplier together with various filters, which automatically move in front of the window, was mounted aboard spaceship II. Radiation in the 1.4- to 3-, 5- to 10-, 8- to 21-, and 44- to 110-Å regions were measured. Also measured was the hydrogen Lyman α line at 1216 Å. It was found that radiation in the 44- to 110-Å region was always constant within an accuracy of 88 percent. The radiation flux in the 8- to 21-Å region was constant most of the time, but during flares an increase was observed of 63 percent at one time and of 3.2 times during another flare. In the region below 8 Å, the quiet Sun's radiation was very insignificant, but increased sharply (by more than a factor of 11) during the flare on August 19, 1950. In the 1.4- to 3-Å region, only a background caused by radiation of a nonsolar origin was recorded. The radiation of the quiet Sun was identified with a corona temperature $T = 0.9 \times 10^6$ K. The spectral distribution of the short-wave solar radiation flux over the Earth's atmosphere is determined. Lyman α emission at 1216 Å yields a flux of $5-6 \text{ erg cm}^{-2} \text{ sec}^{-1}$. It was not constant, but did not increase during the above mentioned flare of August 19, 1960.

151. Young, R. M.; and Stober, A. K.: A Soft X-Ray Photoionization Detector. NASA TN D-3169, Accession #N66-16936, Feb. 1966, pp. 1-7.

A direct-current, gas-filled ionization chamber, which is a simple ceramic radiation detector, consists of a ceramic shell incorporating a beryllium window and containing xenon fill gas. The sensitivity is determined by the ion-pair yield and spectral absorption characteristics of xenon along with the transmission properties of beryllium. The fabrication technique for this detector and some observed operating characteristics are also described.

152. Zehnpfennig, T.; Reidy, W. P.; Vaiana, G. S.; and Wiza, J.: The ATM Soft X-Ray Slitless Spectrograph. Astron. J., vol. 73, June 1968, p. S85.

The authors present the general design of a soft X-ray slitless spectrograph to be flown on ATM. The spectrograph consists of an X-ray transmission grating (thin-film plastic replicas shadowed with gold) and an image-forming X-ray telescope with an angular resolution of > 5 seconds of arc and a spectral resolution of 0.2 \AA at 7 \AA .

153. Zhitnik, I. A.; Krutov, V. V.; Maljavkin, L. P.; Mandel'stam, S. L.; and Cheremukhin, G. S.: The X-Ray Photographs and the Spectrum of the Sun in the Region $9.5\text{--}200 \text{ \AA}$. Space Res. VII, 1967, pp. 1263-1280.

Preliminary results are outlined on the solar photographs and spectrum in the $9.5\text{--}200\text{-\AA}$ region obtained by means of instrumentation carried by two geophysical rockets launched on September 20 and October 1, 1965 to an altitude of about 500 km. In both launchings the instrumental equipment consisted of a battery of pin-hole cameras and a spectrograph. The camera battery consisted of 18 cameras. Photographs were recorded on SC-5 Kodak film and UFR-21-3 NIKFI film. A table summarizing the basic data of the cameras in the launch on October 1, 1965 is presented. The Sun photographs are obtained in the following spectrum regions: $\lambda < 10\text{-}$, 8- to 15- , $< 20\text{-}$, $< 25\text{-}$, 44- to 60- , and 170- to 200-\AA . Preliminary estimations for the radiation flux from the region where the X-ray flare occurred give for the spectral interval $\lambda < 25 \text{ \AA} \sim 2 \times 10^{-2} \text{ erg cm}^{-2} \text{ sec}^{-1}$, and for the interval $\lambda < 25 \text{ \AA} \sim 2.6 \times 10^{-1} \text{ erg cm}^{-2} \text{ sec}^{-1}$; the mean intensity of the line $\lambda = 15.0 \text{ \AA}$ (Fe XVII) is about $10^{-2} \text{ erg cm}^{-2} \text{ sec}^{-1}$. The solar spectrum was photographed by means of a grazing incidence spectrograph using SC-5 Kodak film. On the first flight lines in the regions 21.6 to 72.3 \AA and 170 to 195 \AA were recorded. On the second flight lines in the regions 9.5 to 72.3 \AA and 170 to 181 \AA were recorded. A table giving preliminary values of wavelengths determined by these flights for the region 9.5 to 72.3 \AA is presented. A table of lines in the long-wave region of the spectrum is also presented. Many of the X-ray photographs obtained from these experiments are reproduced. Also shown is a table of X-ray flux from active regions in the solar corona during these flights.

AUTHOR INDEX

Acton, L. W. - 1, 2, 3
American Astronomers Report - 4
Anastassiadis, M. - 5
Anderson, K. A. - 6
Argo, H. V. - 7
Arnoldy, R. L. - 8, 9, 10
Atkinson, P. A. - 11
Austin, W. E. - 12, 13, 14
Baez, A. V. - 15
Behring, W. E. - 99
Bergey, J. A. - 7
Blake, R. L. - 16, 17, 18, 19, 20, 21
Boviatsos, D. S. - 5
Bowles, J. A. - 22
Boyd, R. L. F. - 23
Broadfoot, A. L. - 24
Byram, E. T. - 53
Casal, F. G. - 137
Cheremukhin, G. S. - 153
Chitnis, E. V. - 25
Chubb, T. A. - 3, 16, 17, 18, 19, 20, 26, 27, 28, 29, 30, 31, 32, 33, 72, 94
Clark, T. A. - 123
Cline, T. L. - 34, 65
Conner, J. P. - 35
Cooke, B. A. - 22
Culhane, J. L. - 22, 36, 37, 47
Dicke, R. H. - 38
Dolan, J. F. - 39
Donnelly, R. F. - 40
Drake, J. F. - 136
Dvoryashin, A. S. - 41
Efremov, A. I. - 87
Ellison, M. A. - 42
Elwert, G. - 43, 44, 45
Evans, K. - 46, 47
Evans, W. D. - 7
Fazio, G. G. - 39
Frank, L. A. - 84
Freeman, F. F. - 68
Friedman, H. - 16, 17, 18, 19, 20, 28, 29, 30, 31, 32, 33, 48, 49, 50, 51,
52, 53, 54, 72, 94

Fritz, G. - 54
 Gates, W. - 100
 Giacconi, R. 55, 56, 103, 111
 Gibson, Sr. J. - 136
 Glencross, W. M. - 97
 Goldberg, L. - 57, 58
 Gregory, B. N. - 59, 73
 Gursky, H. - 60
 Hall, L. A. - 61, 64
 Harries, J. R. - 62
 Heroux, L. - 61
 Hindley, K. - 63
 Hinteregger, H. E. - 61, 64
 Holt, S. S. - 34, 65
 Hones, E. W., Jr. - 34
 House, L. L. - 21, 66
 Hudson, H. S. - 67, 105
 Jones, B. B. - 68
 Kale, P. - 25
 Kane, S. R. - 8, 9, 10
 Kawabata, K. - 69
 Korchak, A. A. - 70
 Kreplin, R. W. - 3, 28, 29, 30, 31, 32, 33, 54, 59, 71, 72, 73, 94
 Krutov, V. V. - 153
 Kundu, M. R. - 74, 75
 Kupperian, J. E., Jr. - 31
 Landini, M. - 76, 77, 78, 79
 Lebedev, A. A. - 150
 Levitskii, L. S. - 41
 Lichtman, S. W. - 53
 Lin, R. P. - 80
 Lindsay, J. C. - 55, 81, 82, 99
 Lundbak, A. - 83
 Machlum, B. - 84
 Malitson, H. H. - 85
 Maljavkin, L. P. - 153
 Mandel'shtam (Mandel'stam), S. L. - 86, 87, 88, 89, 90, 153
 Mangus, J. D. - 91
 Manley, O. - 103
 Manson, J. E. - 92
 Masley, A. J. - 149
 Maxwell, A. - 93
 May, T. C. - 149
 Meekins, J. F. - 3, 54, 94

Meisel, D. D. - 95
Muney, W. S. - 55, 96, 133
Negus, C. R. - 97
Neupert, W. M. - 98, 99, 100, 101
News Notes - 102
Ney, E. P. - 122
Nichols, W. A. - 32
Pankratov, A. K. - 41, 139
Paolini, F. R. - 103
Pecker, C. - 104
Peterson, L. E. - 67, 105
Podmoshensky, A. L. - 150
Pounds, K. A. - 11, 22, 36, 37, 46, 47, 106, 108, 109
Purcell, J. D. - 12, 13, 14, 131
Reidy, W. P. - 55, 103, 110, 111, 152
Rense, W. A. - 112, 138
Rohrlich, F. - 104
Rossi, B. - 56
Rugge, H. R. - 113, 114, 140, 141
Russell, P. C. - 108, 115, 116
Russo, D. - 77, 78, 79
Sakurai, K. - 117
Sandlin, G. D. - 147, 148
Sanford, P. W. - 22, 36, 37
Schwartz, D. A. - 67, 105
Schweizer, W. - 61, 64
Shaw, M. L. - 22, 36
Shklovskii, I. S. - 118
Shklovsky, J. - 119
Shurygin, A. - 90
Singer, S. - 7, 35
Smith, D. - 36
Smith, T. S. - 120
Snider, C. B. - 12
Snijders, R. - 121
Stein, W. A. - 122
Stober, A. K. - 151
Stogsdill, E. E. - 35
Stuhlinger, E. - 123
Swartz, M. - 100, 101
Tagliaferri, G. L. - 77, 78, 79
Takao, K. - 124
Teske, R. G. - 125
Thomas, L. - 126, 127

Tindo, I. - 90
Tousey, R. - 12, 13, 14, 128, 129, 130, 131, 132
Underwood, J. H. - 91, 96, 133
Unzicker, A. E. - 16, 17, 18, 19, 20, 32, 54
Vaiana, G. S. - 103, 110, 111, 152
Van Allen, J. A. - 84, 134, 135, 136
Vasilyev, B. - 90
Venables, F. H. - 127
Vette, J. I. - 137
Violet, T. - 138
Vladimirskii, B. M. - 139
Voron'ko, J. - 90
Walker, A. B. C., Jr. - 113, 114, 140, 141
Watanabe, K. - 131
Watts, R. N., Jr. - 142, 143
White, W. A. - 101, 144
Widing, K. G. - 12, 13, 14, 132, 145, 146, 147, 148
Williams, K. M. - 127
Willmore, A. P. - 37, 109
Wilson, R. - 68
Winckler, J. R. - 6, 8, 9, 10, 149
Wiza, J. - 152
Yefimov, O. N. - 150
Yefremov, A. I. - 150
Young, R. M. - 100, 151
Zehnpfennig, T. - 55, 60, 103, 111, 152
Zhitnik, I. A. - 153

SUBJECT INDEX

Active Sun (coronal condensations, plages, quiet Sun, solar activity IGY, IQSY, etc.): 2, 5, 6, 8, 9, 10, 12, 16, 19, 24, 28, 29, 30, 32, 33, 34, 35, 36, 37, 42, 44, 46, 47, 50, 51, 54, 55, 58, 59, 62, 63, 69, 71, 72, 73, 75, 76, 77, 78, 79, 80, 81, 82, 83, 84, 86, 87, 88, 89, 92, 94, 97, 98, 100, 103, 105, 106, 108, 110, 111, 113, 114, 115, 116, 117, 121, 124, 125, 128, 129, 133, 134, 137, 138, 139, 140, 142, 144, 146, 147, 148, 149, 150, 153.

Characteristic X-Rays ($K\alpha$ type emission): 1, 21, 66.

Correlations and Comparisons (with theory, with other experiments, with SID, with solar activity, with microwaves, $H\alpha$, Lyman α , etc.): 2, 5, 6, 8, 9, 10, 16, 20, 24, 31, 34, 35, 36, 37, 40, 41, 42, 43, 44, 45, 46, 47, 48, 49, 50, 53, 55, 57, 58, 59, 62, 67, 69, 71, 72, 73, 74, 75, 76, 77, 78, 79, 80, 81, 82, 83, 84, 87, 88, 89, 90, 96, 97, 99, 100, 103, 104, 105, 106, 108, 110, 111, 115, 116, 117, 121, 124, 125, 126, 127, 128, 129, 133, 134, 135, 137, 139, 141, 142, 144, 148, 149, 150.

Energetic Particle Emission (electrons, protons, flares, cosmic-rays etc.): 1, 6, 8, 9, 10, 40, 41, 62, 65, 80, 93, 117, 118, 121, 122, 135, 139, 143.

Extreme Ultraviolet Radiation (EUV, XUV, UV, Lyman α , $H\alpha$, etc.): 4, 12, 13, 14, 31, 32, 40, 46, 48, 49, 50, 51, 52, 53, 58, 59, 61, 64, 68, 72, 79, 82, 85, 87, 88, 90, 97, 98, 99, 101, 103, 104, 110, 112, 118, 124, 127, 128, 129, 130, 131, 132, 138, 142, 149, 150, 153.

Instrumentation and Analysis (detectors, spectrometers, pinhole cameras, films, X-ray photography, X-ray telescopes, optics, methods, techniques, equations, calculations): 3, 4, 6, 7, 8, 9, 10, 11, 12, 13, 14, 15, 16, 17, 18, 19, 20, 22, 23, 24, 25, 29, 30, 31, 32, 33, 34, 36, 38, 43, 46, 47, 48, 50, 52, 53, 54, 55, 56, 57, 58, 59, 60, 61, 62, 64, 66, 68, 69, 71, 72, 73, 75, 76, 77, 78, 79, 81, 84, 86, 87, 88, 89, 91, 92, 94, 96, 97, 98, 99, 100, 101,

102, 103, 106, 107, 108, 109, 110, 111, 112, 113, 114, 115,
116, 121, 122, 123, 124, 126, 127, 128, 129, 130, 131, 133,
135, 137, 138, 140, 141, 143, 144, 145, 146, 148, 149, 150,
151, 152, 153.

Ionospheric Disturbances (SID, atmospheric absorptions, etc.): 2, 3, 5,
9, 28, 31, 35, 37, 40, 41, 42, 44, 53, 69, 71, 72, 76, 79, 80,
82, 83, 95, 124, 126, 127, 134, 135, 137, 139, 142, 144.

Microwave Emission (radio bursts, radiowaves, etc.): 2, 6, 8, 9, 10,
16, 22, 24, 25, 34, 35, 36, 37, 40, 41, 42, 62, 65, 67, 69, 73,
74, 75, 77, 78, 79, 80, 81, 82, 85, 86, 88, 93, 95, 99, 103, 111,
117, 122, 124, 127, 135, 137, 139, 143, 144, 149.

Nonsolar X-Ray Emission (celestial sources, galactic, Sco X-1, Tau X-1,
background, etc.): 23, 26, 27, 48, 105, 128.

Reviews (general, topic, bibliography, etc.): 23, 26, 42, 48, 49, 50, 52,
57, 58, 63, 74, 82, 85, 87, 88, 89, 90, 106, 128, 129, 130,
142.

Solar Eclipse Experiments: 5, 7, 71, 90, 95.

Solar Flares: 1, 2, 3, 6, 8, 9, 27, 28, 30, 31, 33, 34, 36, 37, 40, 41,
42, 45, 50, 52, 58, 59, 63, 65, 67, 69, 70, 71, 72, 73, 74, 75,
77, 78, 79, 80, 81, 83, 84, 89, 90, 94, 100, 101, 105, 106, 110,
117, 118, 119, 121, 122, 132, 134, 135, 137, 139, 141, 144, 149,
150.

X-Ray Emission (spectra, tables, ions, line, continuum, etc.): 7, 12, 13,
14, 17, 18, 19, 20, 21, 29, 37, 42, 43, 45, 46, 47, 50, 52, 54,
61, 64, 69, 73, 82, 86, 88, 89, 92, 97, 98, 99, 100, 101, 104,
112, 113, 114, 120, 122, 128, 129, 130, 132, 137, 138, 140, 141,
144, 145, 146, 147, 148, 153.

X-Ray Flight Experiments-

Balloon: 6, 31, 137, 149

Rocket: 4, 7, 12, 13, 14, 16, 17, 18, 19, 20, 22, 24, 28, 29,
30, 31, 33, 37, 44, 45, 46, 47, 48, 49, 50, 51, 52, 53,
54, 55, 58, 61, 64, 66, 68, 71, 87, 88, 89, 90, 92, 96,
97, 102, 104, 106, 108, 110, 111, 115, 116, 128, 130,
131, 133, 138, 145, 153.

Satellite: 2, 3, 5, 8, 9, 10, 25, 32, 34, 35, 36, 37, 50, 51,
52, 59, 62, 67, 72, 73, 76, 77, 78, 79, 80, 81, 82,
83, 84, 88, 89, 90, 94, 98, 99, 100, 101, 103, 105,
106, 109, 113, 114, 117, 124, 125, 126, 127, 134,
135, 136, 140, 141, 142, 143, 144, 150.

X-Ray Production Mechanisms (bremsstrahlung, synchrotron, inverse-Compton, thermal, nonthermal, recombination, etc.): 1, 2, 6,
10, 27, 28, 33, 34, 37, 39, 43, 44, 45, 58, 65, 67, 69, 70, 74,
75, 79, 80, 86, 88, 89, 93, 106, 111, 117, 118, 119, 120, 121,
122, 125, 130, 139, 149.

APPENDIX

TABLE A-1. TABULATION OF ROCKET AND BALLOON SOLAR X-RAY FLIGHT EXPERIMENTS

Date	Time ^a	SC	Lab	R, B	Designation	Instrumentation	$\Delta\lambda$	Ref
11/18/48	3:34 pm MST	Q	NRL	R		Phosphors	< 8, 1040-1340	131
2/17/49	10:00 am MST	A	NRL	R		Phosphors	< 8, 1040-1340	131
4/11/49	3:05 pm MST	Q	NRL	R		Phosphors	< 8, 1040-1340	131
9/29/49	1730	A	NRL	R	V-2, #49	p.c., i.c.	2-8, 8-20, 1100-1350, 1425-1650, 1725-2100	30, 31, 44, 50, 53, 71, 87, 89
2/17/50	11:01 am MST	Q	NRL	R		Phosphors	< 8, 1040-1340	131
5/1/52	1459	Q	NRL	R	A-9	p.c., i.c.	2-8, 8-20	30, 31, 44, 45, 50, 71, 87, 89
5/5/52	1344	Q	NRL	R	A-10	p.c., i.c.	2-8, 8-20	30, 31, 44, 45, 50, 71, 87, 89
12/15/52	2138	Q	NRL	R	Viking 9	G.c.	< 8, 8-20	31, 44, 87
11/15/53	2240	Q	NRL	R	A-14	p.c., i.c.	2-8, 8-20, 44-100	30, 31, 44, 45, 50, 71, 87, 89
11/25/53	1546	Q	NRL	R	A-15	p.c., i.c.	2-8, 8-20	28, 30, 31, 45, 50, 71, 89
12/1/53	1529	Q	NRL	R	A-16	p.c., i.c.	2-8, 8-20, 44-100	28, 30, 31, 37, 44, 45, 50, 71, 87, 89
10/10/55		Q	NRL	R			2-8, 8-20	45, 50
10/18/55	2250	Q	NRL	R	A-34	p.c., i.c.	< 8, 8-20	30, 31, 50, 71, 89
6/20/56	1905	A	NRL	R-B	Rockoon, 5.31	i.c., G.c. photo. [NaI (Tl)]	3-8, Lyman α	31, 89
7/20/56	1915	A	NRL	R	D-8 (Deacon)	p.c., i.c.	< 8, 8-20, 44-100	30, 31, 45, 50, 71
11/17/56			NRL	R	A-43		44-100	45, 50
8/20/57	1650	A	NRL	R	Dan 20, 7.42 F (Nike-Deacon)	p.c., i.c.	< 8, 8-20, 3-8	50, 71, 89
8/29/57	2113	A	NRL	R	Dan 23, 7.45 F	p.c., i.c.	< 8, 8-20, 3-8	50, 71, 89
9/18/57	1054	A	NRL	R	Nike-Asp 7.49 F		> 1.5	89
6/4/58	5:54 am MST	Q	U. Colorado	R		g.i. spect.	80-1216	138
3/30/59	8:15 am MST	Q	U. Colorado	R		g.i. spect.	80-1216	138

TABLE A-1. (Continued)

Date	Time ^a	SC	Lab	R, B	Designation	Instrumentation	$\Delta\lambda$	Ref
7/21/59	Morning		USSR	R		p.c.	3-10, 5-15	37, 90
	Evening		USSR	R		p.c.	3-10, 5-15	37, 90
7/24/59	1634	A, (Q)	NRL	R	NN 8.67 CF (Nike-Asp)	p.c., i.c., s.c.	< 8, 8-20, 44-60 (20-200 keV)	33, 50, 71, 89
8/7/59	1705	Q	NRL	R	NN 8.68 CF	p.c., i.c.	2-8, 8-20	33, 50, 71, 89
8/14/59	1600	Q	NRL	R	NN 8.69 CF	p.c., i.c., s.c.	2-8, 8-20, < .6, 44-60	28, 30, 31, 33, 37, 45, 50, 71, 89
8/24/59	2247	A	NRL	R	NN 8.71 CF	p.c., i.c., s.c.	2-8, 8-20, 44-60 (20-200 keV)	28, 33, 50, 71, 89
8/29/59	1610	Q	NRL	R	NN 8.72 CF	p.c., i.c.	2-8, 8-20	33, 50, 71, 89
8/31/59	2252	A	NRL	R	NN 8.73 CF	p.c., i.c., s.c.	2-8, 8-20, 44-60 (20-200 keV)	28, 30, 31, 33, 50, 71, 89
9/1/59	1700	A	NRL	R	NN 8.75 CF	p.c., i.c., s.c.	< .6	28, 33, 50, 71, 89
9/17/59		Q	USSR	R			2-8, 8-20, (20-200 keV)	89
12/21/59	Morning	Q	USSR	R			8-15	89
	Evening	Q	USSR	R			2-10	89
1/29/60			AFCRL	R		g.i. monochromator photoelectric detector	55-310	64
4/19/60	1415	A	NRL	R		p.h.c.	0-80 (20-60)	16, 102
8/11/60	1926		U. Minnesota	B		i.c., G.c.		149
8/17/60		Q	CSRL	B		s.c. (NaI)	> 80 keV	137
10/12/60		A	CSRL	B		s.c. (NaI)	> 80 keV	137
11/23/60		Q	USSR	R			8-15	89
2/15/61			USSR	R			< 10	90
6/21/61	1445	A	NRL	R		p.h.c.	10-100	16
9/27/61		Q	USSR	R			2-8, 8-14	89
	0025	A	U. Leicester	R	SL 40	p.c.	7-15	37
9/28/61	1400-2530		Berkeley- Minnesota	B	122 F Flin Flon	s.c., p.h.a.	20-150 keV	6
10/24/61		Q	CRG USSR	R			8-15	89
10/18/62		Q	USSR				2-10, 8-18	89
3/1/63		Q	U. Leicester	R	SL 84	p.c.	7-15	37

TABLE A-1. (Concluded)

Date	Time ^a	SC	Lab	R, B	Designation	Instrumentation	$\Delta\lambda$	Ref
4/4/63			NRL	R		B.c.s. (EDDT, KAP, ML), p.h.c.	2-8, 5-25, 20-80	20
5/2/63			AFCRL	R		g.i. monochromator photoelectric detector spect.	55-310	58, 64
5/10/63			NRL	R		B.c.s. (KAP, EDDT, OHS) G.c., p.h.c.	44-630	4, 13, 14, 145
7/25/63			NRL	R		B.c.s. (KAP)	2-8, 5-25, 20-90	17, 19, 20, 58, 88
7/27/63			NRL	R		g.i. spect., B.c.s.	1-25	18
9/20/63			NRL	R			33-188	4, 13, 14, 58, 145
3/30/64	Near noon		AFCRL	R		g.i. monochromator photoelectric detector p.h.c.	55-312	58, 61
8/11/64	0540	Q	U. Leicester	R		p.h.c.	< 25, 44-70	116
12/17/64	0335	A	U. Leicester	R		p.h.c.		115
3/17/65	1510	Q	ASE, GSFC	R	NAS 4.63 GS	g.i. spect.	8-12	55, 110, 111
6/23/65	1435.5		Kitt Peak	R		p.h.c.	8-24, 8-18, 0-20, 0-12	24
9/20/65			USSR	R		p.h.c., spect.	< 10, 8-15, < 20, < 25, 44-60, 170-200	153
10/1/65			USSR	R		p.h.c., spect.	< 10, 8-15, < 20, < 25, 44-60, 170-200	88, 153
10/20/65		Q	NRL	R		g.i., spect.		12
11/3/65	1900		AFCRL	R		G.c., g.i. monochromator photoelectric detector	30-128	58, 92
2/1/66		Q	NRL	R		g.i. spect.	0-150, 160-410	12
4/28/66		A	NRL	R		g.i.s.		12
5/5/66	0414	Q	U. Leicester	R	SL 304	B.c.s. (KAP), p.c.	8-20, 11-25	46, 47, 97
5/15/66	0500		MSSL, U. Leicester	R	CO6 (Centaure)	g.i. spect. p.c.	< 5	22
5/20/66	1510		GSFC	R	NASA 4.95 GS	g.i. spect., p.c.	2-11, 8-20, 3-75	133
7/27/66		Q	NRL	R		g.i. spect.		148
10/4/66	2029	Q	NRL	R		B.c.s. (EDDT, KAP) G.c., p.h.c. (g.i.)	1.7-8.3 5-25	54, 58
11/12/66	1200		LASL	R	Nike-Tomahawk	G.c., B.c.s.	16-40	7
	1407		LASL	R	Nike-Tomahawk	G.c., B.c.s.	16-40	7
	1445		LASL	R	Nike-Tomahawk	G.c., B.c.s.	16-40	7
8/8/67		Q	U. Leicester	R		g.i. p.c.	8-20, Lyman α	97
10/3/67			GSFC	R		g.i. spect.	6-11, 8-20, 27-40, 44-60	96
3/20/68	0527		ARUCL	R	SL 408	g.i.s., p.h.c.	~ 12-70, ~ 140-500	68

a. Expressed as UT unless otherwise noted.

TABLE A-2. TABULATION OF SATELLITE SOLAR X-RAY FLIGHT EXPERIMENTS

Designation	Period of Observation	Instrumentation	$\Delta\lambda$	Ref
1963-21 C	6/63-7/63	i. c.	< 8, 8-12, 44-60	106, 126
1964-01 D	1/11/64-3/65	i. c., photometers	2-8, 8-14, 8-16, 44-55, 44-60	25, 73, 78, 79, 127
Ariel (UK-1, S51, 1962 omicron)	4/26/62-11/1/62	p. h. a., p. c.	4.7-5.4, 5.4-6.4, 6.2-7.9, 7.3-9.7, 9.7-13.8	37, 82, 89, 106, 109
Explorer 33	7/1/66-1/30/68	G. c.	2-12	134, 135, 136
Explorer 35	7/19/67-1/30/68	G. c.	2-12	136
Explorer 37	3/5/68	G. c.	0.1-60, 1080-1350	142
IMP III	12/22/65 6/25-27/66	G. c., i. c.	> 40 keV (electron) (10-100 keV)	80
IMP F	6/67	p. c.	> 4 keV (X-ray) > 80 keV (electron) > 2.1 MeV (proton)	62
Injun I	7/61-8/61	G. c.	< 14	84
IRIS (ESRO II B)	5/17/68	G. c.	1-20, 44-70	143
Mariner V	6/14/67-11/21/67	G. c.	2-8	136
OGO I(A), III(B)	9/5/64-6/30/66	i. c.	10-50 keV (10-10 keV, 16-106 keV, 106- 150 keV) 80 keV-1 MeV	8, 9, 10, 34
OSO I	3/7/62-5/17/62	g. i. s., s. c., i. c.	20-100 keV, < 8, 50-400	81, 82, 89, 98, 99
OSO II	3/7/62-3/65	G. c., i. c.	0.1-10, 1-8, 8-20, 44-60	73, 144

TABLE A-2. (Concluded)

Designation	Period of Observation	Instrumentation	$\Delta\lambda$	Ref
OSO III	7/7/66-3/22/67	Positron detector, B.c.s.	1.3-20, 20-400, 7.7-12.5 keV, 12.5- 22 keV	34, 67, 100, 101, 105, 125
OSO IV	10/23/67-6/68	Spectroheliograph B.c.s. p.c.s., p.h.a.	0.5-3.9 1.4-8.4 8-18, 44-60	36, 94, 103
OV1-10 (1966-111B)	12/66-3/67 4/67-6/67	B.c.s., s.c., p.h.a., p.c.	7-25	113, 114, 140, 141
Sputnik II, III (Spaceship II, III)	8/19-20/60 12/1-2/60	Counters	15-20 keV 1.4-3, 8-21 5-10, 44-110 Lyman α	90, 150
SR I (Greb I, 1960 η 2)	6/22/60-11/1/60	i.c.	2-8, 1050-1350	32, 50, 72, 82, 142
SR 3	6/29/61-11/26/61	i.c.	2-8, 8-20	3, 89
SR 4	1/64-7/64	i.c.	2-8, 8-14, 8-16, 44-55, 44-60	89, 142
SR 7 (1965-16 D)	3/65-7/31/65	i.c., G.c.	0.5-3, 0-8, 8-12, 8-16, 0-20, 44-55, 44-60	73, 76, 77
SR 8 (Explorer 30 1965-93 A)	11/65-8/31/66	i.c., G.c.	1-8, 8-16, 1-20, 44-60, 1080-1350, 1225-1350, 0.5-3	59, 76, 83, 124, 142
Vela satellites	10/17/63-7/17/64	s.c.	0.5-15	35

TABLE A-3. TABULATION OF OBSERVED SOLAR SPECTRAL
LINES (1- to 100-Å) BY FLIGHT EXPERIMENT

[illegible]

TABLE A-3. (Continued)

No.	Date of Observation	R, B, S	λ Observed (Å)	λ Predicted (Å)	Ion	Transition	Remarks	Reference
2	7/25/63	R	18.54	18.627	O VII	$1s^2\ ^1S_0-1s3p\ ^1P_1$	Doub. by deflec.	17, 19, 88, 89
			18.61	18.969	O VIII	$1s\ ^2S_{1/2}-2p\ ^2P_{3/2, 1/2}$	p. sys. Doub., Broad Wings, Ly α Ly α	
			18.8	18.97	O VIII		Ly β	
			18.9	20.97	N VII	$1s\ ^2S_{1/2}-3p\ ^2P_{3/2, 1/2}$	Very weak, Ly β	
			20.5	20.910	N VII		Broad	
			21.55	21.602	O VII	$1s^2\ ^1S_0-1s2p\ ^1P_1$	Broad	
			21.6	21.60	O VII		Broad	
			21.80	21.804	O VII		Broad	
			21.70	23.2	O VII		Broad, Uid., (Poss. N VI)	
			24.7	24.78	N VII		Ly α	
			24.8	24.781	N VII		Broad, Ly α	
			26.9	27.0	C VI		Ly γ	
			27.6				Uld.	
			28.5	28.46	C VI		Ly β	
			30.0	15.01 \pm 2	Fe XVII			
3	7/27/63	R	30.9	15.6 \pm 2				18
			31.8	16.01 \pm 2	O VIII		Ly β	
			33.75	33.74	C VI		Ly α	
			13.7	13.8	Fe XVII			
			15.0	15.0	Fe XVII			
			15.2	15.26	Fe XVII			
			16.0	16.0	O VIII			
			16.7	16.8	Fe XVII			
			17.05	17.05	Fe XVII			
			17.7	17.8	O VII			
			18.9	18.97	O VIII			

TABLE A-3. (Continued)

No.	Date of Observation	R, B, S	λ Observed (Å)	λ Predicted (Å)	Ion	Transition	Remarks	Reference
3	7/27/63	R	20.8	20.9	N VII			18
			21.5	21.6	O VII			
			21.7	21.8	O VII			
			22.0	22.07				
			24.8	24.8	N VII		(Poss. O VI)	
4	9/20/63	R	33.74		C VI	$1s^2 2s-2p^2 P^0$		13
			(39.28)		Si XI	$2s^2 2p^2^3 P-2s^2 2p3d^3 D^0$	Derived	
			40.27		C V	$1s^2^1 S-1s2p^1 P^0$		
			40.73		C V	$1s^2^1 S-1s2p^3 P^0$		
			(40.91, .95)		Si XII	$2s^2 2s-3p^2 P^0$	Derived	
			41.49				Utd.	
			(42.51, .54, .58)		S X	$2s^2 2p^2^4 S^0-2s^2 2p^2 3d^4 P$	Derived	
			43.76		Si XI	$2s^2^1 S-2s3p^1 P^0$		
			44.02, .16		Si XII	$2p^2 P^0-3d^2 D$		
			49.22		Si XI	$2s2p^1 P^0-2s3d^1 D$		
			50.35		Fe XVI	$3s^2 2s-4p^2 P^0$		
			50.52		Si X	$2s^2 2p^2^3 P^0-2s^2 3d^2 D$		
			50.69		Si X			
			50.70		Si X			
			52.9		Fe XV	$3s^2^1 S-3s4p^1 P^0$		
			54.14		Fe XVI	$3p^2 P^0-4d^2 D$		
			54.18		S IX	$2s^2 2p^2^3 P-2s^2 2p^2 3s^3 D^0$		
			55.34		Si IX	$2s^2 2p^2^3 P-2s^2 2p3d^3 D^0$		
			57.88, .92		Mg X	$2s^2 2s-3p^2 P^0$		
			61.00, .02, .07		Si VIII	$2s^2 2p^2^4 S^0-2s^2 2p^2 3d^4 P$		

TABLE A-3. (Continued)

No.	Date of Observation	R, B, S	λ Observed (Å)	λ Predicted (Å)	Ion	Transition	Remarks	Reference
4	9/20/63	R	61.61		Si IX	$2s^2 2p^2 \ ^3P - 2s^2 2p 3s \ ^3P^0$		13
			61.85		Si VIII	$2s^2 2p^2 \ ^2D^0 - 2s^2 2p^2 3d \ ^2D, \ ^2F$		
			62.75		Mg IX	$2s^2 \ ^1S - 2s 3p \ ^1P^0$		
			63.29		Mg X	$2p \ ^2P^0 - 3d \ ^2D$		
			63.72		Fe XVI	$3p \ ^2P^0 - 4s \ ^2S$		
			65.85		Mg X	$2p \ ^2P^0 - 3s \ ^2S$		
			66.24		Fe XVI	$3d \ ^2D - 4f \ ^2F^0$		
			67.20		Mg IX	$2s 2p \ ^3P^0 - 2s 3d \ ^3D$		
			69.62		Si VIII	$2s^2 2p^2 \ ^4S^0 - 2s^2 2p^2 \ 3s \ ^4P$		
			69.95		Mg IX	$2p^2 \ ^1D - 2p 3d \ ^1F^0$		
			70.00		Fe XV	$3s 3d \ ^3D - 3s 4f \ ^3F^0$		
			72.31		Mg IX	$2s 2p \ ^1P^0 - 2s 3d \ ^1D$		
			88.08, .12?		Ne VIII	$2s \ ^2S - \ ^3p \ ^2P^0$		
			2 x 44.16		Si XII			
5	9/20/65	R	21.6	21.60 21.80	O VII O VII		(21.55, 21.7)	153
			33.75	33.74	C VI		(33.75), Ly α	
			40.3	40.27	C V		(40.26)	
			42.2	42.51 42.54 42.58	S X S X S X		(42.54)	
			43.2	21.60 x 2	O VII		(43.18)	
			44.0	43.76 44.02 44.05 44.16 44.22 44.25	Si XI Si XII Mg X Si XII Si IX Si IX		(43.75), blend (44.18)	

TABLE A-3. (Continued)

No.	Date of Observation	R, B, S	λ Observed (Å)	λ Predicted (Å)	Ion	Transition	Remarks	Reference
5	9/20/65	R	45.3	45.66	Si XII		(45.66)	153
			46.1	46.26	Si XI		(46.32)	
				46.30	Si XI			
				46.40	Si XI			
			47.5	47.61	Si XI		(47.6)	
				47.65	Si XI			
				47.65	Si X			
				47.79	Si X			
			49.4	49.22	Si XI		(49.23)	
				49.26	Si XI			
			50.6	50.52	Si X			
				50.56	Fe XVI			
				50.69	Si X			
			52.1	52.07	Si X		(52.09)	
			52.7	52.16	Si X			
				52.81	Si IX		(52.83)	
				52.84	Si IX			
			54.1	54.14	Fe XVI		(54.16)	
				54.18	S IX			
			55.34	55.30	Si IX		(55.34)	
				55.36	Si IX			
				55.40	Si IX			
			57.6	57.88	Mg X		(57.9)	
				57.92	Mg X			
			59.0	58.88	Si VIII		(59.03)	
				58.91	Si IX			
				58.96	Fe XIV			
				59.00	Si IX			
				59.08	Si IX			
			61.05	60.99	Si VIII		(61.06)	
				61.02	Si VIII			
				61.07	Si VIII			
				61.80	Si VIII			

TABLE A-3. (Continued)

No.	Date of Observation	R, B, S	λ Observed (Å)	λ Predicted (Å)	Ion	Transition	Remarks	Reference
5	9/20/65	R	61.8	61.85	Si VIII		(61.85)	153
				61.90	Si VIII			
				61.91	Si VIII			
				61.85	Si IX			
				61.92	Mg IX			
				61.96	Mg IX			
				62.75	Mg IX			
				62.81	Si VIII			
				62.85	Si VIII			
				62.68	Fe XVI			
				63.15	Mg X			
				63.23	Si VIII			
				63.27	Si VIII			
				63.29	Mg X			
				67.09	Mg IX			
				67.14	Mg IX			
				67.24	Mg IX			
			67.0	69.95	Mg IX		(67.15)	
				69.95	Fe XV			
				69.99	Fe XV			
				70.05	Fe XV			
				72.23	Mg IX			
				72.31	Mg IX			
				9.17	Mg XI			
				11.1	Ne IX			
				11.1	Na X			
				11.54	Ne IX			
	10/1/65	R	9.5	12.14	Ne X		(69.99)	
				12.26	Fe XVII			
				12.4	Ne IX			
				13.45	Ne IX			
				13.7	Ne IX			
				13.82	Fe XVII			
				13.82	Fe XVII			

TABLE A-3. (Continued)

No.	Date of Observation	R, E, S	λ Observed (Å)	λ Predicted (Å)	Ion	Transition	Remarks	Reference
6	10/1/65	R	14.2	14.82	O VIII		Ly δ , (15.0)	153
			14.9	15.01	Fe XVII			
			15.20	15.18	O VIII		Ly γ , (15.25)	
			15.6	15.26	Fe XVII			
			16.0	16.006	O VIII		Ly β , (16.0)	
			16.85	16.77	Fe XVII		(16.72)	
			17.1	17.05	Fe XVII		(17.01, 17.05)	
			18.9	18.97	O VIII		Ly α , (18.8, 18.9)	
			20.5	20.91	N VII		Ly β , (20.8)	
			21.6	21.60	O VII		(21.55, 21.7)	
			21.80	21.80	O VII			
			24.7	24.78	N VII		Ly α , (24.8)	
			26.9	27.0	C VI		Ly γ	
			27.6					
			28.5	28.46	C VI		Ly β	
			30.0	15.01 x 2	Fe XVII			
			30.9	15.26 x 2	Fe XVII			
			30.9	15.6 x 2	Fe XVII			
			31.8	16.006 x 2	O VIII		Ly β , blend	
			33.9	16.77 x 2	Fe XVII		Ly α , (33.75);	
				33.74	C VI		(Blend)	
			35.6	17.05 x 2	Fe XVII		Uld.	
			36.6				Uld.	
			37.7	18.97 x 2	O VIII		Ly α	

TABLE A-3. (Continued)

No.	Date of Observation	R, B, S	λ Observed (\AA)	λ Predicted (\AA)	Ion	Transition	Remarks	Reference
6	10/1/65	R	38.7				Uld.	153
			39.6				Uld.	
			40.9	40.91 40.95	Si XII Si XII		(40.92)	
			41.8	20.91 x 2	N VII		Ly β	
			43.8	43.76 44.02	Si XI Si XII		(43.75) (44.18)	
				44.05 44.16	Mg X Si XII			
				44.22 44.25	Si IX Si IX			
			45.9	45.66	Si XII		(45.66)	
			47.9	47.61 47.65 47.65 47.79	Si XI Si XI Si X Si X		(47.6)	
			49.2	49.22 49.26	Si XI Si XI		(49.23)	
			50.6	50.52 50.56 50.69	Si X Fe XVI Si X		(50.7)	
7	2/1/66 7/27/66	R	33.73	33.73	C VI	$1s^2s-2p^2p^0$	Derived	148
			40.27	40.27 (40.93)	C V Si XII	$1s^21s-1s2p^1p^0$ $2s^2s-3p^2p^0$		
			43.76	43.76	Si XI	$2s^21s^0-2s3p^1p^0$		
			44.18	44.16	Si XII	$2p^2p^0-3d^2D$		
			45.49	45.48	Si XII	$2p^2p^0-3s^2s$		
			45.73	45.66	Si XII			
			46.37	46.3	Si XI	$2s2p^3p^0-2s3d^3D$		

TABLE A-3. (Continued)

No.	Date of Observation	R, P, S	λ Observed (Å)	λ Predicted (Å)	Ion	Transition	Remarks	Reference
7	2/1/66 7/27/66	R	49.22	49.22	Si XI	$2s2p\ ^1p^0-2s3d\ ^1D$	Derived	148
			50.51	50.52	Si X	$2p\ ^2p^0-3d\ ^2D$		
			50.68	50.69	Si X			
			(52.30)	(52.30)	Si XI	$2s2p\ ^1p^0-2s3s\ ^1S$		
			52.97	52.91	Fe XV	$3s^2\ ^1S-3s4p\ ^1P^0$		
			54.14	54.14	Fe XVI	$3p\ ^2p^0-4d\ ^2D$		
			54.67	54.73	Fe XVI			
			55.10	55.1	Si IX	$2p^2\ ^3P-2p3d\ ^3P^0$		
			55.31	55.3	Si IX	$2p^2\ ^3P-2p3d\ ^3D^0$		
			57.87	57.90	Mg X	$2s\ ^2S-3p\ ^2P^0$		
			58.97	58.96	Fe XIV			
			59.61	59.58	Fe XIV	$3s^23p\ ^3P^0-3s^24d\ ^3D$	Blend	
			61.05	61.03	Si VIII	$2p^2\ ^4S^0-2p^23d\ ^4P$		
			61.60	61.7	Si IX	$2p^2\ ^3P-2p3s\ ^3P^0$		
			62.74	62.75	Mg IX	$2s^2\ ^1S-2s3p\ ^1P^0$		
			62.98	62.88	Fe XVI			
			63.28	63.29	Mg X	$2p\ ^2p^0-3d\ ^2D$		
			63.72	63.72	Fe XVI	$3p\ ^2p^0-4s\ ^2S$		
			65.67	65.67	Mg X	$2p\ ^2p^0-3s\ ^2S$		
			65.89	65.85	Mg X			
			66.35	66.26	Fe XVI	$3d\ ^2D-4f^2\ F^0$		
			67.20	67.2	Mg IX	$2s2p\ ^3P^0-2s3d\ ^3D$	Blend	
			69.96	70.0	Fe XV	$3s3d\ ^3D-3s4f\ ^3F^0$		
			71.00	71.00	Fe XIV	$3s^23p\ ^3P^0-3s^24s\ ^2S$		
			71.95	(71.96)	Fe XIV		Derived	
			72.31	72.31	Mg IX	$2s2p\ ^1p^0-2s3d\ ^1D$		

TABLE A-3. (Continued)

No.	Date of Observation	R, B, S	λ Observed (Å)	λ Predicted (Å)	Ion	Transition	Remarks	Reference
7	2/1/66 7/27/66	R	74.85	74.86	Mg VIII		Blend	148
			75.03	75.03	Mg VIII	$2s^2 2p^2 \ ^3P - 2s^2 3d^2 \ ^3D$		
			76.01	76.01	Fe XIII	$3s^2 3p^2 \ ^3P - 3s^2 3p4s \ ^3P^0$	Derived	
			76.38	(76.48)	Fe XIII		Derived	
			76.48	(76.55)	Fe XIII			
			77.31	77.34	Ni XI	$3p^6 \ ^1S - 3p^5 4s \ ^1P^0$		
			77.74	77.74	Mg IX	$2s2p \ ^1P^0 - 2s3s \ ^1S$		
			78.71	78.70	Ni XI	$3p^6 \ ^1S - 3p^5 4s \ ^3P^0$	Blend	
			79.48	79.48	Fe XII	$3p^3 \ ^4S^0 - 3p^2 4s \ ^4P$		
			80.03	(80.00)	Fe XII		Derived	
			80.50	(80.49)	Fe XII		Derived	
			82.80	82.82	Mg VIII	$2s^2 2p^2 \ ^2P^0 - 2s^2 3s \ ^2S$		
			83.58	83.6	Mg VII	$2p^2 \ ^3P - 2p3d \ ^3P^0$	Blend	
			84.01	84.0	Mg VII	$2p^2 \ ^3P - 2p3d \ ^3D^0$		
			86.84	86.77	Fe XI	$3p^4 \ ^3P - 3p^3 4s \ ^3D^0$	Blend	
			87.03	87.02	Fe XI		Blend with	
				88.00	Fe XI			
			88.10	88.03	Fe XI		Ne VIII	
				88.17	Fe XI			
			88.10	88.10	Ne VIII	$2s \ ^2S - 3p \ ^2P^0$	Poss. blend Fe XI	
			88.98	89.10	Fe XI	$3p^4 \ ^1D - 3p^3 4s \ ^1D^0$		
			89.20	89.18	Fe XI	$3p^4 \ ^3P - 3p^3 4s \ ^3S^0$		
			89.73	89.77	Fe XI	$3p^4 \ ^1D - 3p^3 4s \ ^3D^0$		
			90.17	90.20	Fe XI		Blend	
			90.47	90.34	Fe XI			
			91.57	91.53	Ni X	$3d \ ^2D - 4f \ ^2F^0$		
			91.78	91.79	Ni X			
			94.01	94.01	Fe X	$3p^5 \ ^2P^0 - 3p^4 4s \ ^2D$		

TABLE A-3. (Continued)

No.	Date of Observation	R, B, S	λ Observed (Å)	λ Predicted (Å)	Ion	Transition	Remarks	Reference
7	2/1/66 } 7/27/66 }	R	95.39	95.34 } 95.37 }	Fe X	$3p^5 2p^0 - 3p^4 4s^2 P$	Blend	148
			96.08	96.12	Fe X	$3p^5 2p^0 - 3p^4 4s^2 P$	Blend	
			96.79	96.79	Fe X			
			97.14	97.12	Fe X	$3p^5 2p^0 - 3p^4 4s^2 P$		
			97.52	97.54	Ne VII	$2s^2 1S - 2s3p^1 P^0$	Blended Fe X. 97.59	
			97.53	97.59	Fe X		Blended or masked (Ne VII, 97.54)	
			97.86	97.84	Fe X			
			98.24	98.27	Ne VIII	$2p^2 P^0 - 3d^2 D$		
8	5/5/66	R	11.45	11.45	Ne IX	$1s^2 1S_0 - 1s3p^1 P_1$		46, 47
			11.56		Ne IX	$1s^2 1S_0 - 1s3p^1 P_1$		
			12.12		Fe XVII	$1s^2 2s^2 2p^6 1S_0 - 1s^2 2s^2 2p^5 4d^1 P_1$	Blends Ne X	
			12.13	12.12	Fe XVII	$1s^2 2s^2 2p^6 1S_0 - 1s^2 2s^2 2p^5 4d^1 P_1$	Blends Ne X	
			12.13	12.13	Ne X	$1s^2 S_{1/2} - 2p^2 P_{1/2, 3/2}$		
			12.24		Ni XIX	$1s^2 2s^2 2p^6 1S_0 - 1s^2 2s^2 2p^5 3d^1 P_1$		
			12.26	12.26	Fe XVII	$1s^2 2s^2 2p^6 1S_0 - 1s^2 2s^2 2p^5 4d^3 D_1$		
			12.42	12.42	Ni XIX	$1s^2 2s^2 2p^6 1S_0 - 1s^2 2s^2 2p^5 3d^1 P_1$		
			12.53				Utd.	
			12.64	12.64	Ni XIX	$1s^2 2s^2 2p^6 1S_0 - 1s^2 2s^2 2p^5 3d^3 D_1$		
			12.80	12.80	Ni XIX	$1s^2 2s^2 2p^6 1S_0 - 1s^2 2s^2 2p^5 3d^3 P^1$	(Disag. in notation in reports) $3P_1$	
			13.45	13.45	Ne IX	$1s^2 1S_0 - 1s2p^1 P_1$		
			13.55	13.55	Ne IX	$1s^2 1S_0 - 1s2p^3 P_1$		
			13.65			$1s^2 2s - 1s2p2s$	Utd., (Poss. Ne VIII)	
			13.77	13.77	Ni XIX	$1s^2 2s^2 2p^6 1S_0 - 1s^2 2s^2 2p^5 3s^1 P_1$		
			13.82	13.82	Fe XVII	$1s^2 2s^2 2p^6 1S_0 - 1s^2 2s^2 2p^5 3p^1 P_1$	(Disag. in trans. in reports) $1s^2 2s^2 2p^5 3p^1 P_1$	
			14.03	14.03	Ni XIX	$1s^2 2s^2 2p^6 1S_0 - 1s^2 2s^2 2p^5 3s^3 P_1$		
			14.25	14.25	Fe XVIII	$1s^2 2s^2 2p^7 1P_3/2 - 1s^2 2s^2 2p^6 (1D) 3d^2 D_{3/2}$		
			14.29	14.29	Fe XVIII	$1s^2 2s^2 2p^7 1P_3/2 - 1s^2 2s^2 2p^6 3d$		
			14.40	14.40	Fe XVIII	$1s^2 2s^2 2p^7 1P_3/2 - 1s^2 2s^2 2p^6 (1P) 3d^2 D_{3/2}$		
			14.82	14.82	O VIII	$1s^2 S_{1/2} - 5p^3 P_{1/2, 3/2}$	Very weak, Ly δ	

TABLE A-3. (Continued)

No.	Date of Observation	R, B, S	λ Observed (Å)	λ Predicted (Å)	Ion	Transition	Remarks	Reference
8	5/5/66	R	15.01	15.01	Fe XVII	$1s^2 2s^2 2p^6 \text{ } ^1S_0 - 1s^2 2s^2 2p^6 3d \text{ } ^1P_1$	Seriously blended, Ly γ	46, 47
			15.17	15.17	O VIII	$1s \text{ } ^2S_{1/2} - 4p \text{ } ^2P_{1/2, 3/2}$		
			15.26	15.26	Fe XVII	$1s^2 2s^2 2p^6 \text{ } ^1S_0 - 1s^2 2s^2 2p^6 3d \text{ } ^3D_1$		
			15.45	15.45	Fe XVII	$1s^2 2s^2 2p^6 \text{ } ^1S_0 - 1s^2 2s^2 2p^6 3d \text{ } ^3P_1$		
			15.62	15.62	Fe XVIII	$1s^2 2s^2 2p^6 \text{ } ^3P_{3/2} - 1s^2 2s^2 2p^6 \text{ } ^1D \text{ } ^3D_{3/2}$	Seriously blended Ly β	
			15.88	15.88	Fe XVIII	$1s^2 2s^2 2p^6 \text{ } ^3P_{3/2} - 1s^2 2s^2 2p^6 \text{ } ^3P \text{ } ^3P_{3/2}$		
			15.96	16.01	O VIII	$1s \text{ } ^4S_{1/2} - 3p \text{ } ^4P_{1/2}$		
			16.01		O VIII	$1s \text{ } ^2S_{1/2} - 3p \text{ } ^2P_{1/2, 3/2}$		
			16.3				Uld. Uld.	
			16.6					
			16.77		Fe XVII	$1s^2 2s^2 2p^6 \text{ } ^1S_0 - 1s^2 2s^2 2p^6 3s \text{ } ^1P_1$		
			17.05	16.77	Fe XVII	$1s^2 2s^2 2p^6 \text{ } ^1S_0 - 1s^2 2s^2 2p^6 3s \text{ } ^3P_1$		
9	10/4/66	R	17.77	17.05	O VII	$1s^2 \text{ } ^1S_0 - 1s 4p \text{ } ^1P_1$	Ly α	54
			18.63	18.97	O VII	$1s^2 \text{ } ^1S_0 - 1s 3p \text{ } ^1P_1$		
			18.94		O VIII	$1s \text{ } ^2S_{1/2} - 2p \text{ } ^2P_{1/2}$		
			18.97		O VIII	$1s \text{ } ^2S_{1/2} - 2p \text{ } ^2P_{1/2, 3/2}$		
			21.60		O VII	$1s^2 \text{ } ^1S_0 - 1s 2p \text{ } ^1P_1$	Uld. (Poss. Fe K) Uld.	
			21.80		O VII	$1s^2 \text{ } ^1S_0 - 1s 2p \text{ } ^3P_1$		
			1.91		Ca XX	$1s \text{ } ^2S_{1/2} - \infty$		
			2.26	2.267	Ca XX	$1s \text{ } ^2S_{1/2} - 7p \text{ } ^2P_{1/2, 3/2}$		
			2.33	2.314	Ca XX	$1s \text{ } ^2S_{1/2} - 6p \text{ } ^2P_{1/2, 3/2}$		
				2.331	Ca XX	$1s \text{ } ^2S_{1/2} - 5p \text{ } ^2P_{1/2, 3/2}$		
				2.361	Ca XX	$1s \text{ } ^2S_{1/2} - 4p \text{ } ^2P_{1/2, 3/2}$		
				2.417	Ca XX	$1s \text{ } ^2S_{1/2} - 3p \text{ } ^2P_{1/2, 3/2}$		
	2.549	Ca XX	$1s \text{ } ^2S_{1/2} - 3p \text{ } ^2P_{1/2, 3/2}$					
2.64	2.987	Ar XVIII	$1s \text{ } ^2S_{1/2} - 4p \text{ } ^2P_{1/2, 3/2}$					
3.05	3.020	Ca XX	$1s \text{ } ^2S_{1/2} - 2p \text{ } ^2P_{1/2, 3/2}$					
3.77	3.733	Ar XVIII	$1s \text{ } ^2S_{1/2} - 2p \text{ } ^2P_{1/2, 3/2}$					

TABLE A-3. (Continued)

No.	Date of Observation	R, B, S	λ Observed (Å)	λ Predicted (Å)	Ion	Transition	Remarks	Reference
9	10/4/66	R	4.41				Utd.	54
			5.73				Utd.	
			5.85				Utd.	
			6.11	6.186	Si XIV	$1s^2 S_{1/2} - 2p^2 P_{1/2, 3/2}$		
			6.52				Utd.	
			6.58				Utd.	
			6.70	6.7	Si XIII	$1s^2 {}^1S_0 - 1s2p {}^1P_1$		
			6.74				Utd.	
			7.05				Utd.	
			7.42	7.47	Mg XI	$1s^2 {}^1S_0 - 1s4p {}^1P_1$		
			7.5	7.47	Mg XI	$1s^2 {}^1S_0 - 1s4p {}^1P_1$		
			7.73	7.757	Al XII	$1s^2 {}^1S_0 - 1s2p {}^1P_1$		
			7.70	7.677	Na XI	$1s^2 S_{1/2} - 7p^2 P_{1/2, 3/2}$		
			7.79	7.735	Na XI	$1s^2 S_{1/2} - 6p^2 P_{1/2, 3/2}$		
			7.82	7.853	Na XI	$1s^2 S_{1/2} - 5p^2 P_{1/2, 3/2}$		
			8.06	8.021	Na XI	$1s^2 S_{1/2} - 4p^2 P_{1/2, 3/2}$		
			9.15	9.16	Mg XI	$1s^2 {}^1S_0 - 1s2p {}^1P_1$		
			9.19	9.23	Mg XI	$1s^2 {}^1S_0 - 1s2p {}^3P_1$		
			9.32	9.29	Mg XI	Satellite (1)		
			9.291	9.291	Ne X	$1s^2 S_{1/2} - 7p^2 P_{1/2, 3/2}$		
			9.33	9.362	Ne X	$1s^2 S_{1/2} - 6p^2 P_{1/2, 3/2}$		
			9.71	9.708	Ne X	$1s^2 S_{1/2} - 4p^2 P_{1/2, 3/2}$		
			11.56	11.53	Ni XIX	$2s^2 2p^6 {}^1S_0 - 2s2p^6 3p {}^1P_1$		
				11.558	Ne IX	$1s^2 {}^1S_0 - 1s3p {}^1P_1$		
				11.59	Ni XIX	$2s^2 2p^6 {}^1S_0 - 2s2p^6 3p {}^3P_1$		
			12.13	12.12	Fe XVII	$2p {}^1S_0 - 4d {}^3D_1$		
				12.134	Ne X	$1s^2 S_{1/2} - 2p^2 P_{1/2, 3/2}$		
			12.26	12.26	Fe XVII	$2p {}^1S_0 - 4d {}^1P_1$		
			13.44	13.44	Ne IX	$1s^2 {}^1S_0 - 1s2p {}^1P_1$		
				13.46	Mn XVI	$2p {}^1S_0 - 4d {}^3D_1$		
			13.56	13.55	Ne IX	$1s^2 {}^1S_0 - 1s2p {}^1P_1$		
				13.61	Mn XVI	$2p {}^1S_0 - 4d {}^1P_1$		

TABLE A-3. (Continued)

No.	Date of Observation	R, B, S	λ Observed (Å)	λ Predicted (Å)	Ion	Transition	Remarks	Reference
9	10/4/66	R	13.70	13.66	Ne IX	Satellite (1)		54
			13.82	13.77	Ni XIX	$2s^2 2p^6 \ ^1S_0 - 2s^2 2p^5 3s \ ^1P_1$		
				13.820	Fe XVII	$2p \ ^1S_0 - 3p^1 \ ^1P_1$		
			13.83	13.83	Ne IX	Satellite (2)		
			13.87	13.887	Fe XVII	$2p \ ^1S_0 - 3p^1 \ ^3P_1$		
				14.08	Ni XIX	$2s^2 2p^6 \ ^1S_0 - 2s^2 2p^5 3s \ ^3P_1$		
			14.23	14.25	Fe XVIII	$2p^5 \ ^2P_{3/2} - 2p^4 \ (^1D) 3d \ ^2D_{5/2}$		
			14.57	14.524	O VIII	$1s \ ^2S_{1/2} - 7p \ ^2P_{1/2, 3/2}$		
				14.634	O VIII	$1s \ ^2S_{1/2} - 6p \ ^2P_{1/2, 3/2}$		
			14.82	14.821	O VIII	$1s \ ^2S_{1/2} - 5p \ ^2P_{1/2, 3/2}$		
			15.01	15.012	Fe XVII	$2p^6 \ ^1S_0 - 2p^5 3d \ ^1P_1$		
			15.06	15.06	Cr XV	$2p \ ^1S_0 - 4d \ ^3D_1$		
			15.13	15.176	O VIII	$1s \ ^2S_{1/2} - 4p \ ^2P_{1/2, 3/2}$		
			15.25	15.21	Cr XV	$2p \ ^1S_0 - 4d \ ^1P_1$		
				15.238	Mn XVI	$2p \ ^1S_0 - 3p^1 \ ^1P_1$		
				15.261	Fe XVII	$2p^6 \ ^1S_0 - 2p^5 3d \ ^3D_1$		
				15.312	Mn XVI	$2p \ ^1S_0 - 3p^1 \ ^3P_1$		
			15.45	15.453	Fe XVII	$2p^6 \ ^1S_0 - 2p^5 3d \ ^3P_1$		
			15.69	15.62	Fe XVIII	$2p^5 \ ^2P_{3/2} - 2p^4 \ (^1D) 3s \ ^2D_{5/2}$		
				15.71	Mn XVII	$2p^6 \ ^2P_{3/2} - 2p^4 \ (^1D) 3d \ ^2D_{5/2}$		
			16.00	16.006	O VIII	$1s \ ^2S_{1/2} - 3p \ ^2P_{1/2, 3/2}$		
				16.01	Fe XVIII	$2p^5 \ ^2P_{3/2} - 2p^4 \ (^3P) 3s \ ^4P_{3/2}$		
			16.07	16.06	Mn XVII	$2p^5 - 2p^4 3d$		
			16.86	16.774	Fe XVII	$2p^6 \ ^1S_0 - 2p^5 3s \ ^1P_1$		
				16.882	Mn XVI	$2p \ ^1S_0 - 3d \ ^1P_1$		
				16.889	Cr XV	$2p \ ^1S_0 - 3p^1 \ ^1P_1$		
			17.04	16.965	Cr XV	$2p \ ^1S_0 - 3p^1 \ ^3P_1$		
				17.051	Fe XVII	$2p^6 \ ^1S_0 - 2p^5 3s \ ^3P_1$		
			17.11	17.08	O VII	$1s^2 \ ^1S_0 - 1snp \ ^1P_1$		
				17.096	Mn XVI	$2p \ ^1S_0 - 3d \ ^3P_1$		
			17.41	17.42	O VII	$1s^2 \ ^1S_0 - 1s5p \ ^1P_1$		
			17.64	17.59	Mn XVII	$2p^5 \ ^2P_{3/2} - 2p^4 \ (^3P) 3s \ ^2P_{3/2}$		
			17.78	17.73	Mn XVII	$2p^5 \ ^2P_{3/2} - 2p^4 \ (^3P) 3s \ ^4P_{3/2}$		
				17.77	O VII	$1s^2 \ ^1S_0 - 1s4p \ ^1P_1$		

TABLE A-3. (Continued)

No.	Date of Observation	R, B, S	λ Observed (Å)	λ Predicted (Å)	Ion	Transition	Remarks	Reference
9	10/4/66	R	18.63	18.587	N VII	$1s^2 S_{1/2} - \infty$	Uld. (Poss. O _K)	54
				18.627	O VII	$1s^2 {}^1S_0 - 1s3p {}^1P_1$		
				18.654	Mn XVI	$2p {}^1S_0 - 3s {}^1P_1$		
				18.670	N VII	$1s^2 S_{1/2} - 1s {}^2P_{1/2, 3/2}$		
			18.63	18.682	N VII	$1s^2 S_{1/2} - 14p {}^2P_{1/2, 3/2}$		
				18.698	N VII	$1s^2 S_{1/2} - 13p {}^2P_{1/2, 3/2}$		
				18.717	N VII	$1s^2 S_{1/2} - 12p {}^2P_{1/2, 3/2}$		
			18.96	18.882	N VII	$1s^2 S_{1/2} - 8p {}^2P_{1/2, 3/2}$		
				18.935	Mn XVI	$2p {}^1S_0 - 3s {}^3P_1$		
				18.969	O VIII	$1s^2 S_{1/2} - 2p {}^2P_{1/2, 3/2}$		
				18.974	N VII	$1s^2 S_{1/2} - 7p {}^2P_{1/2, 3/2}$		
				19.015	Cr XV	$2p {}^1S_0 - 3d {}^3P_1$		
			20.87	20.863	Cr XV	$2p {}^1S_0 - 3s {}^1P_1$		
				20.910	N VII	$1s^2 S_{1/2} - 3p {}^2P_{1/2, 3/2}$		
			21.60	21.602	O VII	$1s^2 {}^1S_0 - 1s2p {}^1P_1$		
			21.80	21.81	O VII	$1s^2 {}^1S_0 - 1s2p {}^3P_1$		
			22.07	22	Ca XIV	$2p^3 {}^4S - 3s {}^4P$		
			23.28					
			23.74	23.77	N VI	$1s {}^1S - np {}^1P$		
			24.78	24.781	N VIII	$1s^2 S_{1/2} - 2p {}^2P_{1/2, 3/2}$		
			24.98	24.898	N VI	$1s^2 {}^1S_0 - 1s3p {}^1P_1$		
10	11/12/66	R	16.01		O VIII	$1s^2 S_{1/2} - 3p {}^2P_{1/2, 3/2}$	Ly β	7
			18.627		O VII	$1s^2 {}^1S_0 - 1s3p {}^1P_1$	Ly α	
			18.97		O VIII	$1s^2 S_{1/2} - 2p {}^2P_{1/2, 3/2}$		
			21.6		O VII	$1s^2 {}^1S_0 - 1s2p {}^1P_1$	Ly α	
			21.8		O VII	$1s^2 {}^1S_0 - 1s2p {}^3P_1$		
			24.78		N VII	$1s^2 S_{1/2} - 2p {}^2P_{1/2, 3/2}$	Ly α	
			24.9		N VI	$1s^2 {}^1S_0 - 1s3p {}^1P_1$		

TABLE A-3. (Continued)

No.	Date of Observation	R, B, S	λ Observed (Å)	λ Predicted (Å)	Ion	Transition	Remarks	Reference
10	11/12/66	R	28.47		C VI	$1s^2 S_{1/2}-3p^2 P_{1/2, 3/2}$	Ly β	7
			28.79		N VI	$1s^2 {}^1S_0-1s2p {}^1P_1$		
			29.08		N VI	$1s^2 {}^1S_0-1s2p {}^3P_1$		
			33.7		C VI	$1s^2 S_{1/2}-2p^2 P_{1/2, 3/2}$	Ly α	
			40.27		C V	$1s^2 {}^1S_0-1s2p {}^1P_1$		
			40.73		C V	$1s^2 {}^1S_0-1s2p {}^3P_1$		
11	2/23/67	S (1966-111B)	8.44	8.421	Mg XII	$1s^2 S_{1/2}-2p^2 P_{1/2, 3/2}$	Blend	113, 114
				8.459	Na XI	$1s^2 S_{1/2}-3p^2 P_{1/2, 3/2}$		
			8.55		Mg XII	Satellite (?)		
			9.18	9.16	Mg XI	$1s^2 {}^1S_0-1s2p {}^1P_1$		
				9.23	Mg XI	$1s^2 {}^1S_0-1s2p {}^3P_1$		
			9.33	9.29	Mg XI	Satellite (1)		
				9.362	Ne X	$1s^2 S_{1/2}-6p^2 P_{1/2, 3/2}$		
				9.39	Mg XI	Satellite (2)		
			9.53	9.48	Ne X	$1s^2 S_{1/2}-5p^2 P_{1/2, 3/2}$	Blend	
			9.75	9.708	Ne X	$1s^2 S_{1/2}-4p^2 P_{1/2, 3/2}$		
			10.05	9.97	Ni XIX	$2p^6 {}^1S_0-2p^5 4d {}^3D_1$		
				10.025	Na XI	$1s^2 S_{1/2}-2p^2 P_{1/2, 3/2}$		
			10.25	10.10	Ni XIX	$2p^6 {}^1S_0-2p^5 4d {}^1P_1$		
				10.239	Ne X	$1s^2 S_{1/2}-3p^2 P_{1/2, 3/2}$		
			10.61					
			10.82					
			11.05	11.00	Na X	$1s^2 {}^1S_0-1s2p {}^1P_1$		
				11.08	Na X	$1s^2 {}^1S_0-1s2p {}^3P_1$		
			11.18	11.16	Na X	Satellite (1)		
			11.31					
			11.57	11.53	Ni XIX	$2s^2 2p^6 {}^1S_0-2s2p^5 3p {}^1P_1$		
				11.558	Ne IX	$1s^2 {}^1S_0-1s3p {}^1P_1$		
				11.59	Ni XIX	$2s^2 2p^6 {}^1S_0-2s2p^5 3p {}^3P_1$		
			11.76		Ne IX	$1s-3p$ satellite (?)		

TABLE A-3. (Continued)

No.	Date of Observation	R, B, S	λ Observed (Å)	λ Predicted (Å)	Ion	Transition	Remarks	Reference	
11	2/23/67	S (1966-111B)	12.14	12.12	Fe XVII	$2p^6\ ^1S_0-2p^6 4d\ ^1P_1$		113, 114	
				12.134	Ne X	$1s\ ^2S_{1/2}-2p\ ^2P_{1/2, 3/2}$			
			12.27	12.26	Fe XVII	$2p^6\ ^1S_0-2p^6 4d\ ^3D_1$			
			12.45	12.42	Ni XIX	$2p^6\ ^1S_0-2p^6 3d\ ^1P_1$			
			12.64	12.60	Ni XIX	$2p^6\ ^1S_0-2p^6 3d\ ^3D_1$			
			12.85	12.80	Ni XIX	$2p^6\ ^1S_0-2p^6 3d\ ^3P_1$			
			13.01						
			13.48	13.44	Ne IX	$1s^2\ ^1S_0-1s2p\ ^1P_1$			} Blend
				13.55	Ne IX	$1s^2\ ^1S_0-1s2p\ ^3P_1$			
			13.71	13.66	Ne IX	Satellite (1)			} Blend
			13.82	13.77	Ni XIX	$2p^6\ ^1S_0-2p^6 3s\ ^1P_1$			
				13.82	Fe XVII	$2p^6\ ^1S_0-3p\ ^1P_1$			
				13.83	Ne IX	Satellite (2)			
			13.92	13.89	Fe XVII	$2p^6\ ^1S_0-3p\ ^3P_1$			
			14.02	14.03	Ni XIX	$2p^6\ ^1S_0-2p^6 3s\ ^3P_1$			
			14.10	14.10	Ni XVIII	$2p^6 3s\ ^2S-2p^6 3s^2\ ^2P_{1/2}$			} Seriously blended
			14.27	14.25	Fe XVIII	$2p^6-2p^6 3d$			
				14.29	Fe XVIII	$2p^6\ ^1P-2p^6 (^1D) 3d\ ^2D$			} Blended
			14.39	14.37	Ni XVIII	$2p^6 3s\ ^2S-2p^6 3s^2\ ^2P_{3/2}$			
				14.40	Fe XVIII	$2p^6\ ^2P-2p^6 (^3P) 3d\ ^2D$			
			14.56						
			14.68	14.634	O VIII	$1s\ ^2S_{1/2}-6p\ ^2P_{1/2, 3/2}$			} Weak
			15.00	15.012	Fe XVII	$2p^6\ ^1S_0-2p^6 3d\ ^1P_1$			
			15.25	15.261	Fe XVII	$2p^6\ ^1S_0-2p^6 3d\ ^3D_1$			
			15.45	15.453	Fe XVII	$2p^6\ ^1S_0-2p^6 3d\ ^3P_1$			
			15.61	15.62	Fe XVIII	$2p^6\ ^2P-2p^6 (^1D) 3s\ ^2D$			
			15.88	15.88	Fe XVIII	$2p^6\ ^2P-2p^6 (^3P) 3s\ ^2P$			
			16.01	16.006	O VIII	$1s\ ^2S_{1/2}-3p\ ^2P_{1/2, 3/2}$			
			16.30	16.01	Fe XVIII	$2p^6\ ^2P-2p^6 (^3P) 3s\ ^4P$			
			16.77	16.774	Fe XVII	$2p^6\ ^1S_0-2p^6 3s\ ^1P_1$			} Weak
			17.06	17.051	Fe XVII	$2p^6\ ^1S_0-2p^6 3s\ ^3P_1$			
			17.42	17.206	Fe XVI	$2s^2 2p^6 3s\ ^2S-2s^2 2p^6 3s^2\ ^2P_{3/2}$			} Badly blended
				17.491	Fe XVI	$2s^2 2p^6 3s\ ^2S-2s^2 2p^6 3s^2\ ^2P_{1/2}$			
			17.64	17.59	Mn XVII	$2p^6\ ^2P_{3/2}-2p^6 (^2P) 3s\ ^2P_{3/2}$			
				17.73	Mn XVII	$2p^6\ ^2P_{3/2}-2p^6 (^2P) 3s\ ^4P_{3/2}$			

TABLE A-3. (Concluded)

No.	Date of Observation	R, B, S	λ Observed (Å)	λ Predicted (Å)	Ion	Transition	Remarks	Reference
11	2/23/67	S (1966-111B)	17.78	17.77	O VII	$1s^2 \text{ } ^1S_0 - 1s4p \text{ } ^1P_1$		113, 114
			18.35		Mg XI	$1s^2 \text{ } ^1S_0 - 1s2p \text{ } ^1P_1$		
			18.54	2 x 9.17				
			18.64	18.627	O VII	$1s^2 \text{ } ^1S_0 - 1s3p \text{ } ^1P_1$		
			18.96	18.969	O VIII	$1s^2 \text{ } ^1S_{1/2} - 2p \text{ } ^2P_{1/2, 3/2}$		
			20.90	20.910	N VII	$1s^2 \text{ } ^1S_{1/2} - 3p \text{ } ^2P_{1/2, 3/2}$	Very weak	
			21.60	21.602	O VII	$1s^2 \text{ } ^1S_0 - 1s2p \text{ } ^1P_1$		
			21.80	21.80	O VII	$1s^2 \text{ } ^1S_0 - 1s2p \text{ } ^3P_1$		
			22.08	(22)	Ca XIV	$2p^3 \text{ } ^4S - 3s \text{ } ^4p$		
			23.12	2 x 11.558	Ne IX	$1s^2 \text{ } ^1S_0 - 1s3p \text{ } ^1P_1$		
			23.29					
			24.22	2 x 12.12	Fe XVII	$2p^6 \text{ } ^1S_0 - 2p^5 4d \text{ } ^1P_1$		
			24.28	2 x 12.13	Ne X	$1s^2 \text{ } ^1S_{1/2} - 2p \text{ } ^2P_{1/2, 3/2}$		
			24.58	2 x 12.26	Fe XVII	$2p^6 \text{ } ^1S_0 - 2p^5 4d \text{ } ^3D_1$		
			24.78	24.781	N VII	$1s^2 \text{ } ^1S_{1/2} - 2p \text{ } ^2P_{1/2, 3/2}$		

Special Tabular Abbreviations

Poss.: Possibly

Doub.: Doubled

Doub. by deflect. p. sys.:

Disag. in trans. in reports:

Doubled by deflection of pointing system

Disagreement in transition notation in reports

TABLE A-4. LIST OF OBSERVED SOLAR
SPECTRAL LINES (1- to 100-Å)

λ Observed (Å)	Ion	λ Predicted (Å)	No.
1.91			9
2.26			9
2.33	Ca XX	2.267	9
	Ca XX	2.314	9
	Ca XX	2.331	9
	Ca XX	2.361	9
	Ca XX	2.417	9
2.64	Ca XX	2.549	9
3.05	Ar XVIII	2.987	9
	Ca XX	3.020	9
3.77	Ar XVIII	3.733	9
4.41			9
5.73			9
5.85			9
6.11	Si XIV	6.186	9
6.52			9
6.58			9
6.70	Si XIII	6.7	9
6.74			9
7.05			9
7.42	Mg XI	7.47	9
7.5	Mg XI	7.47	9
7.73	Al XII	7.757	9
7.70	Na XI	7.677	9
7.79	Na XI	7.735	9
7.82	Na XI	7.833	9
8.06	Na XI	8.021	9
8.44	Mg XII	8.421	11
	Na XI	8.459	11
8.55	Mg XII		11

TABLE A-4. (Continued)

λ Observed (\AA)	Ion	λ Predicted (\AA)	No.
9.15	Mg XI	9.16	9
9.18	Mg XI	9.16	11
	Mg XI	9.23	11
9.19	Mg XI	9.23	9
9.32	Mg XI	9.29	9
	Ne X	9.291	9
9.33	Mg XI	9.29	11
	Ne X	9.362	9, 11
	Mg XI	9.39	11
9.5	Mg XI	9.17	2, 6
9.53	Ne X	9.48	11
9.71	Ne X	9.708	9
9.75	Ne X	9.708	11
10.05	Ni XIX	9.97	11
	Na XI	10.025	11
10.25	Ni XIX	10.10	11
	Ne X	10.239	11
10.61			11
10.82			11
10.9-11.9 (Line group)	Ne IX	11.1	2, 6
	Na X	11.1	2, 6
	Ne IX	11.54	2, 6
	Ne X	12.14	2, 6
11.05	Na X	11.00	11
	Na X	11.08	11
11.18	Na X	11.16	11
11.31			11
11.45	Ne IX	11.45	8
11.56	Ni XIX	11.53	9
	Ne IX		8
11.57	Ne IX	11.558	9
	Ni XIX	11.59	9
11.57	Ni XIX	11.53	11
	Ne IX	11.558	11
	Ni XIX	11.59	11
11.76	Ne IX		11

TABLE A-4. (Continued)

λ Observed (\AA)	Ion	λ Predicted (\AA)	No.
12.12	Fe XVII		8
12.13	Fe XVII	12.12	8, 9
	Ne X	12.13	8
	Ne X	12.134	9
12.14	Fe XVII	12.12	11
	Ne X	12.134	11
12.24	Ni XIX		8
12.26	Fe XVII	12.26	8, 9
12.27	Fe XVII	12.26	11
12.42	Fe XVII	12.26	2, 6
12.42	Ni XIX	12.42	8
12.45	Ni XIX	12.42	11
12.53			8
12.64	Ni XIX	12.60	11
	Ni XIX	12.64	8
12.80	Ni XIX	12.80	8
12.85	Ni XIX	12.80	11
13.01			11
13.1-13.6 (Line group)	Ne IX	13.45	2, 6
	Ne IX	13.7	2, 6
	Fe XVII	13.82	2, 6
13.44	Ne IX	13.44	9
	Mn XVI	13.46	9
13.45	Ne IX	13.45	8
13.48	Ne IX	13.44	11
	Ne IX	13.55	11
13.55	Ne IX	13.55	8
13.56	Ne IX	13.55	9
	Mn XVI	13.61	9
13.65			8
	Ne IX	13.66	9
13.70	Fe XVII	13.8	3
	Fe XVII	13.82	2
13.71	Ne IX	13.66	11
13.77	Ni XIX	13.77	8

TABLE A-4. (Continued)

λ Observed (\AA)	Ion	λ Predicted (\AA)	No.
13.82	Ni XIX	13.77	9, 11
	Fe XVII	13.820	8, 9, 11
	Ne IX	13.83	9, 11
13.87	Fe XVII	13.887	9
13.92	Fe XVII	13.89	11
14.02	Ni XIX	14.03	11
14.03	Ni XIX	14.03	8
14.08	Ni XIX	14.03	9
14.10	Ni XVIII	14.10	11
14.2			2, 6
14.23	Fe XVIII	14.25	9
14.25	Fe XVIII	14.25	8
	Fe XVIII	14.25	11
14.27	Fe XVIII	14.29	11
14.29	Fe XVIII	14.29	8
14.39	Ni XVIII	14.37	11
	Fe XVIII	14.40	11
14.40	Fe XVIII	14.40	8
14.56			11
14.57	O VIII	14.524	9
	O VIII	14.634	9
14.68	O VIII	14.634	11
14.82	O VIII	14.82	8
	O VIII	14.821	9
14.9	O VIII	14.82	6
	Fe XVII	15.01	2, 6
15.00	Fe XVII	15.0	3
	Fe XVII	15.012	2, 11
15.01	Fe XVII	15.01	8
	Fe XVII	15.012	9
	Cr XV	15.06	9
15.13	O VIII	15.176	9
15.17	O VIII	15.17	8
15.20	O VIII	14.82	2
	O VIII	15.18	2, 6
	Fe XVII	15.26	2, 3, 6

TABLE A-4. (Continued)

λ Observed (\AA)	Ion	λ Predicted (\AA)	No.
15.25	Cr XV	15.21	9
	Mn XVI	15.238	9
	Fe XVII	15.261	2, 9, 11
	Mn XVI	15.312	9
15.26	Fe XVII	15.26	8
15.45	Fe XVII	15.45	8
	Fe XVII	15.453	9, 11
15.6			2, 6
15.61	Fe XVIII	15.62	11
15.62	Fe XVIII	15.62	8
15.69	Fe XVIII	15.62	9
	Mn XVII	15.71	9
15.88	Fe XVIII	15.88	8, 11
15.96	O VIII	16.01	8
16.00	O VIII	16.0	3
	O VIII	16.006	2, 6, 9
	Fe XVIII	16.01	9
	O VIII	16.01	2
16.01	O VIII		8, 10
	O VIII	16.006	11
	Fe XVIII	16.01	11
16.07	Mn XVII	16.06	9
16.30			8, 11
16.6			8
16.7	Fe XVII	16.8	3
16.72	Fe XVII	16.774	2
16.77	Fe XVII	16.77	8
16.77	Fe XVII	16.774	11
16.85	Fe XVII	16.77	2, 6
16.86	Fe XVII	16.774	9
	Mn XVI	16.882	9
	Cr XV	16.889	9
17.01 } 17.05 }	Fe XVII	17.051	2
17.04	Cr XV	16.965	9
	Fe XVII	17.051	9
17.05	Fe XVII	17.05	3, 8

TABLE A-4. (Continued)

λ Observed (\AA)	Ion	λ Predicted (\AA)	No.
17.06	Fe XVII	17.051	11
17.1	Fe XVII	17.05	2, 6
17.11	O VII	17.08	9
	Mn XVI	17.095	9
17.41	O VII	17.42	9
17.42	Fe XVI	17.206	11
	Fe XVI	17.491	11
17.64	Mn XVII	17.59	9, 11
	Mn XVII	17.73	11
17.65 } 17.72 }	O VII	17.768	2
17.7	O VII	17.8	3
17.77	O VII		8
17.78	Mn XVII	17.73	9
	O VII	17.77	9, 11
18.35	Mg XI	2 x 9.17	11
18.54			11
18.54 } 18.61 }	O VII	18.627	2
18.627	O VII		10
18.63	O VII		8
	N VII	18.587	9
	O VII	18.627	9
	Mn XVI	18.654	9
	N VII	18.670	9
	N VII	18.682	9
	N VII	18.698	9
	N VII	18.717	9
18.64	O VII	18.627	11
18.8 } 18.9 }	O VIII	18.969	2
18.9	O VIII	18.97	2, 3, 6
18.94	O VIII	18.97	8
18.96	N VII	18.882	9
	Mn XVI	18.935	9
	O VIII	18.969	9, 11
	N VII	18.974	9
	Cr XV	19.015	9

TABLE A-4. (Continued)

λ Observed (\AA)	Ion	λ Predicted (\AA)	No.
18.97	O VIII		8, 10
20.5	N VII	20.91	6
	N VII	20.97	2
20.8	N VII	20.9	3
	N VII	20.910	2
20.87	Cr XV	20.863	9
	N VII	20.910	9
20.90	N VII	20.910	11
21.5	O VII	21.6	3
21.55	O VII	21.602	2
21.60	O VII		8, 10
	O VII	21.60	2, 5, 6
	O VII	21.602	9, 11
	O VII	21.80	2, 5, 6
21.70	O VII	21.8	3
	O VII	21.804	2
21.80	O VII		8, 10
	O VII	21.80	11
	O VII	21.81	9
22.0		22.07	3
22.07	Ca XIV	22	9
22.08	Ca XIV	(22)	11
23.12	Ne IX	2 x 11.558	11
23.2			2
23.28			9
23.29			11
23.74	N VI	23.77	9
24.22	Fe XVII	2 x 12.12	11
24.28	Ne X	2 x 12.13	11
24.58	Fe XVII	2 x 12.26	11
24.7	N VII	24.78	2, 6
24.78	N VII		10
	N VII	24.781	11
	N VIII	24.781	9

TABLE A-4. (Continued)

λ Observed (\AA)	Ion	λ Predicted (\AA)	No.
24.8	N VII	24.781	2
	N VII	24.8	3
24.9	N VI		10
24.98	N VI	24.898	9
26.9	C VI	27.0	2, 6
27.6			2, 6
28.47	C VI		10
28.5	C VI	28.46	2, 6
28.79	N VI		10
29.08	N VI		10
30.0	Fe XVII	15.01 x 2	2, 6
	Fe XVII	15.26 x 2	6
30.9	Fe XVII	15.6 x 2	2, 6
31.8	O VIII	16.006 x 2	6
	O VIII	16.01 x 2	2
33.7	C VI		10
33.73	C VI	33.73	7
33.74	C VI		4
33.75	C VI	33.74	2, 5
33.9	Fe XVII	16.77 x 2	6
	C VI	33.74	6
	Fe XVII	17.05 x 2	6
35.6			6
36.6			6
37.7	O VIII	18.97 x 2	6
38.7			6
(39.28)	Si XI		4

TABLE A-4. (Continued)

λ Observed (\AA)	Ion	λ Predicted (\AA)	No.
39.6			6
40.27	C V		4, 10
	C V	40.27	7
40.3	C V	40.27	5
40.73	C V		4, 10
40.9	Si XII	40.91	6
	Si XII	40.95	6
(40.91, .95)	Si XII		4
40.96	Si XII	(40.93)	7
41.49			4
41.8	N VII	20.91 x 2	6
42.2	S X	42.51	5
	S X	42.54	5
	S X	42.58	5
(42.51, .54, .58)	S X		4
43.2	O VII	21.60 x 2	5
43.76	Si XI		4
	Si XI	43.76	7
43.8	Si XI	43.76	6
	Si XII	44.02	6
	Mg X	44.05	6
	Si XII	44.16	6
	Si IX	44.22	6
	Si IX	44.25	6
44.0	Si XI	43.76	5
	Si XII	44.02	5
	Mg X	44.05	5
	Si XII	44.16	5
	Si IX	44.22	5
	Si IX	44.25	5
44.02, .16	Si XII		4
44.18	Si XII	44.16	7

TABLE A-4. (Continued)

λ Observed (\AA)	Ion	λ Predicted (\AA)	No.
45.3	Si XII	45.66	5
45.49	Si XII	45.48	7
45.73	Si XII	45.66	7
45.9	Si XII	45.66	6
46.1	Si XI	46.26	5
	Si XI	46.30	5
	Si XI	46.40	5
46.37	Si XI	46.3	7
47.5	Si XI	47.61	5
	Si XI	47.65	5
	Si X	47.65	5
	Si X	47.79	5
47.9	Si XI	47.61	6
	Si XI	47.65	6
	Si X	47.65	6
	Si X	47.79	6
49.2	Si XI	49.22	6
	Si XI	49.26	6
49.22	Si XI		4
	Si XI	49.22	7
49.4	Si XI	49.22	5
	Si XI	49.26	5
50.35	Fe XVI		4
50.51	Si X	50.52	7
50.52	Si X		4
50.6	Si X	50.52	5, 6
	Fe XVI	50.56	5, 6
	Si X	50.69	5, 6
50.68	Si X	50.69	7
50.69	Si X		4
50.70	Si X		4
52.1	Si X	52.07	5
	Si X	52.16	5

TABLE A-4. (Continued)

λ Observed (\AA)	Ion	λ Predicted (\AA)	No.
52.30	Si XI	(52.30)	7
52.7	Si IX	52.81	5
	Si IX	52.84	5
52.9	Fe XV		4
52.97	Fe XV	52.91	7
54.1	Fe XVI	54.14	5
	S IX	54.18	5
54.14	Fe XVI		4
	Fe XVI	54.14	7
54.18	S IX		4
54.67	Fe XVI	54.73	7
55.10	Si IX	55.1	7
55.31	Si IX	55.3	7
55.34	Si IX		4
	Si IX	55.30	5
	Si IX	55.36	5
	Si IX	55.40	5
57.6	Mg X	57.88	5
	Mg X	57.92	5
57.87	Mg X	57.90	7
57.88, .92	Mg X		4
58.97	Fe XIV	58.96	7
59.0	Si VIII	58.88	5
	Si IX	58.91	5
	Fe XIV	58.96	5
	Si IX	59.00	5
	Si IX	59.08	5
59.61	Fe XIV	59.58	7
61.00, .02, .07	Si VIII		4

TABLE A-4. (Continued)

λ Observed (\AA)	Ion	λ Predicted (\AA)	No.
61.05	Si VIII	60.99	5
	Si VIII	61.02	5
	Si VIII	61.03	7
	Si VIII	61.07	5
	Si VIII	61.80	5
61.60	Si IX	61.7	7
61.61	Si IX		4
61.8	Si VIII	61.85	5
	Si VIII	61.90	5
	Si VIII	61.91	5
61.85	Si VIII		4
62.74	Mg IX	62.75	7
62.75	Mg IX		4
62.98	Fe XVI	62.88	7
63.0	Si IX	61.85	5
	Mg IX	61.92	5
	Mg IX	61.96	5
	Mg IX	62.75	5
	Si VIII	62.81	5
	Si VIII	62.85	5
	Fe XVI	62.88	5
	Mg X	63.15	5
	Si VIII	63.23	5
	Si VIII	63.27	5
	Mg X	63.29	5
63.28	Mg X	63.29	7
63.29	Mg X		4
63.72	Fe XVI		4
	Fe XVI	63.72	7
65.67	Mg X	65.67	7
65.85	Mg X		4
65.89	Mg X	65.85	7
66.24	Fe XVI		4
66.35	Fe XVI	66.26	7
	Fe XVI	66.37	7

TABLE A-4. (Continued)

λ Observed (\AA)	Ion	λ Predicted (\AA)	No.
67.0	Mg IX	67.09	5
	Mg IX	67.14	5
	Mg IX	67.24	5
67.20	Mg IX		4
	Mg IX	67.2	7
69.62	Si VIII		4
69.9	Mg IX	69.95	5
	Fe XV	69.95	5
	Fe XV	69.99	5
	Fe XV	70.05	5
69.95	Mg IX		4
69.96	Fe XV	70.0	7
70.00	Fe XV		4
71.00	Fe XIV	71.00	7
71.95	Fe XIV	(71.96)	7
72.26	Mg IX	72.23	5
	Mg IX	72.31	5
72.31	Mg IX		4
	Mg IX	72.31	7
74.85	Mg VIII	74.86	7
75.03	Mg VIII	75.03	7
76.01	Fe XIII	76.01	7
76.38	Fe XIII	(76.48)	7
76.48	Fe XIII	(76.55)	7
77.31	Ni XI	77.34	7
77.74	Mg IX	77.74	7
78.71	Ni XI	78.70	7
79.48	Fe XII	79.48	7

TABLE A-4. (Continued)

λ Observed (\AA)	Ion	λ Predicted (\AA)	No.
80.03	Fe XII	(80.00)	7
80.50	Fe XII	(80.49)	7
82.80	Mg XIII	82.82	7
83.58	Mg VII	83.6	7
83.9	Ne VIII	85.0	1
84.01	Mg VII	84.0	7
86.84	Fe XI	86.77	7
87.03	Fe XI	87.02	7
	Fe XI	88.00	7
88.08, .12	Ne VIII		4
88.10	Fe XI	88.03	7
	Ne VIII	88.10	7
	Fe XI	88.17	7
2 x 44.16	Si XII		4
88.98	Fe XI	89.10	7
89.20	Fe XI	89.18	7
89.73	Fe XI	89.77	7
90.17	Fe XI	90.20	7
90.47	Fe XI	90.34	7
91.57	Ni X	91.53	7
91.78	Ni X	91.79	7
94.01	Fe X	94.01	7
95.39	Fe X	95.34	7
	Fe X	95.37	7

TABLE A-4. (Concluded)

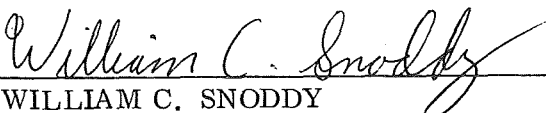
λ Observed (\AA)	Ion	λ Predicted (\AA)	No.
96.08	Fe X	96.12	7
96.79	Fe X	96.79	7
97.14	Fe X	97.12	7
97.52	Ne VII	97.54	7
97.53	Fe X	97.59	7
97.86	Fe X	97.84	7
98.24	Ne VIII	98.27	7

A SOLAR X-RAY ASTRONOMY SUMMARY AND BIBLIOGRAPHY

By Robert M. Wilson, John M. Reynolds,
and Stanley A. Fields

The information in this report has been reviewed for security classification. Review of any information concerning Department of Defense or Atomic Energy Commission programs has been made by the MSFC Security Classification Officer. This report, in its entirety, has been determined to be unclassified.

This document has also been reviewed and approved for technical accuracy.


WILLIAM C. SNODDY
Chief, Space Thermophysics Division


G. B. HELLER
Director, Space Sciences Laboratory

DISTRIBUTION

TM X-53991

INTERNAL

DIR

Dr. Eberhard M. Rees
Mr. James T. Shepherd

DEP-T

Mr. Cook

AD-S

Dr. Ernst Stuhlinger
Dr. George Bucher

S&E-P

Mr. Kroeger

S&E-CSE-DIR

Dr. Haeussermann

S&E-AERO-DIR

Dr. E. Geissler

S&E-ASTR-DIR

Mr. Brooks Moore
Mr. W. P. Horton

S&E-ASTR-RP

Mr. Richard Hoover

S&E-ASTN-DIR

Mr. K. Heimbürg

S&E-SSL-DIR

Mr. G. B. Heller
Mr. R. V. Hembree

S&E-SSL-X

Dr. J. Dozier
Mr. H. Weathers
Dr. A. Weber

S&E-SSL-N

Dr. Rudolf Decher
Dr. A. DeLoach

S&E-SSL-P

Dr. R. Naumann
Mr. J. McGuire

S&E-SSL-S

Dr. W. H. Sieber

S&E-SSL-T

Mr. W. Snoddy
Mr. J. Milligan
Mr. E. Miller
Mr. G. Arnett
Mr. B. Jones
Mr. S. Fields (15)
Mr. J. Reynolds (15)
Mr. B. Wilson (15)
Mr. J. Fountain
Dr. K. Schocken
Mr. H. Bennett
Mr. B. Denman

S&E-SSL-C

Mr. Bill Bass
Reserve (25)

PD-DIR

Dr. W. Lucas

PD-MP

Mr. J. Downey
Mr. H. Gierow
Mr. H. Dudley
Mr. P. Schwindt
Mr. J. Oliver
Mr. S. Larson
Mr. R. Potter

DISTRIBUTION (Concluded)

PM-DIR

Dr. W. A. Mrazek

PM-MO-MGR

Dr. F. A. Speer

A&TS-PAT

Mr. L. D. Wofford, Jr.

PM-PR-M

A&TS-MS-H

A&TS-MS-IP (2)

A&TS-MS-IL (8)

A&TS-TU (6)

EXTERNAL

NASA Headquarters

Washington, D. C. 20546

ATTN:

Dr. Nancy G. Roman - SG

Mr. R. E. Halpern - SG

Dr. John E. Naugle - S

Goddard Space Flight Center

Mr. J. H. Underwood - 614

Dr. E. Boldt - 611

Dr. S. Holt - 611

Dr. P. Serlemitsos - 611

Saint Louis University

Physics Department

Saint Louis, Missouri

ATTN: Dr. J. F. McGee

University of South Florida

Dept. of Astronomy

Tampa, Florida

ATTN:

Dr. H. K. Eichhorn-von Wurmb,

Chairman Astron. Dept.

Dr. S. Sofia

Dr. E. Devinney

Scientific and Technical Information

Facility (25)

P. O. Box 33

College Park, Maryland 20740

ATTN: NASA Representative (S-AK/RKT)